Runx1 C-terminal Domains During Hematopoietic Development and Leukemogenesis: A Dissertation

RUNX1 C-TERMINAL DOMAINS DURING HEMATOPOIETIC DEVELOPMENT AND LEUKEMOGENESIS

A Dissertation Presented

By

Christopher R. Dowdy

Submitted to the Faculty of the
University of Massachusetts Graduate School of Biomedical Sciences, Worcester
In partial fulfillment of the requirements for the degree of

DOCTOR OF PHILOSOPHY

May 25th, 2012

Department of Cell Biology

RUNX1 C-TERMINAL DOMAINS DURING HEMATOPOIETIC DEVELOPMENT AND LEUKEMOGENESIS

A Dissertation Presented
By

Christopher R. Dowdy

The signatures of the Dissertation Defense Committee signify completion and approval as to style and content of the Dissertation

_____
Gary S. Stein, Ph.D., Thesis Advisor

_____
Lucio Castilla, Ph.D., Member of Committee

_____
Alan Rosmarin, MD, Member of Committee

_____
Hong Zhang, Ph.D., Member of Committee

_____
Janice Telfer, Ph.D., Member of Committee

The signature of the Chair of the Committee signifies that the written dissertation meets the requirements of the Dissertation Committee

_____
Anthony Imbalzano, Ph.D., Chair of Committee

The signature of the Dean of the Graduate School of Biomedical Sciences signifies that the student has met all graduation requirements of the school.

_____
Anthony Carruthers, Ph.D.,
Dean of the Graduate School of Biomedical Sciences

Department of Cell Biology
May 25th, 2012

Acknowledgements

Firstly, I want to thank my advisor Gary, as well as Janet, Andre and Jane for their constant advice and guidance throughout my time in the lab. I never would have thought a large multiple PI lab could run so well, and my experiences here have taught me the true value of collaboration. It has truly been a pleasure working with everyone in the lab these years. The wisdom of senior members like Kaleem, Dana, and Shirwin coupled with the eagerness and altruism everyone here has made my time here enlightening as well as humbling. I am proud to come from a lab so deeply immersed in the collaborative spirit.

I want to thank Steve Baker for teaching me about statistics, Rachel Gerstein for everything I know about flow and B-cells, and everyone in the lab. Every member of the lab has helped make this possible, from teaching me the finer points of a specific technique to helping me see things from a new perspective.

I also wish to acknowledge my committee members, Tony, Lucio, Alan and Hong, for all of their support, advice and constructive criticism. Their influence has taught me how to simultaneously see the big picture and maintain focused on the details.

I especially need to thank my wonderful wife Pam. Without her unwavering support, this endeavor would not have been possible. Words cannot express the depth of my gratitude.

Abstract

Runx1 is a master regulator of hematopoiesis, required for the initiation of definitive hematopoiesis in the embryo and essential for appropriate differentiation of many hematopoietic lineages in the adult. The roles of Runx1 in normal hematopoiesis are juxtaposed with the high frequency of Runx1 mutations and translocations in leukemia. Leukemia associated Runx1 mutations that retain DNA-binding ability have truncations or frame shifts that lose C-terminal domains. These domains are important for subnuclear localization of Runx1 and protein interactions with co-factors. The majority of leukemia associated Runx1 translocations also replace the C-terminus of Runx1 with chimeric fusion proteins. The common loss of Runx1 C-terminal domains in hematopoietic diseases suggests a possible common mechanism. We developed a panel of mutations to test the functions of these domains in vitro, and then developed mouse models to examine the consequences of losing Runx1 C-terminal domains on hematopoietic development and leukemogenesis in vivo.

We previously observed that overexpression of a subnuclear targeting defective mutant of Runx1 in a myeloid progenitor cell line blocks differentiation. Gene expression analysis before differentiation was initiated revealed that the mutant Runx1 was already deregulating genes important for maturation. Furthermore, promoters of the suppressed

genes were enriched for binding sites of known Runx1 co-factors, indicating a non-DNA-binding role for the mutant Runx1.

To investigate the in vivo function of Runx1 C-terminal domains, we generated two knock-in mouse models; a C-terminal truncation, $Runx1^{Q307X}$, and a point mutant in the subnuclear targeting domain, $Runx1^{HTY350\text{-}352AAA}$. Embryos homozygous for $Runx1^{Q307X}$ phenocopy a complete Runx1 null and die in utero from central nervous system hemorrhage and lack of definitive hematopoiesis. Embryos homozygous for the point mutation $Runx1^{HTY350\text{-}352AAA}$ bypass embryonic lethality, but have hypomorphic Runx1 function. $Runx1^{HTY350\text{-}352AAA}$ results in defective growth control of hematopoietic progenitors, deregulation of B-lymphoid and myeloid lineages, as well as maturation delays in megakaryocytic and erythroid development.

Runx1 localizes to subnuclear domains to scaffold regulatory machinery for control of gene expression. This work supports the role of transcription factors interacting with nuclear architecture for greater biological control, and shows how even subtle alterations in that ability could have profound effects on normal biological function and gene regulation.

Table of Contents

List of Figures and Tables

List of Symbols, Abbreviations or Nomenclature

5-flourouracil (5-FU)
Acute Myeloid Leukemia (AML)
Core Binding Factor (CBF)
Colony Forming Unit (CFU)
Common Lymphoid Progenitor (CLP)
Chronic Myelomonocytic Leukemia (CMML)
Common Myeloid Progenitor (CMP)
Central Nervous System (CNS)
Electrophoretic Mobility Shift Assay (EMSA)
Granulocyte Monocyte Progenitor (GMP)
Familial Platelet Disorder (FPD)
Hematopoietic Stem Cell (HSC)
In Vitro Transcription and Translation (IVTT)
Myeloid Dysplastic Syndromes (MDS)
Megakaryocyte Erythroid Progenitor (MEP)
Multipotent Progenitor (MPP)
Subnuclear Targeting Defective mutant (mSTD)
Nuclear Localization Signal (NLS)
Nuclear Matrix-Intermediate Filament (NMIF)
Nuclear Matrix Targeting Signal (NMTS)
Refractory Anemia with Excess Blasts (RAEB)
Runt Homology Domain (RHD)

Preface

Portions of this thesis have appeared in:

Dowdy CR, Xie R, Frederick D, Zaidi SK, Gerstein RL, Lian JB, van Wijnen AJ, Stein JL, Stein GS. A Germline Point Mutation in Runx1 Uncouples its Role in Definitive Hematopoiesis from Differentiation. Manuscript in preparation.

Dowdy CR, Xie R, Frederick D, Hussain S, Zaidi SK, Vradii D, Javed A, Li X, Jones SN, Lian JB, van Wijnen AJ, Stein JL, Stein GS. Definitive hematopoiesis requires Runx1 C-terminal-mediated subnuclear targeting and transactivation. *Human molecular genetics.* Mar 15 2010;19(6):1048-1057.

Targeting vector construction and Southern blots shown in Figure 15 were performed by Ronglin Xie and Dana Frederick. Cloning and targeting vector components shown in Figure 21A was performed by Ronglin Xie.

Sectioning and histological staining in Figure 16, was performed by Sadiq Hussain and Dana Frederick. Sectioning and histological staining in Figure 27B, Figure 29F, Figure 31D and Figure 31E were performed by Dana Frederick.

Western blot in Figure 20 was performed by Dana Frederick.

Figure 2 is reproduced with permission from Stein et al., *Trends in Cell Biology* 2003; 13(11):584-92 (License Number: 2895480524553).

Figure 3 and Figure 32 are adapted with permission from Larsson and Karlsson, *Oncogene* 2005; 24(37):5676-92 (License Number: 2895470995227).

Chapter 1: General Introduction

Runx Proteins

Runx1, Runx2 and Runx3 are the three DNA-binding alpha subunits of the Core Binding Factor (CBF) heterodimeric transcription factor. The shared beta subunit (CBFbeta) protects the alpha subunit from degradation and greatly increases the DNA-binding affinity for the complex, while not binding DNA itself.[1,2] The expression of Runx factors is tissue specific, while they all bind the same consensus sequence (Figure 1). The three alpha subunits historically have several different names from the manners in which they were isolated. The consensus binding sequence is contained within many viral enhancers and earned the Runx proteins the names Polyomavirus Enhancer Binding Protein 2 (PEBP2)[3] and CBF from the core murine leukemia virus enhancer.[4] Runx1 was originally named Acute Myeloid Leukemia 1 (AML1) when it was identified as the target on chromosome 21 of the leukemic (8;21) translocation.[5] Runx2 is important in bone biology, which earned the Runx proteins the names Nuclear Matrix Protein 2 (NMP2)[6], Osteoblast-specific Complex (OBSC)[7] and Osteoblast-specific Factor 2 (OSF2).[8] The DNA-binding domain of all 3 Runx factors is homologous to the *Drosophila* protein Runt. Therefore, the term Runt-related transcription factor (RUNX) has been formally adopted by researchers studying all three of the CBF alpha subunits.[9]

All three Runx factors are lineage determining transcription factors. Runx1 is essential for embryonic hematopoiesis.[10] Runx2 is required for ossification in bone.[11,12] Runx3 is implicated in gastric and neuronal development.[13,14] All three Runx factors contain several highly conserved domains (Figure 1), including the DNA-binding Runt homology domain (RHD) at the N-terminus[15], and a nuclear matrix targeting signal (NMTS) responsible for subnuclear targeting at the C-terminus.[16] The RHD dimerizes with CBFbeta and binds the consensus DNA sequence TGTGGT. Gene regulation is carried out through protein-protein interactions with co-factors, mediated by additional domains.[17-23] The NMTS in Runx proteins is a 30-40 amino acid sequence that targets Runx to distinct subnuclear foci, associated with transcriptional activity.[24,25] Runx factors are thought to anchor to the nuclear matrix and act as a scaffold, associating regions of DNA with other factors via its many interaction domains.[26,27] Playing a functional role in the three dimensional architecture of the nucleus dramatically increases the potential mechanisms for Runx factors to regulate gene expression.[28,29]

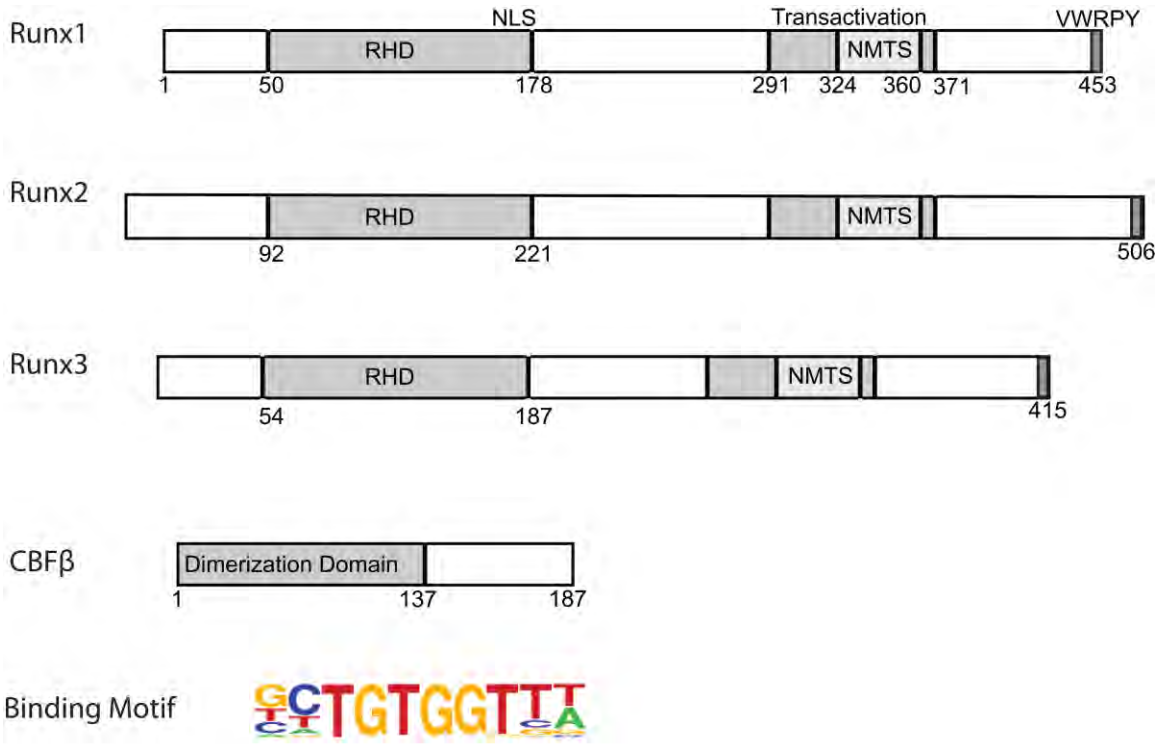

Figure 1: Schematic of Runx transcription factors

All three Runx transcription factors have a conserved Runt Homology Domain (RHD) which dimerizes with CBFbeta and binds the consensus DNA motif.[30] The RHD also contains the Nuclear Localization Signal (NLS) at the C-terminal end. All three Runx proteins also have a conserved Nuclear Matrix Targeting Signal (NMTS) and several conserved co-factor interaction domains, including transactivation domains and the VWRPY domain critical for association with the Groucho/TLE co-repressor. Shown are the amino acid lengths for human Runx1, Runx2 and Runx3. The amino acid lengths of the mouse proteins are 451, 513, and 410, respectively. CBFbeta increases the DNA-binding ability of each Runx factor by forming a heterodimer via its dimerization domain and the RHD. Both human and mouse CBFbeta contain 187 amino acids.

Nuclear Architecture

The nuclear matrix is a ribonucleoprotein network extending from the inner nuclear envelope throughout the nucleus.[31] Electron microscopy, with much higher resolution than light microscopy and better staining techniques, allowed the observation of a highly structured nucleus with many substructures that contained little or no DNA. The nuclear matrix is functionally defined as the non-chromatin structures of the nucleus observed under the electron microscope in unextracted cells.[31] Release of the ribonucleoprotein particles would not occur with only removal of the nuclear envelope or treatment with DNase, but required digestion with ribonucleases.[32] This indicated that the nuclear matrix contained structural RNA. Early studies of the nuclear matrix found an RNase resistant scaffolding made up of protein fibers connected to nuclear lamina.[33] The current model states the nuclear matrix is a network of branched filaments that connect to the nuclear lamina.[34-36] Other components of the nuclear matrix have either direct or indirect interactions with these filaments.[31]

The nuclear matrix serves important roles in DNA replication and transcription. Newly synthesized DNA and replication factories are attached to the nuclear matrix.[37-39] Transcription machinery, RNA polymerase II, splicing factories and many transcription factors also remain in the nuclear matrix after DNase digestion.[31,40] In addition to tethering important complexes involved in gene expression, over 400 proteins are associated with the nuclear matrix.[41] Some of these proteins, like the Runx transcription

factors and ALL1, act as scaffolds to organize other regulatory factors.[42,43] Associating chromatin remodeling enzymes, transcription factors and signaling molecules all together at the same three-dimensional space as DNA allows for combinatorial control of gene expression, greatly increasing potential regulation by these transcription factors.[44]

Most transcription factors have a nuclear localization signal (NLS) that marks them for translocation into the nucleus. Once inside the nucleus, a DNA binding domain determines its sequence specificity and a nuclear matrix targeting signal (NMTS) is required for proper interactions within the nuclear matrix. The first transcription factors identified with a NMTS were Runx1 and Runx2.[25] The Runx NMTS targets it to matrix associated transcriptional domains.[24] Currently, many transcription factors have an identified NMTS, including steroid receptors, PIT1, YY1, SATB1, and even the leukemia associated Runx1/ETO, which has distinct subnuclear targeting from Runx1.[45-51]

Cancer cells exhibit massive gene deregulation and profound morphological changes in their nuclei.[52,53] Several aspects of the nuclear architecture are altered in the cancer cell, suggesting a functional connection between nuclear organization and gene expression.[44] Nuclear architecture assembles DNA and proteins in three-dimensional space and is important for many biological functions (Figure 2). These complex spatial organizations of the genome with factors that influence its expression are very important for appropriate gene regulation, and are often perturbed in disease.[16,26-29,54-57]

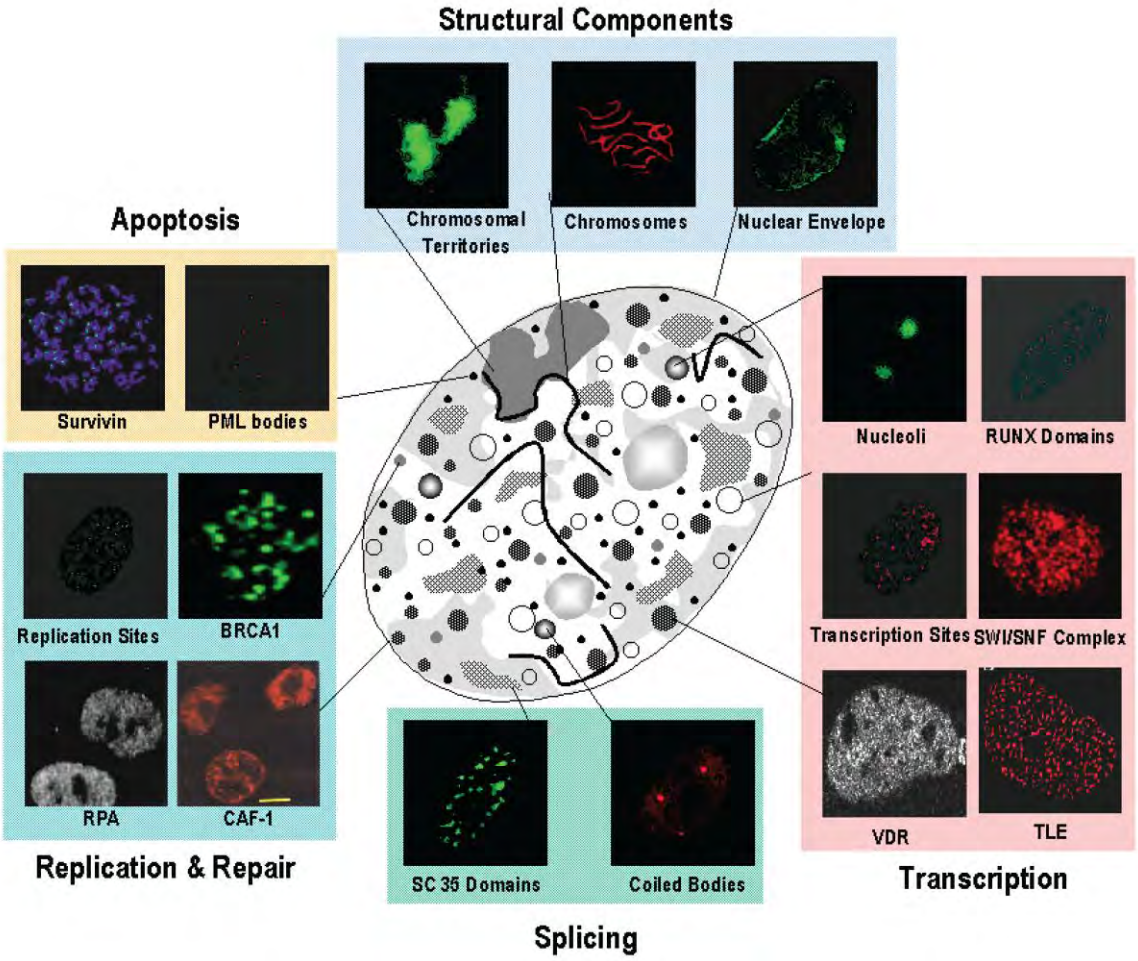

Figure 2: Nuclear architecture functionally links regulatory information.

Nuclear architecture organizes regulatory signals. Immunofluorescence microscopy reveals distinct subnuclear distribution of important processes, including DNA replication and repair, apoptosis, chromatin remodeling, transcriptional control and RNA processing. All of these domains are associated with the nuclear matrix.

Stein et al., *Trends in Cell Biology* 2003; 13(11):584-92

Runx1 in Normal and Malignant Hematopoiesis

Runx1 plays several important roles throughout normal hematopoiesis. It is required for the initial emergence of the hematopoietic stem cell (HSC) from the hemogenic endothelium in the embryo.[10,58,59] Without Runx1 function, embryos die in utero at embryonic day 12.5, from central nervous system hemorrhage and complete lack of definitive hematopoiesis.[10,58,59] In adults, Runx1 is still required for growth control of hematopoietic progenitors and may play a role in maintaining long term repopulation potential.[60-62] In addition to the stem cell, Runx1 is important in regulating the differentiation of many mature blood lineages (Figure 3).[63]

Runx1 contributes to B and T-lymphoid development. Abrogation of Runx1 expression[64-66], or expression of leukemic dominant negative inhibitors of Runx1 function[67], impede B-lymphopoiesis. Runx factors are expressed in developing T-cells[68] and precise control of Runx1 expression is critical for their maturation. Removal of the C-terminal VWRPY domain of Runx1 results in reduced CD8 single positive T-cells.[69] Runx3 mediated downregulation of Runx1 is required T-cell progenitors to mature through CD4/CD8 double negative stages[70] and to silence CD4 to transition from double positive to CD8 single positive cells.[71,72] Thus, Runx1 plays several distinct roles throughout lymphopoiesis.

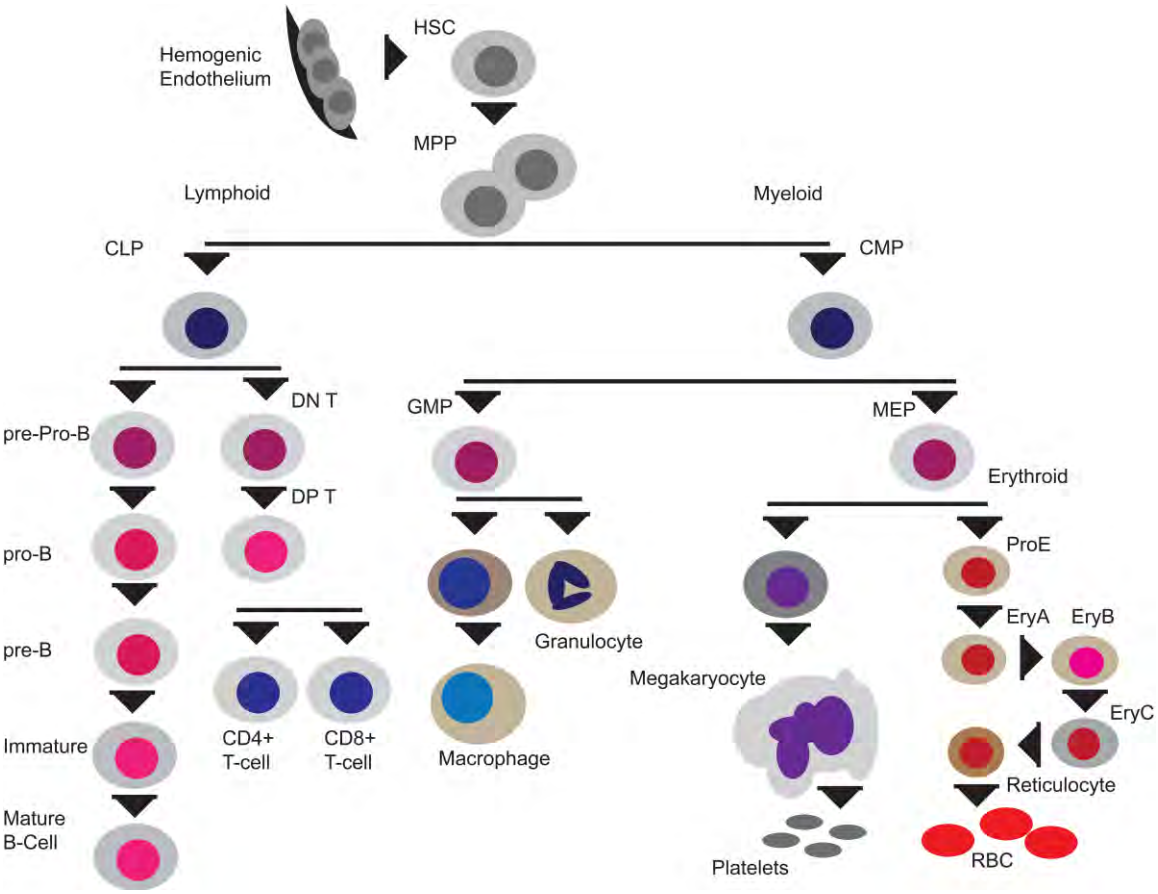

Figure 3: Definitive hematopoiesis.

Runx1 has critical roles in the initial emergence of the hematopoietic stem cell (HSC) from the hemogenic endothelium. In addition, Runx1 is important for differentiation into multi-potent progenitors (MPP), common lymphoid progenitors (CLP), common myeloid progenitors (CMP), and further committed cell types in both lymphoid and myeloid hematopoietic lineages.

Adapted from Larsson and Karlsson, *Oncogene* 2005; 24(37):5676-92

Reproduced with permission

License Number: 2895470995227

Megakaryocyte maturation requires Runx1 function.[66] Runx1 controls expression of the thrombopoietin receptor, and many other genes critical for megakaryocyte development.[73-76] Point mutations in Runx1 are responsible for familial platelet disorders[77,78] and abrogated platelet production is a common finding in animal models with Runx1 mutations.[63,79]

Runx1 is a key factor during myeloid development.[79-81] Runx1 was initially cloned as the target on chromosome 21 of the myeloid leukemic (8;21) translocation.[5] CSF1R, the receptor for myeloid growth factors M-CSF and GM-CSF is one of the most well characterized targets of Runx1 regulation.[82-84] Runx1 also directly regulates the myeloid specific transcription factor PU.1 at the level transcription[85] as well as interaction with co-factors.[86] Disrupting Runx1 function in myeloid cells blocks differentiation and contributes to a transformed phenotype.[87] There is a critical role for Runx1 during myelopoiesis, and disruption of Runx1 function can drive leukemogenesis.

Runx1 and CBFbeta are the most common targets of mutation or translocation in human acute myeloid leukemias (AML).[88,89] The (8;21) translocation is found in 12-15% of de novo adult AML and is a major contribution to secondary AML in patients who received cytotoxic chemotherapy.[88-91] In addition to AML, Runx1 mutations are found in chronic myelomonocytic leukemia (CMML), myeloid dysplastic syndromes (MDS), refractory anemia with excess blasts (RAEB) and familial platelet disorder (FPD) which also have

predisposition toward AML.[77,78,88,92-95] Disruption of Runx1 contributes to many types of hematopoietic disease.

Leukemia associated point mutations of Runx1 are either missense mutations in the DNA-binding RHD, or truncations removing C-terminal domains including the NMTS.[96] RHD mutations cause dominant negative inhibition, or are hypomorphic depending on what degree of DNA-binding is maintained.[97] CBFbeta greatly increases the DNA binding ability of Runx1 and reduction of CBFbeta dosage causes phenotypes similar to Runx1 ablation.[98-101] The C-terminus of Runx1 does not contact DNA or CBFbeta, therefore the disease mechanism of C-terminal mutation must involve functions other than DNA-binding.

The C-terminus of Runx1 contains many known co-factor interaction domains and the NMTS. The (8;21) translocation removes the NMTS and the chimeric fusion protein displays altered subnuclear targeting.[49,51] NMTS mutants of Runx1 within myeloid cell lines disrupt subnuclear localization, alter gene transcription and affect a transformation like phenotype.[87] These data suggest that loss of C-terminal domains of Runx1 in the disease associated mutations and translocations may represent a common disease mechanism. Greater understanding of these functional domains is required to understand how their loss contributes to disease. The following studies examine the functional roles of Runx1 C-terminal domains during normal hematopoiesis and leukemic development.

Expression of Runx1 mutations in hematopoietic cell lines and primary cells in vitro, followed by generation of a knock-in mouse models of Runx1 C-terminal truncation and a Runx1 C-terminal point mutation, revealed the contributions of distinct domains in Runx1 throughout its many roles in hematopoiesis.

Chapter 2: Runx1 C-Terminal Mutants Alter Growth Control and Differentiation in Hematopoietic Cells

Runx1 is a key hematopoietic transcription factor required for definitive hematopoiesis and a frequent target of leukemia-related mutations and chromosomal translocations. Leukemia-associated mutations occur in the DNA-binding domain at the N-terminus, or within C-terminal domains responsible for subnuclear targeting and co-factor interactions. Fusion proteins generated from leukemia-related translocations often retain DNA binding activity, but display loss of subnuclear targeting and associated transactivation functions encoded by the C-terminus of the protein. We purpose that the common loss of Runx1 C-terminal domains observed in these mutants could be a common mechanism of disease progression. To define the precise functions of Runx1 C-terminal domains we developed a panel of mutations and assessed their effects in hematopoietic cells.

Introduction

Runx1 is a master regulator of hematopoiesis, required for the emergence of hematopoietic stem cells (HSC) and appropriate differentiation across hematopoietic lineages.[10,79,80] Runx1 is also a frequent target of for mutation and translocations in leukemia and other hematopoietic disorders.[77,78,92,93,95,102] Mutations observed in patients cluster either in the N-terminal DNA-binding Runt Homology Domain (RHD), or within the C-terminus.[96] Leukemia-associated translocations often retain DNA-binding ability while replacing the C-terminal domains with chimeric fusion protein.[88] The domains disrupted or lost are critical for co-factor interactions and appropriate subnuclear targeting of Runx1.[19-21,25,103] The disease mechanism for DNA-binding mutations is presumably lack of transcription factor binding and therefore lack of gene regulation. For Runx1 C-terminal mutations the biological consequences are not always as straight forward.

Loss of C-terminal functional domains is common among many leukemia-associated Runx1 mutations, therefore we hypothesize that loss of co-factor interaction and aberrant subnuclear targeting may be a common leukemic mechanism. To examine the roles of precise domains within the C-terminus, we developed a panel of Runx1 mutations. Using these mutations in several cellular contexts, we investigated the biological consequences of precise mutations within the C-terminus.

Materials and Methods

Construction of the Runx1 mutant vectors

Wildtype Runx1 in the pcDNA3.1/HISa mammalian expression vector[104] or the pMSCV-IRES-GFP (pMIG) retroviral expression vector[105] was mutated by site directed mutagenesis using a QuikChange Site-Directed Mutagenesis Kit (Stratagene, La Jolla, CA) with the primers shown in Table 1.

Runx1 Mutation	Primers
R174Q	GTGGACGGCCCCCAAGAACCCCGAAGAC
	GTCTTCGGGGTTCTTGGGGGCCGTCCAC
Q307X	CGGCGACCCACGCTAGTTCCCTACTCTG
	CAGAGTAGGGAACTAGCGTGGGTCGCCG
Y352A	TCGCTACCACACCGCCCTGCCGCCGCCC
	GGGCGGCGGCAGGGCGGTGTGGTAGCGA
HTY350-352AAA	GCCTCTCGCTACGCCGCCGCCCTGCCGCCG
	CGGCGGCAGGGCGGCGGCGTAGCGAGAGGC
Y357A	CCTGCCGCCGCCCGCCCCCGGCTCATCA
	TGATGAGCCGGGGGCGGGCGGCGGCAGG

Table 1: Runx1 mutagenesis primers

The forward and reverse primers used to generate the Runx1 mutants in Figure 4 are shown. All primers conformed to the recommended specifications for site directed mutagenesis: 25-45 bases in length, a minimum 40% GC and melting point above 78ºC.

Luciferase assays

HeLa cells were transfected with Fugene 6 (Roche) following manufacturer's instructions. Cells were plated at 200,000 cells per well of a 6-well plate, and 3 wells for each construct was transfected with 500 ng of GM-CSF promoter luciferase reporter (pGL3)[103]; 200 ng of pcDNA3.1/HISa (Invitrogen) empty vector, Runx1 wildtype, Runx1^{Q307X} , Runx1^{Y352A}, Runx1$^{HTY350-352AAA}$ or Runx1^{Y357A}; and 5 ng pHRL-null promoter-less Renilla luciferase.[106] Luciferase activity was measured 24 hours after transfection using the Dual-Luciferase Reporter Assay System (Promega, Madison, WI Cat. No. E1960) in a Glomax Luminometer (Promega) with Glomax 1.6 software.

IVTT protein expression

In vitro transcription and translation (IVTT) of Runx1 wildtype, Runx1^{R174Q}, Runx1^{Y352A}, Runx1$^{HTY350-352AAA}$, Runx1^{Y357A} and Runx1^{Q307X} was performed using the TNT Coupled Reticulocyte Lysate System (Promega) following the manufacturer's instructions. Successful IVTT reactions were tested by Western blot. 2 uL of IVTT lysate was diluted into 30 uL direct lysis buffer (2% SDS, 2 M urea, 10% glycerol, 10 mM Tris-HCl [pH 6.8], 0.002% bromophenol blue, 10 mM DTT, 1× Complete protease inhibitor [Roche], 25 uM MG132 and 1 mM PMSF) and boiled for 5 min. The entire volume was electrophoresed in an 8% SDS-polyacrylamide gel, at 100V for 1.5 hours. Separated proteins were transferred to an Immobilon Membrane (Millipore, Billerica, MA) by semidry transfer for 30min at 10V. Membranes were blocked for at least 1 hour in 5%

nonfat dry milk in PBST (PBS with 0.1% Tween 20) and then probed for 1 hour with primary antibody diluted 1:1000 (AML1(RHD) [Oncogene Science]). After four 5 min washes with PBST, blots were incubated for 1 hour with goat anti-rabbit IgG-HRP secondary antibody diluted 1:4000, washed four times for 5 min in PBST and detected with ECL (Perkin-Elmer, Waltham, MA).

Electrophoretic Mobility Shift Assay (EMSA)

Runx consensus oligonucleotide 5'-CGA GTA TTG TGG TTA ATA CG-3' was end labeled as described previously.[107,108] Upper strands of the oligonucleotides were labeled with ^{32}P for 1 hour at 37°C in a 50 uL volume using T4 Polynucleotide Kinase (New England BioLabs, Beverly, MA) following manufacturer's instructions. The reaction was stopped by heat inactivation at 65°C for 1 hour. Annealing was performed by addition of a twofold excess amount of bottom strand followed by boiling for 5 min and slow cooling to room temperature. Unincorporated nucleotides were removed with a quick-spin G 25 Sephadex column (Roche Molecular Biochemicals, Indianapolis, IN) according to the manufacturer's instructions. 2 uL of IVTT lysate for Runx1 wildtype, $Runx1^{R174Q}$, $Runx1^{Y352A}$, $Runx1^{HTY350\text{-}352AAA}$, $Runx1^{Y357A}$ or $Runx1^{Q307X}$ were used in the binding reaction. Reaction mixtures were prepared using 50 fmol of probe, 50 mM KCl, 1 mM magnesium chloride, 1 mM DTT, 2 mM sodium fluoride, 2 mM sodium vanadate, 10% glycerol, 2 ug of poly(dI-dC)•poly(dI-dC), and DNA binding reactions were carried out

at 25˚C for 20 min. Aliquots were separated in a 4% nondenaturing polyacrylamide gel for 1.5 hours at 200 V. The gel was dried and subjected to autoradiography.

Generation and concentration of retrovirus

The Phoenix retrovirus expression system (Orbigen, San Diego, CA Cat. No. RVK-10001) was used to generate retroviruses for expression of the Runx1 mutant panel per manufacturer's instructions. Phoenix eco cells (a proprietary 293T derivative grown in DMEM with 10% FBS) were co-transfected with 5 ug pMIG plasmid and 2.5 ug φeco plasmid using Superfect (Qiagen). After 24 and 48 hours the media was replaced. Media containing retroviruses was collected and then replaced the 3rd, 4th and 5th days after transduction, as we determined those time points provided the most infectious virus. Collected virus containing media was spun at 25000 rpm for 3 hours and then resuspended in one fifth the original volume to concentrate the virus for better infection.

Transduction of bone marrow cells

Bone marrow cells were isolated by washing the marrow space of femurs and tibiae of 8-12 week old donor mice. 200,000 cells were resuspended in 1 mL of complete media (RPMI with 20% FBS, 6 ng/mL IL-3, 10 ng/mL IL-6, and 10 ng/mL SCF). 1 mL of concentrated virus was added and cells were spun at 2400 rpm for 90 min at 30ºC. Following the spin, cells were incubated at 37ºC for 3 hours before resuspension in fresh

complete media. This infection was repeated then next day. 24 hours after the second infection cells were taken to the University of Massachusetts flow cytometry core facility and sorted for GFP expression.

Colony Forming Unit (CFU) assays

GFP positive transduced bone marrow cells (10,000) were resuspended in Iscove's Modified Dulbecco's Medium (IMDM) without serum, and plated in duplicate (2000 cells per plate) in 35-mm dishes containing Methocult methyl cellulose medium (StemCell Technologies Vancouver, BC, Canada Cat. No. M3434) for CFU assay per the manufacturer's instructions. Colonies were counted by visual inspection after 7 days of incubation at 37°C.

Microarray and qRT-PCR

RNA was prepared from 1 million of the stably transduced 32D cells using TRIzol following the manufacturer's protocol (Invitrogen). For microarray analysis, total RNA was processed by the University of Massachusetts Genomics Core Facility and run on Affymetrix MouseGene 1.0 ST arrays. GeneSpring software (Agilent Technologies) was used to determine which genes had expression changes of at least 1.5 fold, and that gene list was further analyzed using the Database for Annotation, Visualization and Integrated Discovery (DAVID)[30] software suite for gene ontology and promoter motif analysis.

RNA samples for microarray confirmation were treated with DNaseI and 1 ug was subjected to reverse transcription with oligo dT primers. Quantitative PCR was performed on the resulting cDNA using the primers in Table 2.

Gene	qRT-PCR Primer	
Fcgr3	CAGAATGCACACTCTGGAAGC	forward
	GGGTCCCTTCGCACATCAG	reverse
H2-Ea	AAGTCATGGGCTATCAAAGAGGA	forward
	CTCATCGCCGTCAAAGTCAAA	reverse
C3	CCAGCTCCCCATTAGCTCTG	forward
	GCACTTGCCTCTTTAGGAAGTC	reverse
S100a8	AAATCACCATGCCCTCTACAAG	forward
	CCCACTTTTATCACCATCGCAA	reverse
S100a9	ATACTCTAGGAAGGAAGGACACC	forward
	TCCATGATGTCATTTATGAGGGC	reverse
Clec4e	AGTGCTCTCCTGGACGATAG	forward
	CCTGATGCCTCACTGTAGCAG	reverse
mCox	ACGAAATCAACAACCCCGTA	forward
	GGCAGAACGACTCGGTTATC	reverse

Table 2: qRT-PCR primers to confirm microarray data in 32D stable cell lines

Results

Runx1 C-terminal mutations in DNA binding and target activation

In order to study contributions of precise domains within Runx1, we used site-directed mutagenesis to generate a panel of Runx1 mutations (Figure 4). Luciferase assays using HeLa cells transfected with the Runx1 C-terminal mutations showed that the truncation and subnuclear targeting mutants failed to activate the GM-CSF promoter to the same extent as wildtype Runx1 (Figure 5; p=0.012, 0.037 and 0.11 for $Runx1^{Q307X}$, $Runx1^{Y352A}$ and $Runx1^{HTY350\text{-}352AAA}$, respectively). The PPXY domain mutant $Runx1^{Y357A}$ did not reduce activation of the GM-CSF promoter (Figure 5). DNA binding ability was retained in all of the C-terminal mutations, indicating a different mechanism for the deregulation of the GM-CSF promoter (Figure 6).

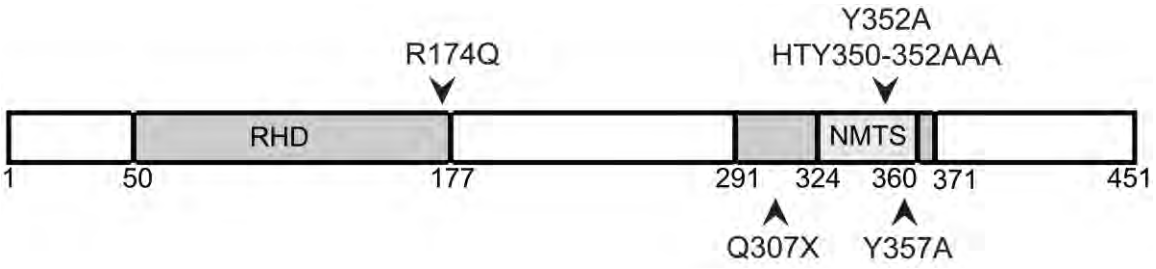

Figure 4: Panel of Runx1 mutations to investigate C-terminal domains

Site directed mutagenesis was used (Table 1) to generate a panel of Runx1 mutants to model: loss of DNA binding (R174Q), C-terminal truncation (Q307X), aberrant subnuclear targeting (Y352A), aberrant subnuclear targeting and loss of co-factor interactions (HTY350-352AAA), and loss of PPXY motif.

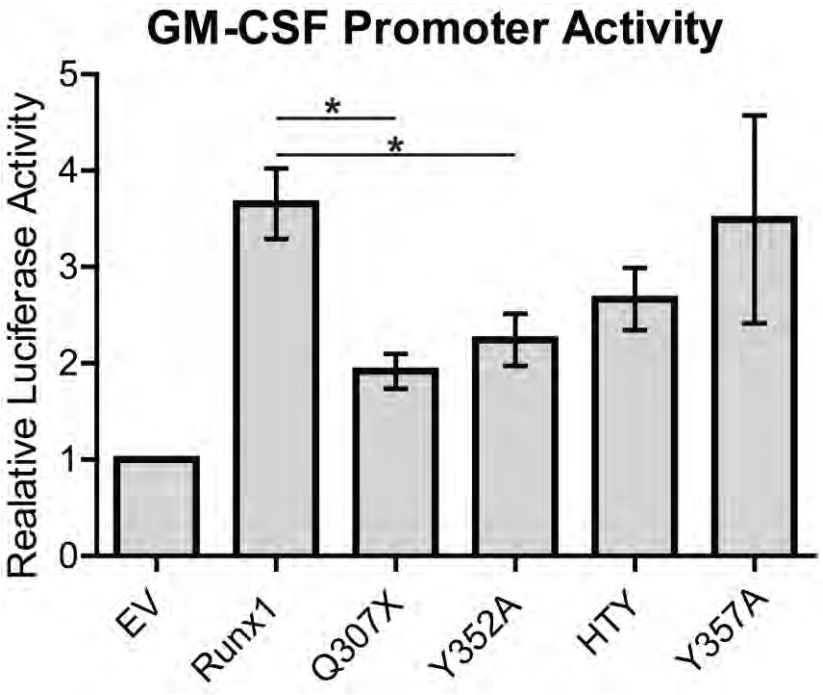

Figure 5: Runx1 C-terminal mutants and promoter activation

HeLa cells were co-transfected with empty vector (EV), wildtype, or mutant Runx1 and a luciferase construct driven by the GM-CSF promoter. Plotted is the relative luciferase activity using renilla as a background control and normalizing to empty vector (n=3 transfections for each construct). *$p<0.05$, calculated by Student's T test.

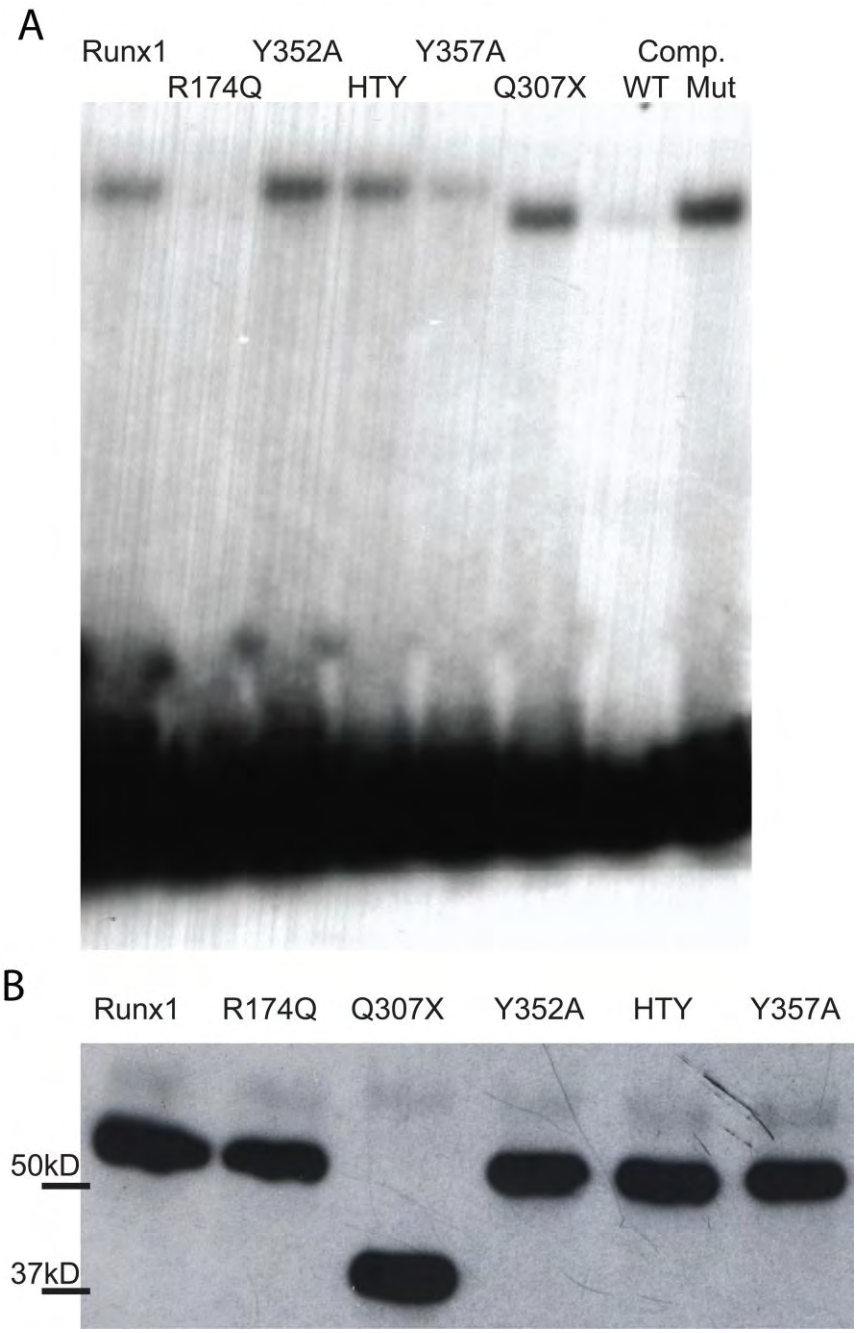

Figure 6: DNA binding is retained in Runx1 C-terminal mutants

(A) IVTT generated wildtype and mutant Runx1 in Electrophoretic Mobility Shift Assay (EMSA) using the Runx consensus oligonucleotide 5'-CGA GTA TTG TGG TTA ATA CG-3'. The rightmost lanes show Q307X with the addition of cold wildtype (WT) or mutant (Mut) competitor oligo. Free probe is visible at the bottom of the gel. (B) Western blot using anti-flag antibody with 2 uL of the IVTT generated lysate as in A.

Transduction of primary cells with Runx1 C-terminal mutations

After establishing DNA binding and promoter activation of the Runx1 mutations in HeLa cells, we transitioned into hematopoietic cells for further experiments. Hematopoietic cells are difficult to transfect, so we used site directed mutagenesis to develop the same panel of mutations in a retroviral expression vector that included an IRES-GFP, pMIG.[105] This vector allowed purification of even a very small percentage of transduced cells by flow cytometry for GFP expression (Figure 7).

Primary bone marrow cells were transduced with the panel of Runx1 mutants and GFP+ cells were sorted for colony forming unit (CFU) assays (Figure 8). Runx1 is known to have a growth suppressive role in hematopoietic progenitors[61,62,109] and overexpression of full length Runx1 suppressed CFU ability of bone marrow cells. Overexpression of empty vector, the DNA-binding mutant (R174Q) or C-terminal truncation (Q307X) had significantly more CFU, suggesting that loss of DNA binding or the C-terminus both result in a non-functional protein. Interestingly, overexpression of the Runx1 C-terminal point mutations had similar CFU to wildtype, indicating that those precise domains are not required for growth suppression.

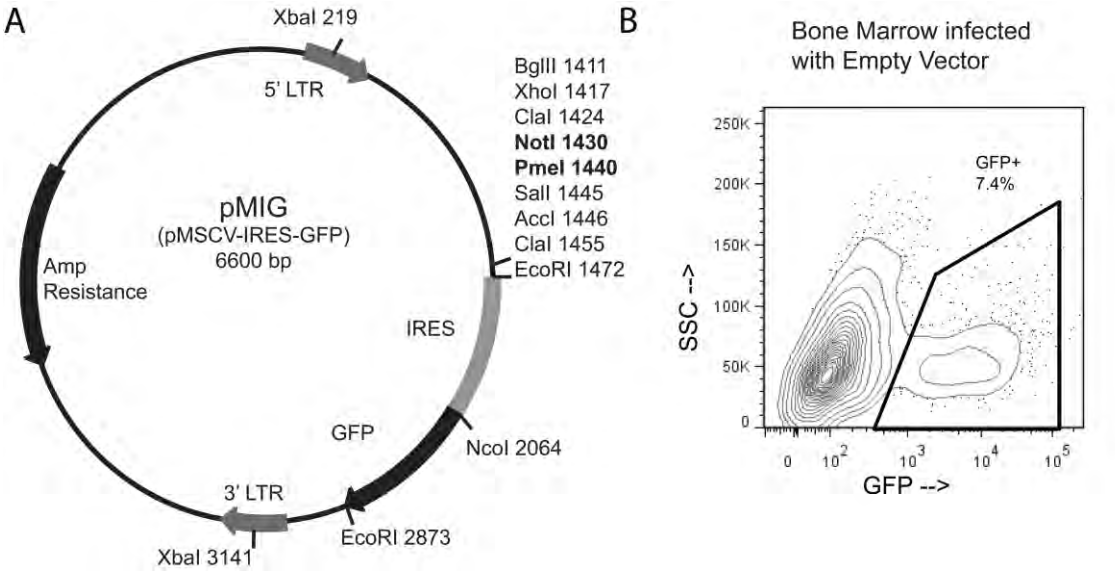

Figure 7: Retroviral constructs allow purification of low yield transduction

(A) The retroviral vector pMIG was used to create a panel of mutants for transduction of hematopoietic cells. Runx1 was cloned between bolded NotI and PmeI restriction sites, and mutations were made from the wildtype plasmid via site directed mutagenesis (Table 1). (B) With the IRES GFP, very low transduction yields could be purified by flow cytometry. Shown is a representative sort of empty vector infected cells.

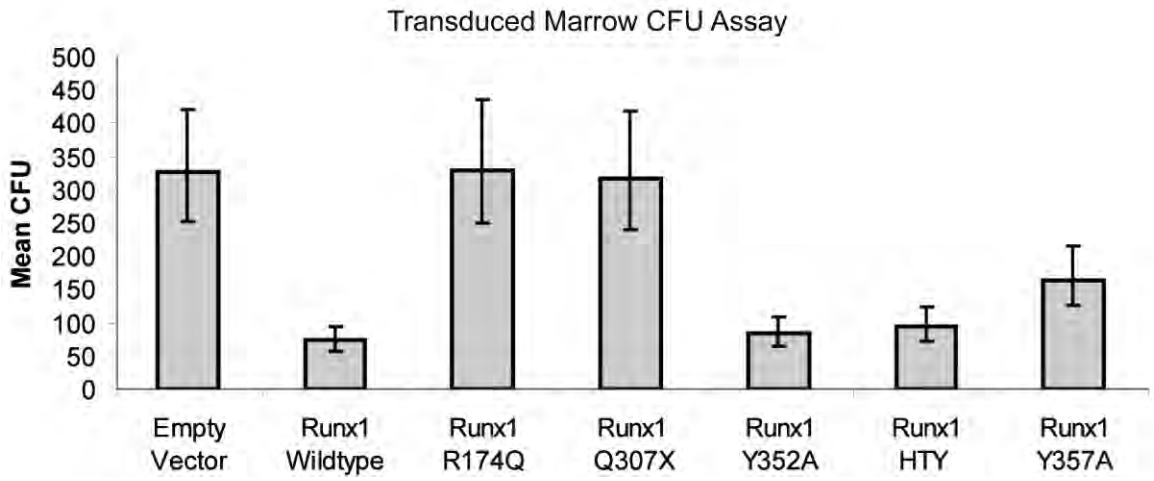

Figure 8: Bone marrow CFU assays with Runx1 C-terminal mutants

Bone marrow cells were retro-virally transduced with empty vector, Runx1 wildtype, Runx1^{R174Q}, Runx1^{Q307X}, Runx1^{Y352A}, Runx1$^{HTY350\text{-}352AAA}$ or Runx1^{Y357A}, sorted for GFP expression and then GFP+ cells (2,000 per plate) were plated in colony forming unit (CFU) assays. The DNA binding mutation and C-terminal truncation had similar colonies to empty vector. Wildtype Runx1 , Runx1^{Y352A}, Runx1$^{HTY350\text{-}352AAA}$ and Runx1^{Y357A} all significantly inhibited colony formation ($p<0.05$, n=6 to 10). Error bars are SEM.

Stable cell lines with Runx1 subnuclear targeting mutant

Our lab previously developed stable cell lines transduced with empty vector, wildtype Runx1 and a subnuclear targeting defective mutant (mSTD) Runx1 in 32D cells.[87] The mSTD mutation is in the human Runx1 cDNA with a point mutation causing Y380A, equivalent to Y352A mutant in the mouse transcript (Figure 4). 32D murine myeloid progenitor cells are IL-3 dependent, and can be forced to differentiate by replacement of IL-3 with GM-CSF in the growth media. We performed CFU assays with these stable cells lines under normal growth and differentiation conditions (Figure 9). Under normal growth conditions, overexpression of both wildtype Runx1 and mSTD Runx1 suppressed colony formation, similar to the results observed in bone marrow cells. After 12 days in differentiation media, empty vector and Runx1 overexpressing cells had differentiated and lost most of their colony forming ability. In contrast, mSTD Runx1 expression caused a differentiation block[87] and those cells maintained colony forming ability. These results highlight the importance of cellular context on Runx1 activity and differences in the effect of Runx1 mutations in progenitor cells versus their further differentiated progeny.

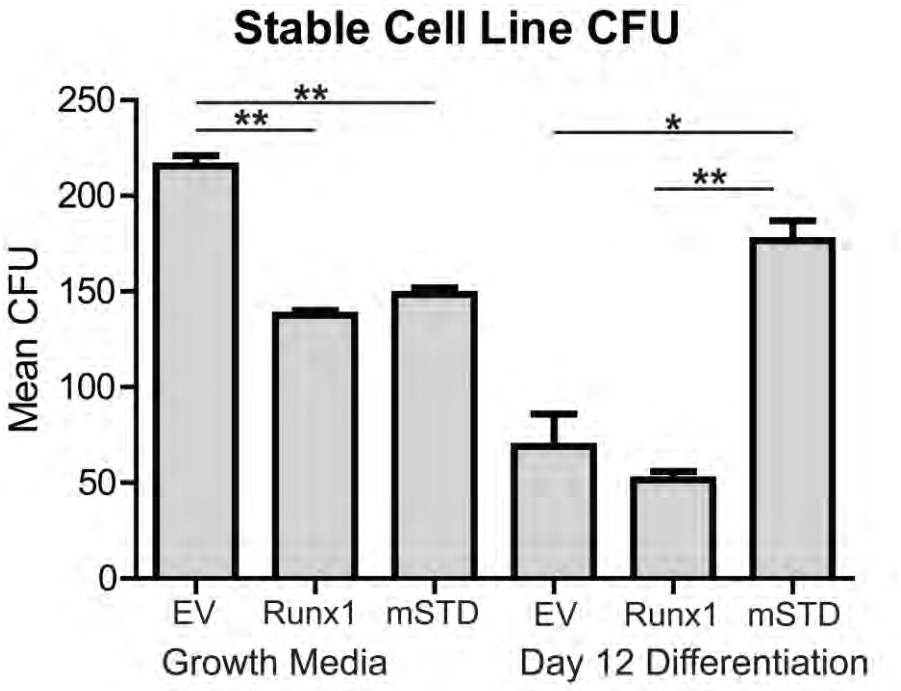

Figure 9: Stable 32D cell line CFU assays

32D stable cell lines overexpressing empty vector, wildtype Runx1 or subnuclear targeting defective mutant Runx1 (mSTD) were plated in CFU assays from growth media, or after 12 days in differentiation medium (n=2 each). Error bars are SEM. * $p<0.05$, ** $p<0.01$, calculated with Student's T test.

Previous characterization of the 32D stable cell lines found deregulation of many myeloid genes.[87] We examined global gene expression of the 32D stable cell lines under normal growth conditions with microarray analysis. Gene expression in wildtype Runx1 overexpressing cells was compared to mSTD overexpressing cells. Four samples were prepared for each cell line. Three were used as replicates in the microarray analysis (Table 3) while the fourth was used to confirm altered gene expression by qRT-PCR (Figure 10). Functional annotation clustering revealed enrichment of several gene ontology terms (Table 4). The terms for deregulated genes correlate with the differentiation block observed in these cells, as they are involved with immune response or important functions of mature monocytes / macrophages. Promoter analysis of genes deregulated in the progenitor cells harboring subnuclear targeting defective Runx1 revealed the predominant DNA binding motifs were not the canonical Runx motif, but motifs of known Runx1 co-factors PU.1, CEBPβ, CEBPα, and ETS1 (Figure 11). Enrichment of co-factor binding motifs indicates a non-DNA binding mediated role for mSTD Runx1 is driving these expression changes, and support the importance of Runx1 scaffolding functions during gene regulation.

Mean Ratio	NCBI Transcript Number	Gene Symbol		Mean Ratio	NCBI Transcript Number	Gene Symbol
Genes down in mutant at least 0.7 fold				Genes up in mutant at least 1.5 fold		
0.348	NM_011346	Sell		2.891	NM_177368	Tmtc2
0.357	NM_010188	Fcgr3		1.901	NM_030174	Mctp1
0.317	NM_017372	Lyz2		2.207	NM_025943	Dzip1
0.232	NM_001033245	Hk3		4.335	NM_010671	Krtap13
0.320	NM_177594	Mtmr9		2.100	NM_010676	Krtap8-2
0.242	NM_010930	Nov		2.653	NM_023326	Bmyc
0.379	NM_173869	Stfa2l1		1.888	NM_008969	Ptgs1
0.370	NM_001082546	BC100530		1.720	NM_011309	S100a1
0.378	NM_031198	Tcfec		2.016	NM_007899	Ecm1
0.275	NM_010640	Klk1b11		2.250	NM_175035	Gimap5
0.247	NM_001033632	Ifitm6		2.163	NM_008486	Anpep
0.542	NM_009230	Soats1		2.223	NM_001024617	Inpp4b
0.531	NM_001077189	Fcgr2b		2.114	NM_008823	Cfp
0.379	NM_011337	Ccl3				
0.546	NM_007800	Ctsg				
0.533	NM_009155	Sepp1				
0.528	NM_030720	Gpr84				
0.422	NM_001082545	Stfa2l1				
0.422	NM_010381	H2-Ea				
0.475	NM_009638	Crisp1				
0.623	NM_009778	C3				
0.519	NM_001080944	Atp8b4				
0.505	NM_177260	Tmem154				
0.529	NM_011313	S100a6				
0.363	NM_013650	S100a8				
0.368	NM_009114	S100a9				
0.499	NM_011612	Tnfrsf9				
0.573	NM_013706	Cd52				
0.686	NM_207237	Man1c1				
0.353	NM_023785	Ppbp				
0.639	NM_013470	Anxa3				
0.535	NM_177686	Clec12a				
0.488	NM_001038604	Clec5a				
0.579	NM_019948	Clec4e				
0.502	NM_001082960	Itgam				
0.366	NM_001024703	Mctp2				
0.459	NM_001001559	Dub2a				
0.481	NM_030691	Igsf6				
0.519	NM_027870	Armcx3				
0.550	NM_008694	Ngp				
0.481	NM_009916	Ccr4				

Table 3: Gene list from microarray data

The mean ratio of expression change shown by microarray analysis was calculated using 32D cells stably expressing wildtype versus mSTD Runx1 with GeneSpring software (n=3 of each). Listed are transcripts of known genes that reached the threshold of either expression 0.7 fold lower or 1.5 fold higher in mSTD expressing cells.

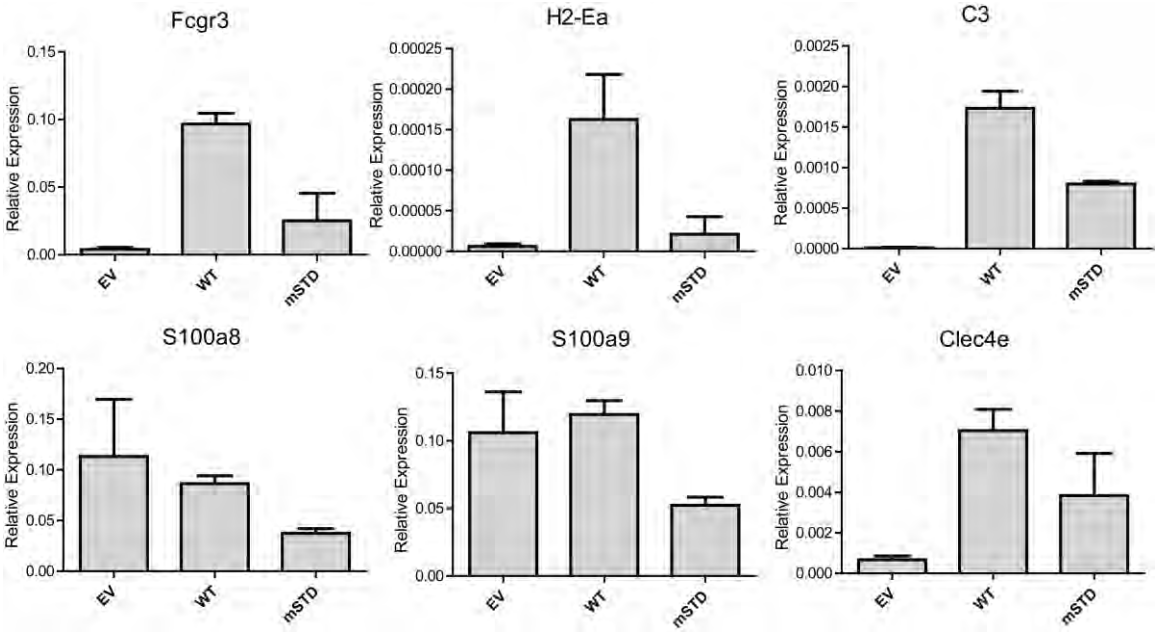

Figure 10: qRT-PCR of 32D stable lines confirms microarray data

Global gene expression of 32D stable cell lines with empty vector (EV), wildtype Runx1 (WT) or subnuclear targeting defective mutant Runx1 (mSTD) was analyzed by microarray analysis (n=3). Altered expression levels of several genes was confirmed by qRT-PCR using an independent sample of each cell line. Relative expression levels shown are normalized to mCox. Mean relative expression is plotted, with error bars showing the range between 2 technical replicates.

Gene Ontology Term	p value	Gene Symbols
Leukocyte chemotaxis and migration	0.00217	S100a9, Itgam, Fcgr3
Cell migration and motility	0.02350	S100a9, Itgam, Ccr4, Fcgr3
Addaptive immune response	0.00056	H2-Ea, C3, Fcgr3, Fcgr2b
Inflammatory response and phagocytosis	0.00096	C3, Fcgr3, Fcgr2b
Positive regulation of immune response	0.00508	H2-Ea, C3, Cfp, Fcgr3
C-type lectin	0.00498	Clec4e, Sell, Clec5a, Clec12a
Antigen processing and presentation	0.00158	H2-Ea, Fcgr3, Fcgr2b
Cystatin protease inhibitors	0.00007	Stfa2, Stfa2la1, Stfa1, Ngp
Calcium binding	0.00001	S100a9, S100a8, S100a6, S100a1

Table 4: Gene Ontology from 32D stable cell microarrays

Gene Ontology terms for the most highly enriched gene clusters comparing stably overexpressing wildtype Runx1 versus mSTD Runx1 (n=3). Genes with a mean difference in expression of at least 1.5 fold were used in the analysis. Shown are the term for a cluster, the calculated Fisher exact p value, and the gene symbols within that cluster. Clustering performed with DAVID bioinformatics resources.[30]

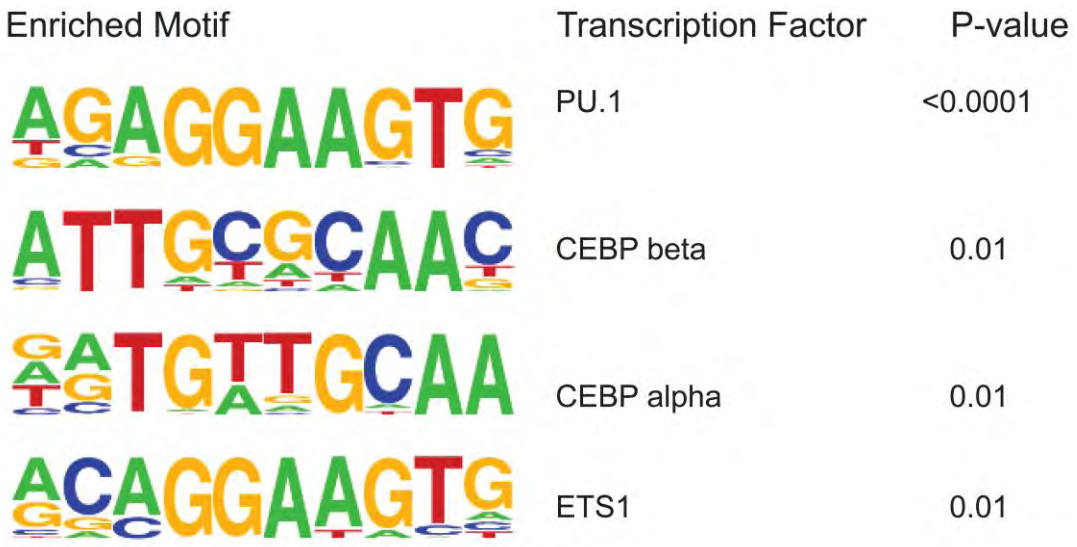

Figure 11: Motif analysis of deregulated genes in 32D stable cell lines

DAVID motif analysis of the deregulated genes in 32D cells overexpressing mSTD Runx1. The enriched motif, transcription factor predicted to bind that motif and p value for the enrichment are shown. P values calculated using Benjamini-Hochberg correction for false discovery rate.

Discussion

Runx1 is a frequent target for mutation and translocation in hematopoietic disease.[77,78,92,93,95,102] The mutations that retain DNA-binding ability lose C-terminal domains[88,96] critical for co-factor interactions and subnuclear targeting.[19-21,25,103] Loss of Runx1 C-terminal domains represents a potential common leukemic mechanism. Therefore, we developed a panel of Runx1 C-terminal mutations to examine the roles of these lost domains in vitro.

Runx factors can suppress cell growth and proliferation.[27,109-113] Within hematopoiesis, this function of Runx1 is highly context dependent[114,115], and so are the consequences of mutations within C-terminal domains. Overexpressed in primary cells, or in a stable cell line, subnuclear targeting defective mutants behave in the same way as wildtype Runx1 in colony forming assays. However, if the cells are pushed toward differentiation the difference between wildtype and mSTD Runx1 are dramatic. Even with the same assay and in the same cells, the effects of altering Runx1 subnuclear targeting differ in the presence of differentiation promoting growth factors. This supports Runx1 relaying external signals while organizing regulatory machinery[26] and connects subnuclear targeting with an additional layer of regulatory control.

While mutations in the C-terminus of Runx1 do not interfere with DNA-binding, they do alter promoter activation. Our group has previously reported that stable overexpression of

mSTD Runx1 blocks differentiation.[87] Examination of global gene expression in these cells before they were given any differentiation signal revealed that deregulation of genes important for monocyte/macrophage cell function was already underway. Importantly, the genes deregulated by mSTD Runx1 did not require Runx1 binding in their promoters. Instead the promoters of deregulated genes were enriched for the binding motifs of several known Runx1 co-factors. Known protein-protein interaction domains for the enriched co-factors are N-terminal to the NMTS and therefore direct interactions should have been maintained.[116-118] These data provide strong evidence for Runx1 scaffolding co-factors and DNA as part of complex regulatory networks.

The context dependent nature of normal Runx1 function during hematopoiesis and of the C-terminal Runx1 mutations supports study of these mutants at endogenous levels in vivo. A point mutation disrupting subnuclear targeting has profound effects on a myeloid progenitor cell line, but additional consequences in other hematopoietic lineages are likely. Runx1 is important during differentiation of many hematopoietic lineages[64,66,75,80,119] and additional non-hematopoietic roles of Runx1 in the hair follicle[120-122] or bone development[123,124] could also be affected. Taken together, these in vitro data on the effects of C-terminal Runx1 mutations support the concept of transcription factors scaffolding regulatory machinery within subnuclear domains and warrant further investigation at endogenous expression levels in vivo.

Chapter 3: Definitive Hematopoiesis Requires Runx1 C-Terminal-Mediated Subnuclear Targeting and Transactivation

Runx1 is a key hematopoietic transcription factor required for definitive hematopoiesis and is a frequent target of leukemia-related chromosomal translocations. The resulting fusion proteins, while retaining DNA binding activity, display loss of subnuclear targeting and associated transactivation functions encoded by the C-terminus of the protein. To define the precise contribution of the Runx1 C-terminus in development and leukemia, we created a knock-in mouse with a C-terminal truncation by introducing a single nucleic acid substitution in the native Runx1 locus. This mutation ($Runx1^{Q307X}$) models genetic lesions observed in patients with leukemia and myeloproliferative disorders. The $Runx1^{Q307X}$ homozygous mouse exhibits embryonic lethality at E12.5 due to central nervous system hemorrhage and a complete lack of hematopoietic stem cell function. While able to bind DNA, $Runx1^{Q307X}$ is unable to activate target genes, resulting in deregulation of various hematopoietic markers. Thus, we demonstrate that the subnuclear targeting and transcriptional regulatory activities of the Runx1 C-terminus are critical for hematopoietic development. We propose that compromising the C-terminal functions of Runx1 is a common disease mechanism for somatic mutations and leukemic fusion proteins observed in human patients.

Introduction

Runx1 is required for the emergence[10,59] and possibly the maintenance[60-62] of hematopoietic stem cells (HSCs) and is important throughout definitive hematopoiesis.[79,125] Runx1 is also frequently mutated in hematological disorders and malignancy. Point mutations and translocations of Runx1 are associated with acute myeloid leukemia (AML), chronic myelomonocytic leukemia (CMML), myeloid dysplastic syndromes (MDS), refractory anemia with excess blasts (RAEB) and familial platelet disorder (FPD) which also has a predisposition toward AML.[77,78,88,92-94] Somatic mutations observed in patients cluster either in the N-terminal DNA-binding Runt Homology Domain (RHD) or within the C-terminus.[96] Runx1 mutations in the C-terminus of CMML patients have been shown to predict transformation to AML.[92] The domains disrupted by the C-terminal mutations are critical for many protein-protein interactions[18-21] and for appropriate subnuclear targeting of Runx1.[25,49,51,87] Consequently, cells harboring these mutations exhibit deregulation of Runx1 target genes.[87] Loss of C-terminal residues critical for subnuclear targeting enhances proliferation of myeloid progenitor cells concomitant with a differentiation block, affecting a transformed phenotype.[87,103] This is reminiscent of the effects of various chromosomal translocations that retain the RHD of Runx1 but replace the C-terminus with segments of other proteins, generating leukemic fusion proteins such as Runx1/ETO, Runx1/Evi1 and Runx1/MDS. The chimeric fusion proteins retain DNA binding ability, but lose co-factor interactions important for gene regulation. These results strongly suggest a role of the Runx1 C-terminus and associated functions in the biology of hematopoiesis and leukemogenesis.

To directly examine the biological relevance of the Runx1 C-terminus in vivo, we introduced a premature translational stop codon after amino acid 307, mimicking Runx1 mutations identified in human MDS/AML and CMML patients (Figure 12) and observed to cause MDS/AML in mouse bone marrow transfer models.[92,96,126,127] The truncated Runx1, Runx1^{Q307X}, lacks the transactivation domain and nuclear matrix targeting signal (NMTS) but retains sequences for the entire endogenous Runx1 mRNA, in contrast to a previous mouse model that replaced a portion of the mRNA with bacterial LacZ sequences.[58] Retaining the full endogenous mRNA avoided interfering with any small RNA mediated regulation. In this study, Runx1^{Q307X} homozygous mice die at embryonic day 12.5 (E12.5) from central nervous system hemorrhages and a lack of HSC function. These results phenocopy the complete DNA binding knockout.[10] We also show deregulation of genes important for hematopoiesis and HSC function in E12.5 Runx1^{Q307X} homozygous embryos. Our results demonstrate that the transactivation and subnuclear targeting domains lost in Runx1^{Q307X} are essential for Runx1 function during development.

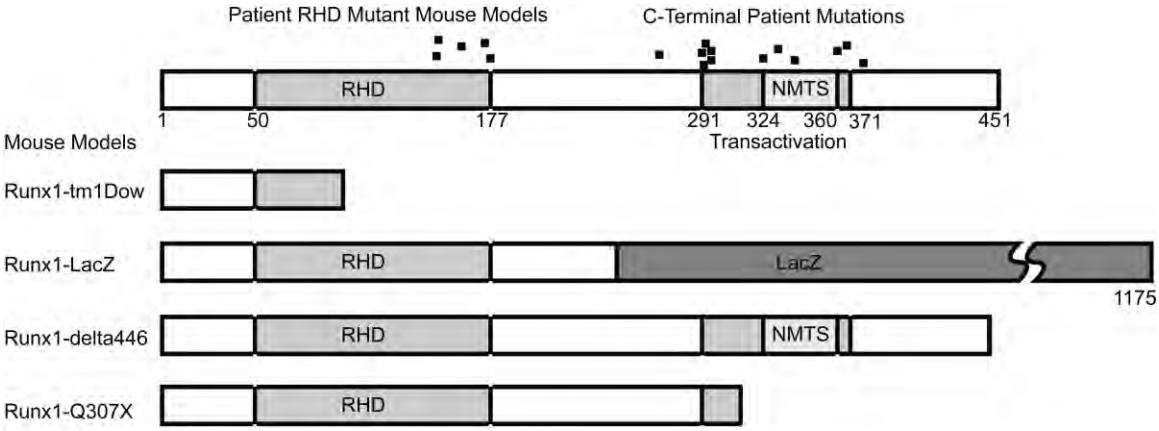

Patient Category	Mutation	Reference
Sporadic MDS, followed by AML	Ser291fsTer300	Harada et al., 2004
Sporadic MDS, followed by AML	Arg292fsTer574	Harada et al., 2004
Sporadic MDS, RAEB in transformation	Thr296fsTer305	Harada et al., 2004
Sporadic MDS, RAEB	Thr296fsTer338	Harada et al., 2004
Sporadic MDS, RAEB	Ala364fsTer570	Harada et al., 2004
Secondary MDS, RAEB in transformation	Leu378fsTer573	Harada et al., 2004
CMML	Ser268fsX578	Kuo et al., 2009
CMML	Arg293X	Kuo et al., 2009
CMML	Gly324fsX565	Kuo et al., 2009
CMML	Pro332fsX573	Kuo et al., 2009
CMML	Met341fsX569	Kuo et al., 2009
CMML	Phe369fsX572	Kuo et al., 2009
Mouse Models	**Mutation**	**Reference**
$Runx1^{tm1Dow}$	Original RHD knockout	Okuda et al., 1996
$Runx1^{tm4Spe}$	Patient RHD mutation: T149A	Matheny et al., 2007
$Runx1^{tm5Spe}$	Patient RHD mutation: R174Q	Matheny et al., 2007
$Runx1^{tm6Spe}$	Patient RHD mutation: L148F	Matheny et al., 2007
$Runx1^{tm7Spe}$	Patient RHD mutation: R177X	Matheny et al., 2007
$Runx1^{tm8Spe}$	Patient RHD mutation: T161A	Matheny et al., 2007
$Runx1^{LacZ}$	Replace exons 7 and 8 with LacZ	Wang, et al., 1996
$Runx1^{delta446}$	Delete final 5 amino acids VWRPY	Nishimura et al., 2004
$Runx1^{Q307X}$	Stop codon in exon 8	This study

Figure 12: Runx1 patient mutations and mouse models.

Diagram of Runx1 with regions of interest highlighted. $Runx1^{Q307X}$ was designed to model several human mutations observed in MDS, AML, RAEB and CMML. Also illustrated are the first RHD knock out mouse, existing mouse models bearing patient mutations in the RHD and previous models with mutations in the Runx1 C-terminus. Runx1-LacZ is broken to illustrate the full length of the chimeric fusion protein.

Materials and Methods

Immunofluorescence microscopy

HeLa cervical carcinoma cells were grown on cover slips coated with 0.05% gelatin and transfected with Fugene 6 (Roche Diagnostics, Indianapolis, IN) following manufacturer's instructions. After 24 hours cells were fixed using formaldehyde (3.7%), and permeabilized with 0.5% Triton X-100 for whole-cell preparations. Nuclear matrix-intermediate filament preparations were obtained as described.[36] Soluble proteins were extracted with cytoskeletal buffer (CSK; 10 mM Pipes, pH 6.8/300 mM sucrose/100 mM NaCl/3 mM MgCl2/1 mM EGTA/20 mM vanadyl riboside complex/1 mM 4-(2-aminoethyl)benzenesulfonyl fluoride) containing 0.5% Triton X-100 for 5 min on ice. After washing in CSK, DNA and associated proteins were removed by digestion with 400 units/mL DNase I for 50 min at 30°C in digestion buffer (10 mM Pipes, pH 6.8/300 mM sucrose/50 mM NaCl/3 mM MgCl2/1 mM EGTA/20 mM vanadyl riboside complex/1 mM 4-(2-aminoethyl)benzenesulfonyl fluoride). A final wash with 0.25 M ammonium sulfate extraction buffer (10 mM Pipes, pH 6.8/250 mM ammonium sulfate/300 mM sucrose/3 mM MgCl2/1 mM EGTA/20 mM vanadyl riboside complex, 1 mM 4-(2-aminoethyl)benzenesulfonyl fluoride) removed remaining cut DNA. Digestion was confirmed by DAPI staining. Runx1 protein was detected by the AML1(RHD) antibody (Oncogene Science, Cambridge, MA; 1:200 dilution) followed by fluorochrome-conjugated Alexa Fluor 488 secondary antibody (Invitrogen Molecular Probes, Eugene, OR; 1:800 dilution). Cells were mounted in Prolong Gold antifade mounting medium (Invitrogen Molecular Probes). Fluorescence and transmitted light images were captured

using a Zeiss Axioplan 2 microscope equipped with a digital charged-coupled device camera (Hamamatsu Photonics, Bridgewater, NJ Cat. No. C4742-95) interfaced with the MetaMorph Imaging System (Universal Imaging Corporation Ltd, Marlow, Buckinghamshire, UK).

Luciferase assays

K562 erythroleukemia or HeLa cells were transfected with Fugene 6 (Roche) following manufacturer's instructions. For both cell types, each well (200,000 cells) of a 6-well plate was transfected with 500 ng of GM-CSF promoter luciferase reporter (pGL3)[103]; 200 ng of pcDNA3.1/HISa (Invitrogen) empty vector, Runx1 wild type or Runx1^{Q307X}; and 5 ng pHRL-null promoter-less Renilla luciferase.[106] Luciferase activity was measured 24 hours after transfection using the Dual-Luciferase Reporter Assay System (Promega, Madison, WI Cat. No. E1960) in a Glomax Luminometer (Promega) with Glomax 1.6 software. Values plotted are the ratios of firefly to Renilla luciferase, normalized to empty vector.

Electrophoretic Mobility Shift Assay (EMSA)

Runx consensus oligonucleotide 5'-CGA GTA TTG TGG TTA ATA CG-3' was end labeled as described previously.[107,108] Upper strands of the oligonucleotides were labeled with ^{32}P for 1 hour at 37°C in a 50 uL volume using T4 Polynucleotide Kinase (New

England BioLabs, Beverly, MA) following manufacturer's instructions. The reaction was stopped by heat inactivation at 65°C for 1 hour. Annealing was performed by addition of a twofold excess amount of bottom strand followed by boiling for 5 min and slow cooling to room temperature. Unincorporated nucleotides were removed with a quick-spin G 25 Sephadex column (Roche Molecular Biochemicals, Indianapolis, IN) according to the manufacturer's instructions. Nuclear extracts from HeLa cells (7.5 ug) transduced with empty vector, wildtype Runx1 or Runx1^{Q307X} were used in the binding reaction. Reaction mixtures were prepared using 50 fmol of probe, 50 mM KCl, 1 mM magnesium chloride, 1 mM DTT, 2 mM sodium fluoride, 2 mM sodium vanadate, 10% glycerol, 2 µg of poly(dI-dC)•poly(dI-dC), and DNA binding reactions were carried out at 25˚C for 20 min. Aliquots were separated in a 4% nondenaturing polyacrylamide gel for 1.5 hours at 200 V. The gel was dried and subjected to autoradiography.

Construction of the Runx1^{Q307X} expression vector

Wild type Runx1 in the pcDNA3.1/HISa expression vector[104] was mutated to Runx1^{Q307X} by site directed mutagenesis using a QuikChange Site-Directed Mutagenesis Kit (Stratagene, La Jolla, CA) with the following primers: forward CGG CGA CCC ACG CTA GTT CCC TAC TCT G, reverse CAG AGT AGG GAA CTA GCG TGG GTC GCC G.

Construction of the Runx1^{Q307X} targeting vector

We targeted the mouse Runx1 locus by homologous recombination using a 3.97 kb SacII-NotI PCR fragment of intron 7 (left arm) and a 4.0 kb NotI-SalI PCR fragment of intron 7 - exon 8 (right arm). Both fragments were generated from mouse AB2.2 genomic DNA by PCR using specific primer pairs (Primers 5' to 3': LAF1 CCG CGG GGC ATC TCT CTC CTT CCT CCA GTG TCT ; LAR1 GAG GGG ATC GAA AAG CTT CCT ; LAF2 AGG AAG CTT TTC GAT CCC CTC; LAR2 GCG GCC GCG ATC ACG GAG AGT GCC TCT GAC AC; RAF1 GCG GCC GCG TGG GCA GGA GCA CTC GCT GT; RAR1 GAG TAG GGA ACT AGC GTG GG; RAF2 CCC ACG CTA GTT CCC TAC TC; RAR2 GAC CAC CCA GAT GCA AAC AGG; RAF3 CGC ACC TTA TCG ATT GCA A; RAR3 GTC GAC CCG ACC AAC AGC CAA ACC CAC CAA). The left arm was created by using two primer pairs that produce 1.3 kb and 2.67 kb fragments (LAF1 to LAR1 and LAF2 to LAR2, respectively) which were ligated using an internal HindIII site to obtain the entire 3.97 kb fragment. The right arm was created using three different primer pairs that produce two overlapping fragments of 1.0 kb containing the stop codon mutation (RAF1 to RAR1 and RAF2 to RAR2) and 3.0 kb (RAF3 to RAR3) which were ligated using an internal ClaI site to obtain the entire 4.0 kb fragment. The 3.97 kb and 4.0kb fragments were cloned in tandem into the pGEM-5Zf(+) vector (Promega). We then inserted a 2.0 kb NotI-NotI cassette containing a floxed neomycin gene (LoxP site - PGK promoter - Neo cDNA - LoxP site) and a 2.2 kb SalI-SalI cassette with the thymidine kinase gene (PGK promoter - TK cDNA). Vectors containing the Neo and TK cassettes were provided by the Transgenic Animal Modeling Core Facility of the

University of Massachusetts Medical School. The final targeting vector and intermediate constructs were subjected to DNA sequencing.

Screening of mouse embryonic stem cells with a Runx1^{Q307X} allele

The targeting vector was linearized with AscI digestion and electroporated into PC3 (129S5/SvEvBrd) embryonic stem (ES) cells (Transgenic Animal Modeling Core Facility, University of Massachusetts Medical School) (i.e., 107 ES cells were transfected with 20 ug linearized construct at 230 V and 500 uF). Positive selection was started 24 hours after electroporation by addition of 180 ug/mL of G418 (Invitrogen Life Technologies, Inc., Carlsbad, CA). Thymadine kinase was used to select against non-homologous recombination events. Resistant clones were transferred into and cultured in 96-well plates. Homologous recombination of the Runx1^{Q307X} allele was established by Southern blot analysis using restriction sites and probes external to the targeting vector. Hybridization was carried out using the PerfectHybtm Plus Hybridization kit (Sigma-Aldrich, St. Louis, MO). Southern blot analysis identified a single clone with a correctly targeted mutation of the Runx1 locus.

Generation of the Runx1^{Q307X} mice

The PC3 ES cell clone with a targeted Runx1^{Q307X} allele was micro-injected into C57BL/6 blastocysts. Chimeric mice with a significant ES cell contribution (as

determined by agouti coat color) were mated with wild type C57BL/6 and germ line transmission of the mutant allele was determined by Southern blot genotyping of tail DNA from offspring and confirmed by PCR (Primers 5' to 3': forward ACT CTG GCA GTC TAG GAA GCC, reverse AGG CGC CGT AGT ATA GAT GGT A). $Runx1^{Q307X}$ heterozygous mice were crossed to generate $Runx1^{Q307X}$ homozygous mice and offspring were subjected to genotyping by PCR and Southern blot analysis.

Histology

Embryos (E12.5) were embedded in paraffin after a sample of tail was taken for genotyping. Six micron sections were stained with hematoxylin and eosin by standard procedures. Images were captured using a Axioskop 40 (Carl Zeiss, Inc., Maple Grove, MN) equipped with a AxioCam HRc and AxioVision Rel. 4.7 software (Zeiss).

Western blotting

Embryos (E12.5) were homogenized with a Dounce homogenizer in 2.0 mL direct lysis buffer (2% SDS, 2 M urea, 10% glycerol, 10 mM Tris-HCl [pH 6.8], 0.002% bromophenol blue, 10 mM DTT, 1× Complete protease inhibitor [Roche], 25 uM MG132 and 1 mM PMSF). HeLa cells were lysed with 500 uL direct lysis buffer per confluent well of a 6-well plate. Cell lysates were boiled for 5 min and equal amounts of protein (embryos) or sample volumes (HeLa cells) were electrophoresed in an 8% SDS-

polyacrylamide gel, at 100V for 1.5 hours. Separated proteins were transferred to an Immobilon Membrane (Millipore, Billerica, MA) by semidry transfer for 30 - 45 min at 10V. Membranes were blocked for at least 1 hour in 5% nonfat dry milk in PBST (PBS with 0.1% Tween 20) and then probed for 1 hour with primary antibody diluted 1:1000 (PU.1, YAP, Cdk2, LaminB [Santa Cruz Biotechnology, Santa Cruz, CA] or AML1(RHD) [Oncogene Science]). After four 5 min washes with PBST, blots were incubated for 1 hour with goat anti-rabbit (or donkey anti-goat) IgG-HRP secondary antibody diluted 1:4000, washed four times for 5 min in PBST and detected with ECL (Perkin-Elmer, Waltham, MA).

Colony Forming Unit (CFU) assays

Fetal livers of E12.5 embryos were isolated, placed in Iscove's Modified Dulbecco's Medium and passed three times through a 26 gauge needle to homogenize the mixture. Cells (20,000) from each liver were plated in duplicate in 35-mm dishes containing Methoculttm methyl cellulose medium (StemCell Technologies Vancouver, BC, Canada Cat. No. M3434), incubated at 37°C and colonies were counted by visual inspection on day 7.

qRT-PCR

RNA was prepared from E12.5 embryos using TRIzol following the manufacturer's protocol (Invitrogen). RNA was treated with DNaseI and 1 ug was subjected to reverse transcription with oligo dT primers. Quantitative PCR was performed on the resulting cDNA using the primers in Table 5.

Gene	qRT-PCR Primer	
Runx1	CCAGCAAGCTGAGGAGCGGCG	forward
	TGACGGTGACCAGAGTG	reverse
MPO	ATGCAGTGGGGACAGTTTCTG	forward
	GTCGTTGTAGGATCGGTACTG	reverse
CEBPdelta	TCGACTTCAGCGCCTACATTG	forward
	CGCTTTGTGGTTGCTGTTGA	reverse
Csf1R	GCGATGTGTGAGCAATGGCAGT	forward
	AGACCGTTTTGCGTAAGACCTG	reverse
Gfi1	AGGAGGCACCGAGAGACTCA	forward
	GGGAGGCAGGGAAGACATC	reverse
Pu.1	TATCAAACCTTGTCCCCAGC	forward
	GCGAATCTTTTTCTTGCTGC	reverse
YAP	CGATCAGACAACAACATGGC	forward
	ATCCTGAGTCATGGCTTGCT	reverse
Bmi1	TCCAGGTTCACAAAACCAGAC	forward
	GTAGTGGGCCATTTCTTCTCC	reverse
p19arf	TTCTTGGTGAAGTTCGTGCGATCC	forward
	ACGTGAACGTTGCCCATCATCATC	reverse
BCL-2	TACCGTCGTGACTTCGCAGAG	forward
	GGCAGGCTGAGCAGGGTCTT	reverse
MCL1	TAAGGACgAAACGGGACTGG	forward
	ACCAGCcCCTACTCCAGCAA	reverse
p21	CTTCTCCCATTTCTTAGTAGCAG	forward
	CCACGGTATTCAACACTGAG	reverse
p27	TCTAAAGCCCACTTATAACCCAG	forward
	CCTGTGCCATCTCTATATTCCT	reverse
p57	GTCTGAGATGAGTTAGTTTAGAGG	forward
	TGCTACATGAACGAAAGGTC	reverse
VEGF	ACTGGACCCTGGCTTTACTG	forward
	GGCAGTAGCTTCGCTGGTAG	reverse
GM-CSF	ATGCCTGTCACGTTGAATGA	forward
	GAAGCTGGATTCAGAGCTGG	reverse
mCox	ACGAAATCAACAACCCCGTA	forward
	GGCAGAACGACTCGGTTATC	reverse

Table 5: qRT-PCR primers used in Runx1^{Q307X} embryos

Results

Loss of Runx1 C-terminal domains causes aberrant subnuclear targeting

The region lost in Runx1^{Q307X} includes the NMTS, a domain required for subnuclear targeting of Runx1 to transcriptionally active sites. In contrast, previous mouse models have focused on the Runt-homology DNA binding domain or substituted the C-terminus with LacZ to track expression (Figure 12). To examine subnuclear targeting of the mutated protein, nuclear matrix-intermediate filament (NMIF) preparations of HeLa cells transduced with wild type Runx1 or Runx1^{Q307X} were examined by in situ immunofluorescence microscopy. Expression of the truncated Runx1^{Q307X} (denoted ΔC in figures) was confirmed by Western blot (Figure 13A). In whole cell preparations, Runx1^{Q307X} retained the characteristic punctate nuclear foci observed with wild type Runx1 (Figure 13B). However, the Runx1^{Q307X} signal was significantly reduced in NMIF preparations, indicating that this mutant has lost the ability to interact with the nuclear matrix (Figure 13B). Thus, our results are consistent with previous observations that the C-terminally encoded NMTS of Runx1 is required for subnuclear targeting.[87,103] We performed luciferase reporter assays to determine if Runx1^{Q307X} is able to activate target promoters. The GM-CSF promoter was activated in the presence of wild type Runx1, but Runx1^{Q307X} activated the promoter to similar levels at the empty vector control, in both HeLa and K562 cells (Figure 13C). Runx1^{Q307X} forms stable protein-DNA complexes in electrophoretic mobility shift assay (EMSA) (Figure 13D). Thus, while Runx1^{Q307X} is capable of binding to DNA, this truncated protein is unable to associate with the nuclear matrix and failed to fully activate target gene promoters.

Runx1 translocations observed in human leukemia patients often lose C-terminal domains critical for subnuclear targeting and protein-protein interactions. Previous mouse models examined complete loss-of-function Runx1 mutations by ablating DNA binding. Other mutants created hypomorphic deletions or fusion proteins produced from chimeric mRNAs lacking endogenous 3'UTR sequences that are required for fidelity of expression. We investigated the biological function of the Runx1 C-terminus by introducing the Runx1^{Q307X} point mutation into the endogenous Runx1 locus by homologous recombination (Figure 14). Southern blot analysis identified ES clones with correctly targeted mutation of the Runx1 locus, from which the mice were generated (Figure 15).

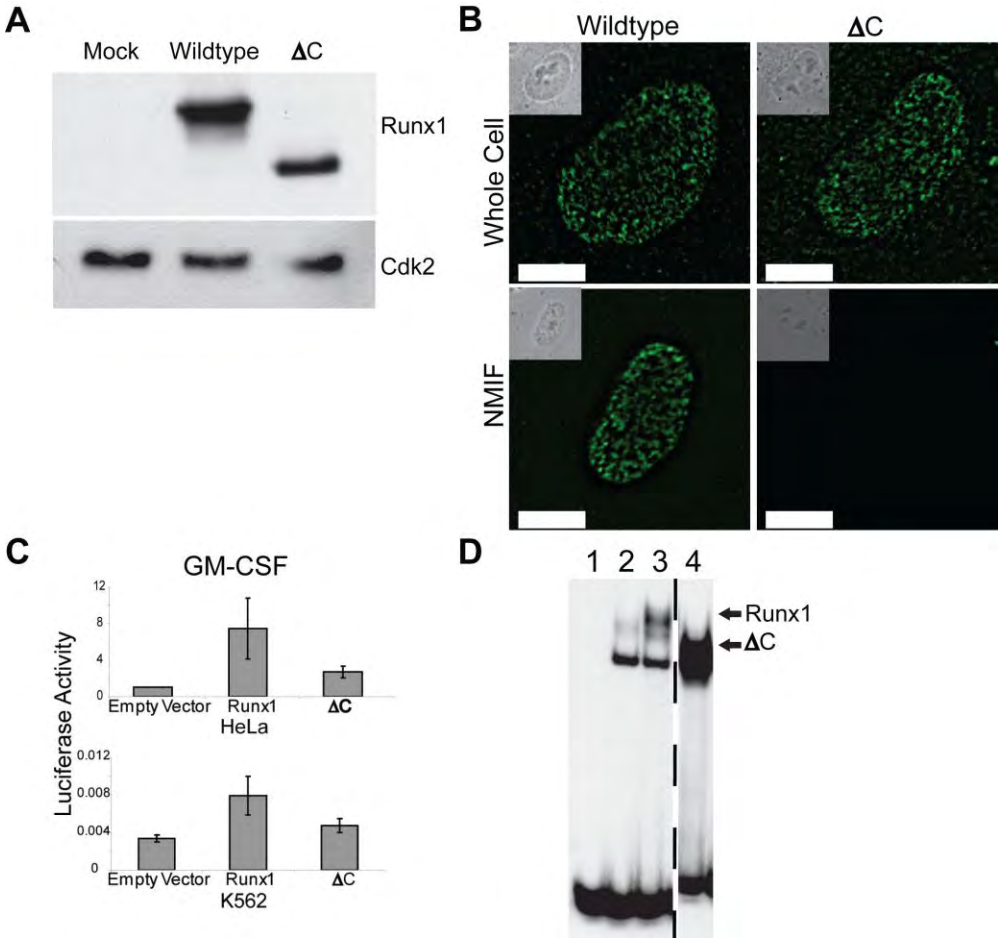

Figure 13: Characterization of Runx1^{Q307X} in vitro

(A) Western blot showing expression of wildtype Runx1 or Runx1^{Q307X} in transfected HeLa cells, with Cdk2 shown as a loading control. (B) Whole cell (upper panels) or NMIF preparations (lower panels) of HeLa cells transfected with wildtype Runx1 or Runx1^{Q307X}. Anti-Runx1 immunofluorescence images are shown with phase contrast insets. Scale bars are 100 um. The signal for Runx1^{Q307X} cells in NMIF preparations decreased by 4.5 fold compared to wild type Runx1, based on observation of at least 200 cells per sample with representative cells shown. (C) Luciferase expression from GM-CSF promoter constructs in the presence of empty vector, wildtype or Runx1^{Q307X} in HeLa and K562 cells. Luciferase activity is normalized to background Renilla and error bars represent the standard deviation between multiple samples (n=3 HeLa, 4 K562). (D) EMSA showing DNA binding activity of wildtype Runx1 and Runx1^{Q307X} from transduced HeLa cell nuclear extracts: lane 1, free probe; lane 2, empty vector; lane 3, wildtype Runx1; lane 4, Runx1^{Q307X}.

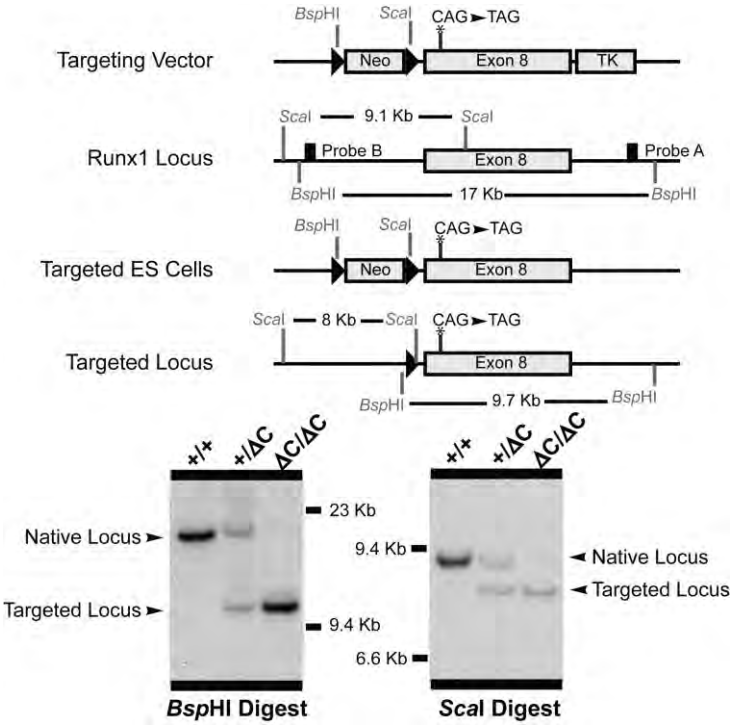

Figure 14: Targeting vector for Runx1^{Q307X} mice

Targeting strategy to replace a portion of Exon 8 with Exon 8 containing the point mutation to cause a stop codon after amino acid 307 (CAG to TAG). Probes A and B and restriction enzyme cut sites are shown. The Neomycin resistance gene (Neo) was removed by using embryonic stem cells containing the sperm-specific PC3Cre, excising Neo during generation of founder mice. Southern blot analysis of genomic DNA from tails of E12.5 embryos was performed using restriction enzymes and probes shown.

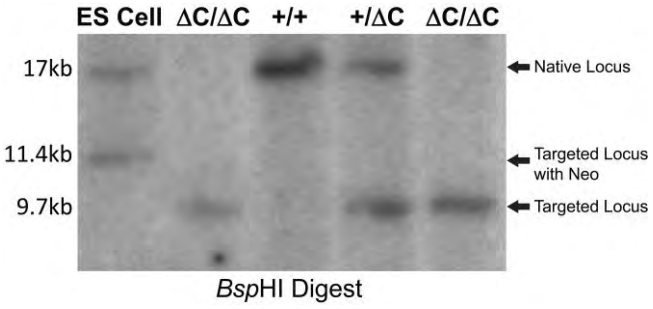

Figure 15: Genotyping of Runx1^{Q307X} mice.

Genotyping by Southern blot, with the ES cells containing the Neo cassette shown as an additional control confirming Neo excision.

Runx1 C-terminal subnuclear targeting and associated transactivation are required during development

Embryos homozygous for the truncated Runx1^{Q307X} died at E12.5 from central nervous system hemorrhage, similar to the Runx1 RHD mutant knockout mice.[10] We observed near Mendelian ratios of wild type, heterozygous and homozygous mutant pups at E11.5 and E12.5 (Table 6). However, no live homozygous Runx1^{Q307X} pups were observed at E13.5 (Table 6). Gross examination of homozygous embryos consistently showed multiple areas of hemorrhage and a pale fetal liver (Figure 16A). The severity of the phenotype ranged from a few small areas of hemorrhage in the spinal cord to large regions of hemorrhage throughout the spinal cord, isthmus and ventral metencephalon (Figure 17). Areas of hemorrhage were examined in more detail with whole mount hematoxylin and eosin staining (Figure 16B and C). The sinusoids of Runx1^{Q307X} homozygous embryo fetal livers were devoid of hematopoietic precursor cells that were present in wild type embryos (Figure 16C middle and lower panels).

Age	Embryos	Litters	+/+	+/ΔC	ΔC/ΔC
E11.5	37	4	9	21	7
E12.5	97	12	27	48	22
Total	134	16	36	69	29
Ratio			1.00	1.92	0.81
E13.5	19*	5	9	10	0

Table 6: Genotyping of embryos from Runx1^{Q307X} heterozygous intercrosses.

Genotyping was performed by Southern blot as shown in Figure 14 or by PCR using the following primers, Forward primer ACT CTG GCA GTC TAG GAA GCC and Reverse primer AGG CGC CGT AGT ATA GAT GGT A. *At E13.5 only live embryos were counted.

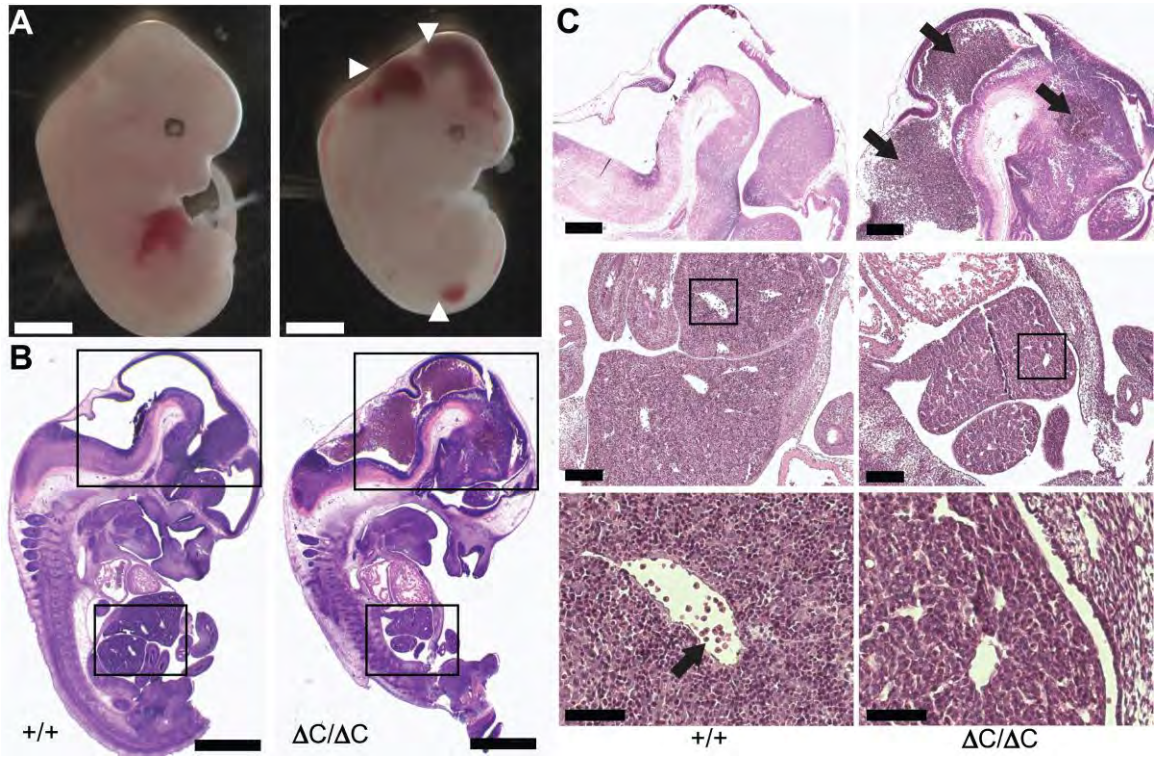

Figure 16: Histology of Runx1^{Q307X} homozygous embryos at E12.5.

(A) Gross image of wild type (left panel) and Runx1^{Q307X} (right panel) E12.5 embryos. White arrowheads note sites of hemorrhage in the Runx1^{Q307X} embryo. Scale bars are 1 mm. (B) Whole mount hematoxylin and eosin staining of embryos in A. Scale bars are 1 mm. (C) Magnification of heads of E12.5, noting hemorrhages with black arrows (upper panels, scale bars are 500 um). Magnification of fetal livers of E12.5 embryos (middle panels, scale bars are 250 um) and magnification showing liver sinusoids (lower panels, scale bars are 100 um) with arrow noting the hematopoietic precursor cells in the wild type sinusoids that are absent from Runx1^{Q307X}.

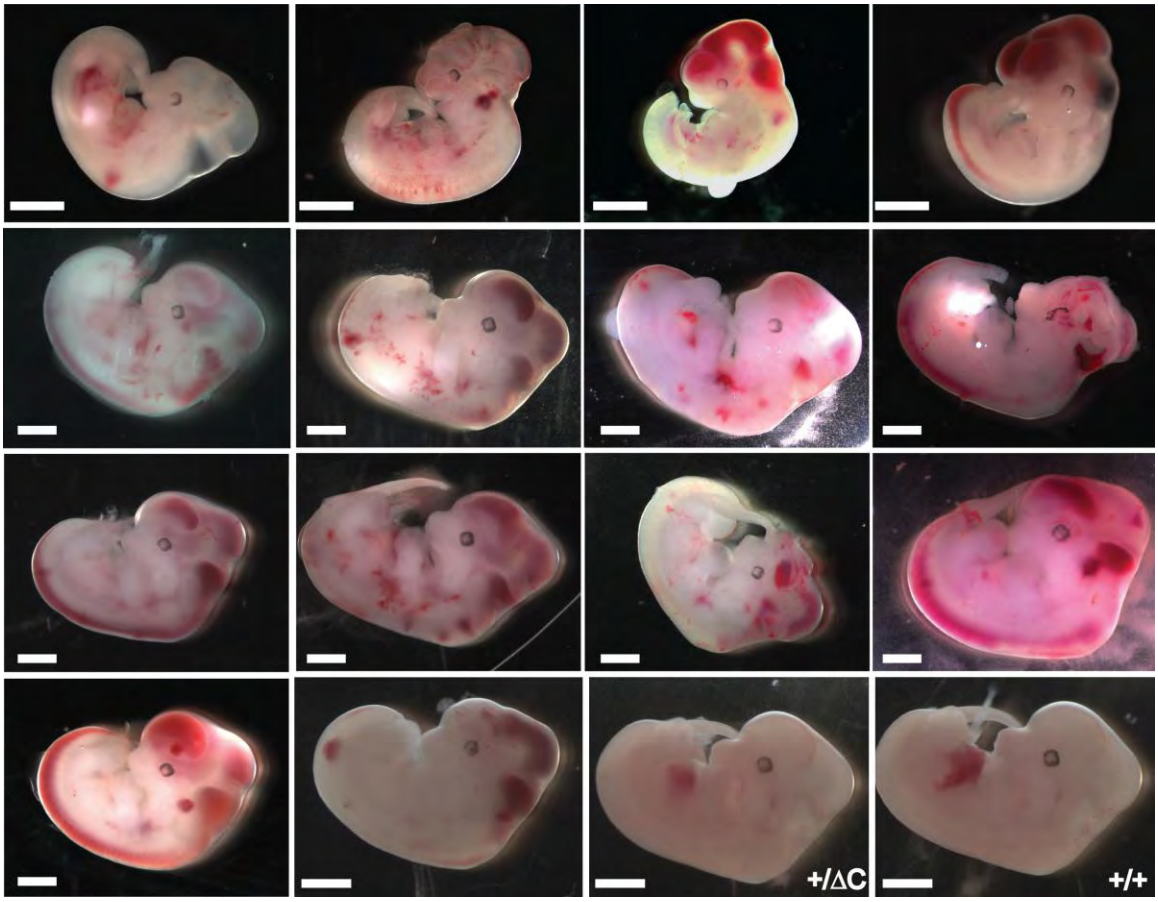

Figure 17: Variation in phenotype of Runx1^{Q307X} homozygous embryos.

E11.5 (top row) and E12.5 Runx1^{Q307X} homozygous embryos display a range of hemorrhage severity. Heterozygous (+/ΔC) and wildtype (+/+) E12.5 embryos are shown for comparison. Scale bars are 1mm.

Consistent with the absence of hematopoietic progenitor cells by histological analysis, fetal liver cells from Runx1^{Q307X} homozygous embryos were unable to form colonies in a methocellulose colony forming unit assay (Figure 18A) despite robust activity of fetal liver cells from their wild type and heterozygous littermates. Runx1 is not required for embryonic primary erythropoiesis and primitive erythrocytes are abundant in the peripheral blood of both wild type and mutant embryos (Figure 18B). Thus, the C-terminal domains of Runx1 are required for in vivo HSC function during development.

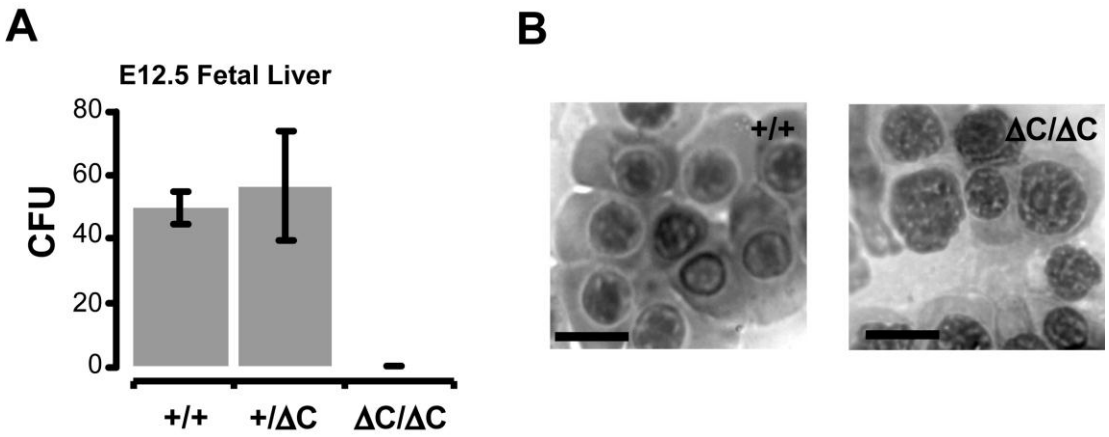

Figure 18: Lack of hematopoietic progenitor cell function in Runx1^{Q307X}.

(A) Colony Forming Unit (CFU) assays using fetal liver cells from wild type, heterozygous or Runx1^{Q307X} homozygous E12.5 embryos (n=3 to 6). (B) Nucleated erythroid progenitors are morphologically normal in peripheral blood smears of wild type and Runx1^{Q307X} E12.5 embryos. Scale bars are 10 um.

Aberrant subnuclear targeting and lost co-factor interactions of Runx1^{Q307X} cause deregulation of Runx1 targets

Runx1 is a key regulator of hematopoiesis and controls many hematopoietic target genes.[66,79,84,85] Considering the severity of the phenotype of the Runx1^{Q307X} homozygous mice, we performed qRT-PCR analysis to measure the effects of Runx1^{Q307X} on Runx1 target genes and markers of hematopoiesis (Figure 19). Expression of hematopoietic transcription factors (Figure 19A) and phenotypic markers (Figure 19B) was decreased in the Runx1^{Q307X} homozygous mice, with a gene dosage dependent reduction generally seen in heterozygous littermates. Runx1 expression was not substantially altered, suggesting that the point mutation does not change the stability of the transcript (e.g., nonsense mediated mRNA decay). Markers for cell survival and proliferation were comparable for the three genotypes (Figure 19C). Genes important for HSC function (Figure 19D) were dramatically down regulated in the Runx1^{Q307X} homozygous mice, confirming the hematopoietic specificity of the mutation. Signaling proteins that are indirect targets were also affected in Runx1^{Q307X} mice (Figure 19E). Interestingly, VEGF was upregulated in the Runx1^{Q307X} homozygous mice, which may contribute to the observed hemorrhages by increasing vascular permeability. Consistent with mRNA expression data, a drop in protein levels of PU.1 and YAP was observed (Figure 20). These results indicate that the loss of key domains responsible for protein-protein interactions with co-factors and subnuclear targeting in Runx1^{Q307X} cause widespread gene deregulation.

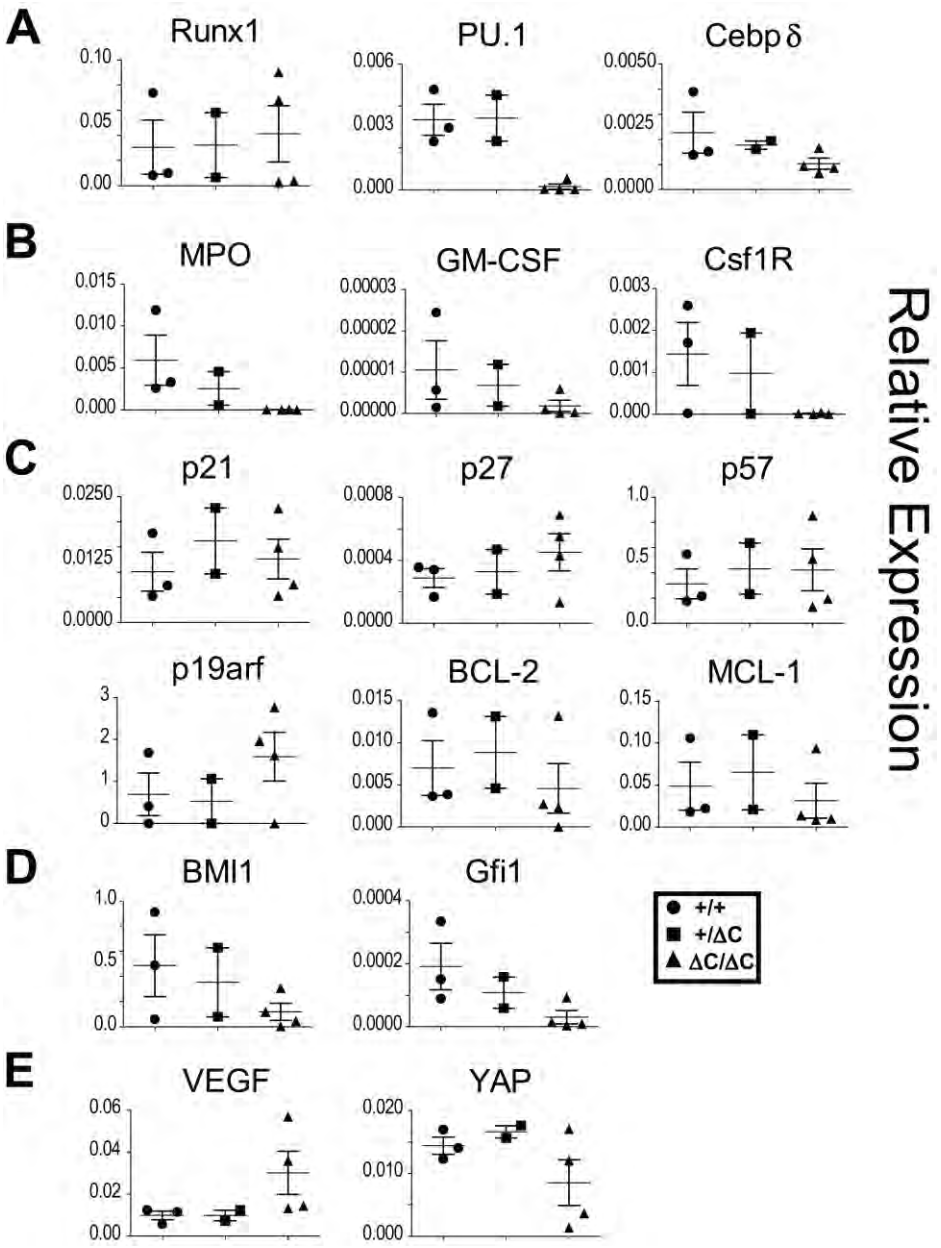

Figure 19: Runx1^{Q307X} causes deregulation of hematopoietic genes.

Relative expression of hematopoietic transcription factors (A), phenotypic markers (B), proliferation and cell survival markers (C), genes required for HSC maintenance (D), and signaling molecules (E) by qRT-PCR in wildtype, heterozygous and homozygous Runx1^{Q307X} E12.5 mice (N= 3, 2, and 4, respectively). Each point represents the mean of technical replicates from one embryo. Results were normalized to mCox expression. See Table 5 for specific primers.

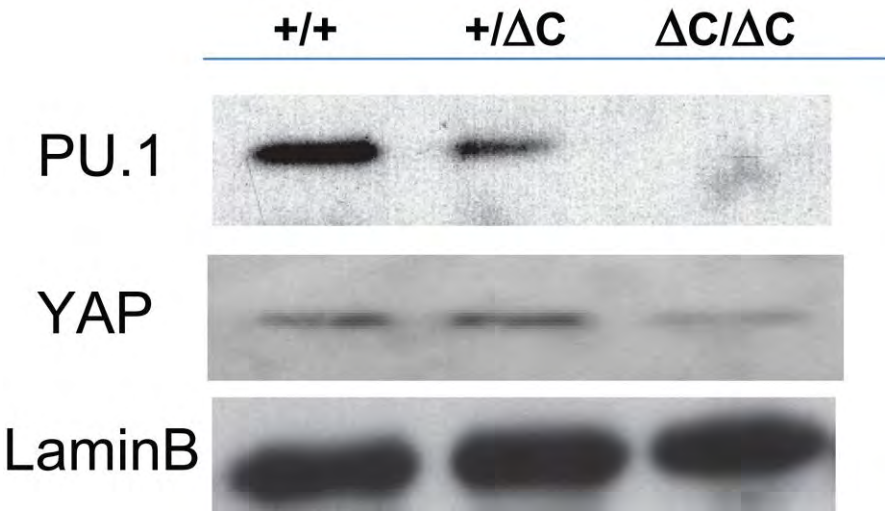

Figure 20: Western blots confirm altered expression.

Altered protein levels were confirmed between wildtype, heterozygous and homozygous Runx1^{Q307X} E12.5 embryos by Western blot for two genes with decreased mRNA.

Discussion

Human leukemias often involve Runx1 translocations that result in a fusion protein retaining the DNA binding domain of Runx1 but losing the C-terminus encompassing subnuclear targeting and transactivation domains. By modeling a loss of function common in many leukemic fusion proteins we sought to shed light on potential common leukemic mechanisms. In this study, we generated a knock-in mouse model that contains a point mutation causing a premature stop codon within exon 8. This mutation truncates the protein after amino acid 307 but maintains the integrity of the endogenous Runx1 mRNA by retaining the extensive 3' untranslated region (UTR) and potential regulation by miRNA.[75,128] In many human leukemias, a naturally occurring truncated protein isoform, AML1a (Runx1/p27[129]), is up regulated, and there is evidence that over expression of AML1a can act as an initiating leukemogenic mutation by inhibiting Runx1 function.[81,130] Taken together, these findings suggest that Runx1 C-terminal domains play important mechanistic roles in leukemogenesis and that loss of subnuclear targeting and transactivation may contribute to the etiology of human leukemia.

Our mouse model with a point mutation in exon 8 complements previous mouse models with mutations in exon 4, which encodes a part of the Runt-homology DNA binding domain. These exon 4 mouse mutations mimic genetic lesions found in leukemia patients[97] and have defined the phenotypic consequences of complete loss of function due to impaired DNA binding. Recent evidence has shown the importance of the Runx1 C-

terminus, which includes subnuclear targeting and transactivation domains, during embryoid body formation with mouse ES cells.[131] Hematopoietic differentiation was lost in embryoid bodies made with Runx1 null ES cells, but rescued by targeted insertion of cDNA for full length Runx1 or Runx1 C-terminal truncations that retained transactivation domains. Recent in vitro studies used a retroviral rescue of Runx1 null cells to assess which domains of Runx1 were important for hematopoietic colony formation.[132] These studies revealed that the C-terminal transactivation domain is required for colony formation, but did not further characterize the rescued cells or address the effects of mutation in vivo.

The Runx1^{Q307X} mutation we have characterized here provides a mouse model for Runx1 C-terminal mutations observed in human patients with MDS, AML, RAEB and CMML.[92,96] A previous mouse model involving the loss of the Runx1 C-terminus replaced exons 7 and 8 with the bacterial LacZ gene to create a fusion protein.[58] This model allowed the tracking of Runx1 expression and supported the concept that Runx1 is required during hematopoietic development. This model also made visualizations of Runx1 expressing cells possible throughout development, pinpointing stages where Runx1 may play important roles. However, the genetic strategy produced a larger Runx1 C-terminal deletion than Runx1^{Q307X} and generated a large Runx1-LacZ fusion protein. During that process the sequences of the 3' UTR were necessarily eliminated. It is now known that the 3' UTR of mRNA can be functionally important, as they support

regulation by miRNAs (e.g., miR-27a).[75] The truncated Runx1^{Q307X} is caused by a single point mutation and retains the endogenous 3'UTR. Therefore, any miRNA mediated regulation of Runx1^{Q307X} should be identical to endogenous. Runx1, Runx2 and Runx3 all have homologous subnuclear targeting signals.[25,75,133] The Runx1^{Q307X} mouse contains a precise mutation that removes only the subnuclear targeting and transactivation domains, thus compromising the function of Runx1 as a scaffolding protein attached to the nuclear matrix, DNA and other proteins within the complicated three dimensional architecture of the nucleus.[21,29] The resulting aberrant subnuclear localization of Runx1^{Q307X} is predicted to trigger a cascade of deregulation. Taking that into account, it is not surprising that this germline mutation has such dramatic consequences for definitive hematopoiesis in the developing embryo.

In this study, we show that Runx1^{Q307X} is no longer associated with the nuclear matrix due to the loss of domains critical for interaction with the nuclear architecture. The region lost in Runx1^{Q307X} corresponds with the mapped interaction domains for many Runx co-factors, including p300, YAP, MOZ, Groucho/TLE1, SUV39H1, Smad3, HDAC1 and HDAC3.[19-21,23,134-140] Runx1^{Q307X} binds DNA but without the transactivation domains or subnuclear targeting it likely obstructs regulation, in a dominant negative fashion, rather than bringing components together. Removal of the C-terminal domains of Runx1 responsible for subnuclear targeting and protein-protein interactions causes the same embryonic lethal phenotype as a DNA binding knockout. Homozygous Runx1^{Q307X}

embryos die at E12.5 from lack of definitive hematopoiesis and central nervous system hemorrhages. Hence, Runx1^{Q307X} is not a hypomorphic mutation but rather results in a phenocopy of RHD mutations. These findings complement the observations with an analogous truncation in the Runx2 gene, which was also a phenocopy of a null mutation.[141] Runx1^{Q307X} contrasts with a mouse mutant lacking the C-terminal VWRPY motif, which has a mild hypomorphic phenotype with defects in thymocyte development, with other hematopoietic lineages being spared.[69] Our results with the Runx1^{Q307X} mouse establish that the subnuclear targeting and transactivation functions of Runx1 are essential for hematopoietic development and are consistent with the observation that human genetic lesions perturbing these functions compromise Runx1 function to contribute to leukemogenesis.

Chapter 4: A Germline Point Mutation in Runx1 Uncouples its Role in Definitive Hematopoiesis from Differentiation

Definitive hematopoiesis requires the master hematopoietic transcription factor Runx1, which is a frequent target of leukemia-related mutations and chromosomal translocations. Several of the resulting fusion proteins generated by these translocations retain the DNA binding activity of Runx1, but lose subnuclear targeting and associated transactivation potential. Complete loss of these functions in vivo resembles Runx1 ablation, which causes embryonic lethality. We generated a knock-in mouse that expresses full length Runx1 mutated in the subnuclear targeting / co-factor interaction domain, Runx1$^{HTY350-352AAA}$. Mutant mice survived to adulthood, and hematopoietic stem cell emergence was unaltered. However, defects were observed in multiple differentiated hematopoietic lineages, precisely at stages where Runx1 is known to play key roles. These findings indicate that subnuclear targeting and associated functions of Runx1 are important in many compartments throughout hematopoietic differentiation. Thus, a germline mutation in Runx1 reveals uncoupling of its roles during embryonic definitive hematopoiesis from subsequent differentiation in the adult across multiple hematopoietic lineages.

Introduction

Hematopoietic stem cell (HSC) emergence in the developing embryo requires the key Runt-related transcription factor Runx1[10], which is stringently regulated during differentiation of hematopoietic lineages.[80,142] Runx1 is one of the most frequent targets of point mutations and translocations in human leukemia[88], and these mutations cluster in either the N-terminal DNA binding domain, or the C-terminal transactivation domains.[92,96] Many Runx1 mutations cause lethality at embryonic day 12.5 in mouse models: defects in DNA binding ability or critical C-terminal functions result in phenocopies of the complete null.[10,58,143] This lethality has made studying the precise roles of Runx1 during hematopoiesis difficult. Genetic restoration of Runx1 expression in Tie2-positive endothelial cells rescued HSC emergence but revealed a secondary genetic bottleneck of Runx1 deficiency related to perinatal respiratory failure.[123] Similar gene replacement experiments in which the Runx1 N-terminus was fused to the C-terminus of Runx2 or Runx3 rescued HSC emergence, but uncovered additional roles of Runx1 in myeloid and T-lymphoid development.[144] A conditional null model developed to bypass embryonic lethality revealed important roles of Runx1 in most adult hematopoietic lineages.[66] However, gaps in knowledge remain about the developmental roles of Runx1 beyond stem cell emergence.

Many transcription factors, including Runx1, localize to specific foci within the nucleus and this localization is critical for biological function.[18-20,25,49,51,87] Subnuclear targeting

defective Runx1 mutants have previously been shown to cause differentiation defects [87] and altered regulation of target genes, including micro RNA precursors.[128] Appropriate subnuclear targeting is associated with Runx1 function as a scaffold within the nucleus, organizes regulatory machinery and mediates combinatorial control of gene expression.[26] In addition, the leukemic fusion protein Runx1-ETO, which loses Runx1 C-terminal domains, exhibits aberrant subnuclear targeting.[45,49,51] We previously characterized a knock-in mouse with a Runx1 C-terminal truncation that removed domains responsible for subnuclear targeting and co-factor interactions.[143] This mutation resulted in a complete phenocopy of mouse models without Runx1 DNA binding ability and was thus not able to address the precise biological contributions of specific domains linked to co-factor interactions and subnuclear targeting of Runx1.

We have previously characterized the Runx1 NMTS in vitro utilizing several point mutations. Those studies showed which residues were the most critical for retention within the nuclear matrix fraction of biochemical fractionations, and for appropriate activation of a M-CSF promoter driven luciferase reporter construct.[103] Those data also showed that while a C-terminal truncation could not completely abolish matrix fraction retention, a point mutation of one or three amino acids near the end of the NMTS could alter fractionation almost as dramatically as the truncation. We developed and characterized stable 32D cell lines expressing that single point mutant[87] and sought to use the triple point mutant, which had a stronger phenotype during the initial in vitro characterization, for in vivo studies.

In this study, we developed a knock-in mouse model, Runx1$^{HTY350-352AAA}$, encoding a triple point mutation in the C-terminal domain required for subnuclear targeting[103] and interaction with biologically important co-factors, including SMAD proteins.[18-20,134,135,145] Mice homozygous for Runx1$^{HTY350-352AAA}$ bypass embryonic lethality. However, this point mutation influences multiple downstream hematopoietic compartments in which there are key roles for wildtype Runx1. Our study establishes that the capability of Runx1 for interaction with regulatory co-factors and the nuclear architecture is required for optimal multi-lineage hematopoietic differentiation. This finding demonstrates that the biological role of Runx1 during embryonic development can be uncoupled from its roles in differentiation of hematopoietic lineages in the adult.

Materials and Methods

Construction of the Runx1$^{HTY350-352AAA}$ targeting vector

We targeted the mouse Runx1 locus by homologous recombination using a 3.97 kb SacII-NotI PCR fragment of intron 7 (left arm) and a 4.0 kb NotI-SalI PCR fragment of intron 7 - exon 8 (right arm). Both fragments were generated from mouse AB2.2 genomic DNA by PCR using specific primer pairs (Primers 5' to 3': LAF1 CCG CGG GGC ATC TCT CTC CTT CCT CCA GTG TCT ; LAR1 GAG GGG ATC GAA AAG CTT CCT ; LAF2 AGG AAG CTT TTC GAT CCC CTC; LAR2 GCG GCC GCG ATC ACG GAG AGT GCC TCT GAC AC; RAF1 GCG GCC GCG TGG GCA GGA GCA CTC GCT GT; RAR1 GAG TAG GGA ACT AGC GTG GG; RAF2 CCC ACG CTA GTT CCC TAC TC; RAR2 GAC CAC CCA GAT GCA AAC AGG; RAF3 CGC ACC TTA TCG ATT GCA A; RAR3 GTC GAC CCG ACC AAC AGC CAA ACC CAC CAA). The left arm was created by using two primer pairs that produce 1.3 kb and 2.67 kb fragments (LAF1 to LAR1 and LAF2 to LAR2, respectively) which were ligated using an internal HindIII site to obtain the entire 3.97 kb fragment. The right arm was created using three different primer pairs that produce two overlapping fragments of 1.0 kb containing the stop codon mutation (RAF1 to RAR1 and RAF2 to RAR2) and 3.0 kb (RAF3 to RAR3) which were ligated using an internal ClaI site to obtain the entire 4.0 kb fragment. The 3.97 kb and 4.0kb fragments were cloned in tandem into the pGEM-5Zf(+) vector (Promega). We then inserted a 2.0 kb NotI-NotI cassette containing a floxed neomycin gene (LoxP site - PGK promoter - Neo cDNA - LoxP site) and a 2.2 kb SalI-SalI cassette with the thymidine kinase gene (PGK promoter - TK cDNA). Vectors containing the Neo and TK

cassettes were provided by the Transgenic Animal Modeling Core Facility of the University of Massachusetts Medical School. The final targeting vector and intermediate constructs were subjected to DNA sequencing before proceeding.

Screening mouse embryonic stem cells for the Runx1$^{HTY350-352AAA}$ allele

The targeting vector was linearized with AscI and electroporated into PC3 (129S5/SvEvBrd) embryonic stem (ES) cells (Transgenic Animal Modeling Core Facility, University of Massachusetts Medical School) (i.e., 107 ES cells were transfected with 20 ug linearized construct at 230 V and 500 uF). Positive selection was started 24 hours after electroporation by addition of 180 ug/mL of G418 (Invitrogen Life Technologies, Inc., Carlsbad, CA). Non-homologous recombination was selected against using thymidine kinase. Resistant clones were transferred into and cultured in 96-well plates. Homologous recombination of the Runx1$^{HTY350-352AAA}$ allele was established by Southern blot analysis using restriction sites and probes external to the targeting vector as in Figure 14. Hybridization was carried out using the PerfectHyb Plus Hybridization kit (Sigma-Aldrich, St. Louis, MO). Southern blot analysis identified a single clone with a correctly targeted mutation of the Runx1 locus.

Generation of the Runx1$^{HTY350-352AAA}$ mice

The PC3 ES cell clone with a targeted Runx1$^{HTY350-352AAA}$ allele was micro-injected into C57BL/6 blastocysts. Chimeric mice with a significant ES cell contribution (as determined by agouti coat color) were mated with wild type C57BL/6 and germ line transmission of the mutant allele was determined by Southern blot genotyping of tail DNA from offspring and confirmed by PCR (Primers 5' to 3': forward ACT CTG GCA GTC TAG GAA GCC, reverse AGG CGC CGT AGT ATA GAT GGT A). This PCR reaction amplifies a 300 bp fragment including the mutation encoding HTY to AAA; CAC ACC TAC to GCC GCG GCA. This creates a new digestion site for SacII which cleaves CCGC^GG. After initial screenings by Southern blot analysis, subsequent generations were genotyped by PCR and restriction enzyme digest (Figure 21B). Runx1$^{HTY350-352AAA}$ heterozygous mice were crossed to generate Runx1$^{HTY350-352AAA}$ homozygous mice and offspring were subjected to genotyping by PCR and Southern blot analysis.

Immunofluorescence microscopy

Bone marrow cells were isolated and spun onto glass slides (100,000 cells per slide). Cells were fixed using formaldehyde (3.7%), and permeabilized with 0.5% Triton X-100 for whole-cell preparations. Nuclear matrix-intermediate filament (NMIF) preparations were obtained as described.[36] Runx1 protein was detected by the AML1(RHD) antibody (Oncogene Science, Cambridge, MA; 1:200 dilution) followed by fluorochrome-conjugated Alexa Fluor 488 secondary antibody (Invitrogen Molecular Probes, Eugene,

OR; 1:800 dilution). Lamin A/C was detected with the N-18 antibody (Santa Cruz; 1:800 dilution) followed by Alexa Fluor 594 (1:800 dilution). Cells were stained with DAPI and then mounted in Prolong Gold antifade mounting medium (Invitrogen Molecular Probes). Fluorescence images were captured using a Zeiss Axioplan 2 microscope equipped with a digital charged-coupled device camera (Hamamatsu Photonics, Bridgewater, NJ Cat. No. C4742-95) interfaced with the MetaMorph Imaging System (Universal Imaging Corporation Ltd, Marlow, Buckinghamshire, UK).

Colony Forming Unit (CFU) assays and ex vivo culture

2000 bone marrow cells were plated in duplicate in 35-mm dishes containing Methocult methyl cellulose medium (StemCell Technologies Vancouver, BC, Canada Cat. No. M3434), incubated at 37°C and colonies were counted by visual inspection on day 7. Bone marrow cells cultured ex vivo were in DMEM supplemented with 10% fetal bovine serum and L-glutamine but without additional cytokines. If media was supplemented with TGF beta, we used a final concentration of 10 ng per ml. When 5-flourouracil (5-FU) was used, mice were given IP injections of 150 mg per kg of 5-FU or vehicle (10% DMSO).

Flow cytometry

Cells were isolated from the bone marrow, spleen, and/or thymus of age matched mice into RPMI Medium without phenol red (Invitrogen) with 1mM EDTA, 0.02% sodium

azide, and 3% fetal bovine serum. Cells were counted and adjusted to 6x10^7 cells per mL for staining. 40 ul of cells was incubated on ice for 20 min with 40 uL of antibody cocktails. Antibodies were all purchased from BD Bioscience and were: B220-PE, Gr1-FITC, CD11b-PE, cKit-APC, Sca1-FITC, CD127-PE-Cy7, CD16/32-v450, CD34-alexaFlour700, AA4.1-FITC, IgM-PerCP-Cy5.5, CD43-APC, CD3-PE, CD4-PE-Cy7, CD8-APC, CD41-FITC, CD71-PE, and Ter119-APC. For lineage exclusion, we used antibodies against Ter119, CD3, CD11b, Gr1 and B220 all conjugated to PE. Propidium iodide staining was performed by the flow cytometry core facility on cells already stained with CD41-FITC and fixed in ethanol. After staining cells were fixed with 1% formaldehyde and processed on an LSRII or FACSCalibur machine by the University of Massachusetts Flow Cytometry core facility. Analysis of CLP and early B progenitors was performed on live cells (stained as above) using a FACS Aria.

qRT-PCR

RNA was prepared from bone marrow cells using TRIzol following the manufacturer's protocol (Invitrogen). RNA was treated with DNaseI and 1 μg was subjected to reverse transcription with oligo dT primers. Sorted CLP were collected into lysis buffer and RNA obtained using an RNAeasy Micro Kit (Quiagen) following the manufacturer's instructions. qRT-PCR was performed on the resulting cDNA using the primer pairs listed in Table 7.

Gene	qRT-PCR Primer	
Runx1	CCAGCAAGCTGAGGAGCGGCG	forward
	TGACGGTGACCAGAGTG	reverse
Runx2	CGGCCCTCCCTGAACTCT	forward
	TGCCTGCCTGGGATCTGTA	reverse
Runx3	GGGCGAGGGAAGAGTTTCAC	forward
	CCTTGATGGCTCGGTGGTA	reverse
Gfi1	AGGAGGCACCGAGAGACTCA	forward
	GGGAGGCAGGGAAGACATC	reverse
Bmi1	TCCAGGTTCACAAAACCAGAC	forward
	GTAGTGGGCCATTTCTTCTCC	reverse
CEBPalpha	AAAGCCAAGAAGTCGGTGGAC	forward
	CTTTATCTCGGCTCTTGCGC	reverse
CEBPdelta	TCGACTTCAGCGCCTACATTG	forward
	CGCTTTGTGGTTGCTGTTGA	reverse
GATA1	GGCAAGACGGCACTCTACC	forward
	CAAGAACGTGTTGTTGCTCTTC	reverse
GATA2	AAAGGGGCTGAATGTTTCG	forward
	GCGTGGGTAGGATGTGTC	reverse
GATA3	TCGGCCATTCGTACATGGAA	forward
	GAGAGCCGTGGTGGATGGAC	reverse
Scl	CATGTTCACCAACAACAACCG	forward
	GGTGTGAGGACCATCAGAAATCTC	reverse
VpreB1	CGTCTGTCCTGCTCATGCT	forward
	ACGGCACAGTAATACACAGCC	reverse
Rag1	CATTCTAGCACTCTGGCCGG	forward
	TCATCGGGTGCAGAACTGAA	reverse
LCN2	GGGAAATATGCACAGGTATCCT	forward
	GCGAACTGGTTGTAGTCCGT	reverse
IRF4	TCTTGTGAAAATGGTTGCCA	forward
	GCAGACCTTATGCTTGGCTC	reverse
Csf1R	GCGATGTGTGAGCAATGGCAGT	forward
	AGACCGTTTTGCGTAAGACCTG	reverse
MPO	ATGCAGTGGGGACAGTTTCTG	forward
	GTCGTTGTAGGATCGGTACTG	reverse
GM-CSF	ATGCCTGTCACGTTGAATGA	forward
	GAAGCTGGATTCAGAGCTGG	reverse
Gr-1	TCGCCAAATATACTTGTTCCTC	forward
	GATTCATTGTCAAGTCAGCCT	reverse
CD11b	ATCTTCTCCCAGAACCTCTC	forward
	GAGTGTTGAAGGATGGAAGG	reverse
Neutrophil Elastase	CCTTGGCAGACTATCCAGCC	forward
	GACATGACGAAGTTCCTGGCA	reverse
MYL9	CTCTGCAGCAGGGAAACC	forward
	CAAACATGGCGAAGACATTG	reverse
Id1	ACTTGGTCTGTCGGAGCAAA	forward
	TAGCAGCCGTTCATGTCGTA	reverse
HB Alpha	ACTTCAAGCTCCTGAGCCACTGC	forward
	GCACGGTGCTCACAGAGGCA	reverse
HB Beta	AACGATGGCCTGAATCACTTG	forward
	AGCCTGAAGTTCTCAGGATCCA	reverse
HB Gamma	TTGGGAAGGCTTCTTGTTGT	forward
	AAGCAGAGGACAAGTTCCCA	reverse
EPO receptor	GGACACCTACTTGGTATTGG	forward
	GACGTTGTAGGCTGGAGTCC	reverse
GATA1	GGCAAGACGGCACTCTACC	forward
	CAAGAACGTGTTGTTGCTCTTC	reverse
Pu.1	TATCAAACCTTGTCCCCAGC	forward
	GCGAATCTTTTTCTTGCTGC	reverse
mCox	ACGAAATCAACAACCCCGTA	forward
	GGCAGAACGACTCGGTTATC	reverse

Table 7: qRT-PCR primers used with Runx1$^{HTY350-352AAA}$ bone marrow

Histology

Soft tissues were fixed in formalin overnight and then embedded in paraffin. Bones for marrow sections were fixed in paraformaldehyde for 3 days under vacuum and then decalcified for 14 days using 0.5 M EDTA prior to embedding. Six micron sections were stained with hematoxylin and eosin by standard procedures. Embryonic day 12.5 embryos were dissected from timed pregnancies and placed in PBS. Images were then captured using a Axioskop 40 (Carl Zeiss, Inc., Maple Grove, MN) equipped with a AxioCam HRc and AxioVision Rel. 4.7 software (Zeiss).

Results

The Runx1$^{HTY350-352AAA}$ homozygous mice bypass embryonic lethality

To investigate the biological importance of Runx1 interactions with regulatory co-factors and the nuclear architecture in vivo, we generated a knock-in mouse model with a Runx1 missense mutation (Runx1$^{HTY350-352AAA}$; denoted HTY in figures and tables). This allele expresses a protein with a triple point mutation in the domain important for subnuclear targeting[103] and interaction with several known co-factors, including SMADs.[18-20,134,135,145] Runx1$^{HTY350-352AAA}$ was introduced into the endogenous Runx1 locus by homologous recombination (Figure 21A), confirmed by Southern blot analysis and PCR assays. An engineered SacII site diagnostic for the HTY to AAA mutation was used to discriminate between the amplified PCR products from the wildtype and mutant alleles (Figure 21B). Genotyping results revealed that Runx1$^{HTY350-352AAA}$ homozygous mice are born at near Mendelian ratios and thus bypass the embryonic day 12.5 lethality associated with Runx1 ablation or C-terminal deletion (Figure 21C). Runx1$^{HTY350-352AAA}$ homozygous embryos at embryonic day 12.5 were similar to wildtype littermates (Figure 21D). The weights of adult wildtype and mutant animals were similar at 12 weeks or 12 months of age (Figure 21E). Runx1 RNA levels in the bone marrow of wildtype and mutant animals are equivalent, indicating that the missense mutation does not destabilize the mRNA (Figure 21F). Immunofluorescence microscopy of whole cell and NMIF preparations of bone marrow cells from wildtype and Runx1$^{HTY350-352AAA}$ homozygous mice showed that while both Runx1 proteins are present within the nuclear matrix, association of the mutant Runx1 protein with the matrix may be decreased (Figure 21G).

Hence, the Runx1$^{HTY350-352AAA}$ mutation appears to retain essential functions of Runx1 during embryonic definitive hematopoiesis. Because Runx1 is required throughout hematopoiesis, we postulated that this mutation could have effects in hematopoietic progenitors or at different stages of hematopoietic lineage progression.

Figure 21: Runx1$^{HTY350-352AAA}$ mouse bypasses embryonic lethality.

(A) Targeting vector for the knock-in mouse contained a floxed Neo cassette as a positive selection marker and a TK cassette for negative selection to ensure homologous recombination in ES cells. (B) Successful targeting to the native Runx1 locus results in a diagnostic SacII site that allows for genotyping by PCR and enzyme digest. From left to right are genotyping results showing the change in digest fragment sizes from a wildtype, heterozygous and homozygous Runx1$^{HTY350-352AAA}$ mouse. (C) Runx1$^{HTY350-352AAA}$ animals were born at Mendelian ratios. (D) Runx1$^{HTY350-352AAA}$ embryos are healthy at embryonic day 12.5 and are comparable to wildtype littermates (3 litters, n=8 WT, 7 HTY). Scale bars are 1mm. (E) Adult wildtype and Runx1$^{HTY350-352AAA}$ mice at 12 weeks or 12 months are equivalent in weight (n=16 WT, 19 HTY for 12 weeks and 15 WT, 9 HTY for 12 months). (F) qRT-PCR for Runx1 in bone marrow cells shows no difference in expression levels (p=0.8 by Student's T test). Each point represents the average of technical replicates from one animal normalized to mCox expression (n=9 WT, 9 HTY). (G) Whole cell and nuclear matrix-intermediate filament (NMIF) preparations of bone marrow from 12 week old wildtype and Runx1$^{HTY350-352AAA}$ animals shows that Runx1 is still present within the nuclear matrix. The heterogeneity of the bone marrow preparations complicated quantification of Runx1 signal, as endogenous expression levels vary widely. Therefore representative Runx1 expressing cells are shown (n=3 WT, 3 HTY). Scale bars are 10 um. All error bars are SEM.

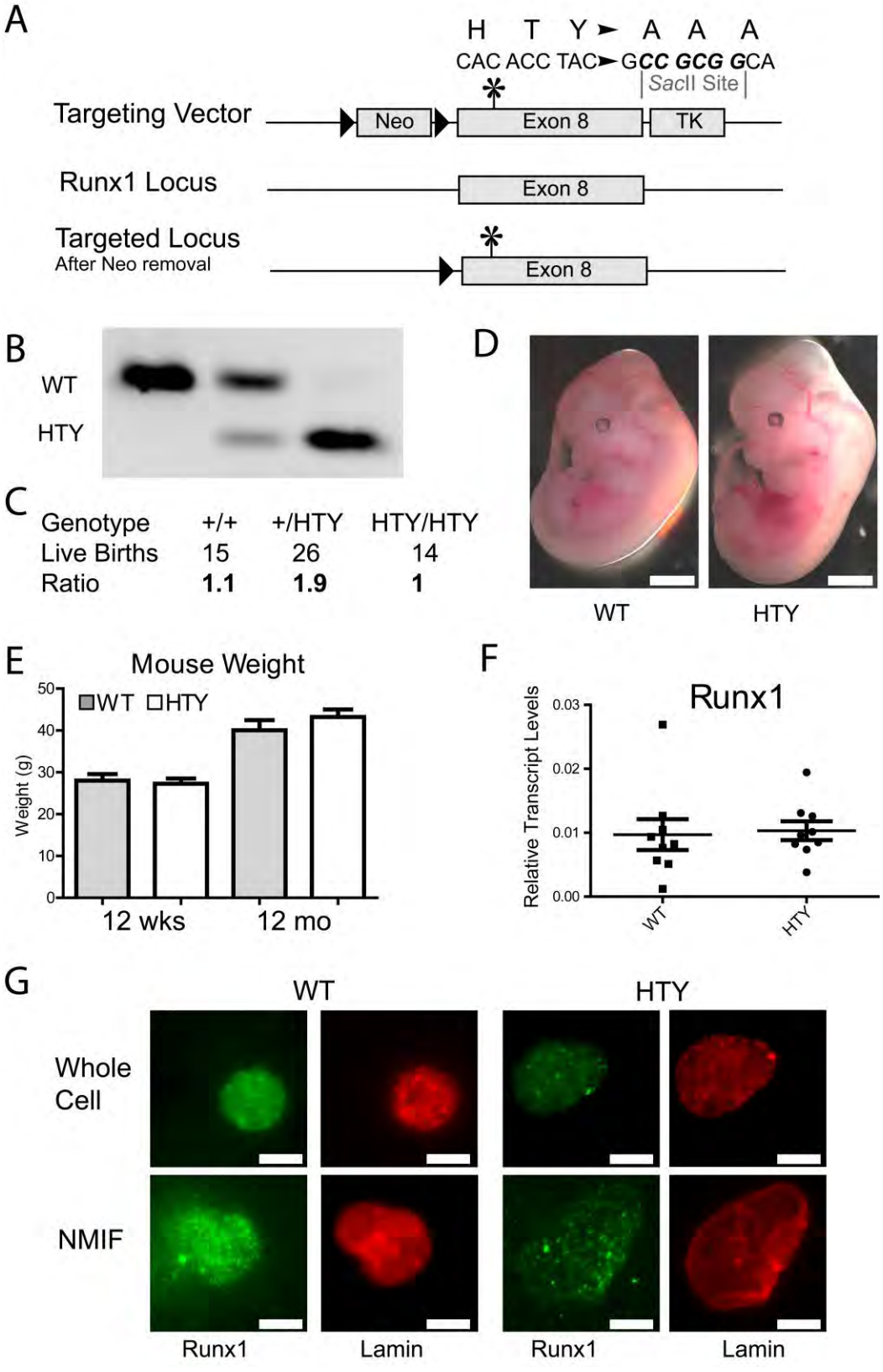
A
H T Y ➤ A A A
CAC ACC TAC➤ GCC GCG GCA
SacII Site
Targeting Vector
Neo
Exon 8
TK
Runx1 Locus
Exon 8
Targeted Locus
After Neo removal
Exon 8
B
WT
HTY
C
Genotype +/+ +/HTY HTY/HTY
Live Births 15 26 14
Ratio 1.1 1.9 1
D
WT
HTY
E
Mouse Weight
WT HTY
Weight (g)
50
40
30
20
10
0
12 wks
12 mo
F
Runx1
Relative Transcript Levels
0.03
0.02
0.01
0.00
WT
HTY
G
WT
HTY
Whole Cell
NMIF
Runx1
Lamin
Runx1
Lamin

Peripheral blood from Runx1$^{HTY350-352AAA}$ mice reveals subtle hematopoeitic defects

As part of the initial characterization of the Runx1$^{HTY350-352AAA}$ mice, blood was collected for complete blood counts at 8 weeks of age (Table 8). Screening of a large number of animals (n=33 wildtype, 26 mutant) revealed subtle, yet consistent and statistically significant, alterations. There were no alterations in white blood cells that reached statistical significance. However, we observed a significant increase in platelet number and size (Table 8, $p<0.001$ and $p=0.012$). We also observed a subtle, sub-clinical anemia. Absolute red blood cell count was increased, but the cell volume was so much smaller that hematocrit was significantly lower than wildtype (Table 8, $p=0.025$). These alterations in the peripheral blood prompted examination of the bone marrow.

Complete Blood Counts at 8 weeks	WT	n=33	HTY	n=26	p value
White Blood Cells	6.38	± 2.33	5.59	± 1.64	0.13
Lymphocytes	5.22	± 2.03	4.52	± 1.48	0.12
Granulocytes	0.71	± 0.42	0.64	± 0.39	0.53
Monocytes	0.45	± 0.29	0.43	± 0.18	0.79
Hematocrit	50.84	± 5.56	47.74	± 5.16	0.025
Mean Corpuscle Volume	51.05	± 3.87	45.20	± 1.34	<0.00001
Red Blood Cells	9.96	± 0.83	10.58	± 1.26	0.035
Hemoglobin	16.62	± 1.00	17.34	± 1.59	0.050
Mean Cell Hemoglobin	16.72	± 0.64	16.45	± 0.73	0.15
Hemoglobin Concentration	32.92	± 2.37	36.42	± 0.73	<0.00001
Red Cell variability	17.61	± 1.77	20.69	± 1.34	<0.00001
Platelet Volume	6.01	± 0.21	6.21	± 0.20	<0.001
Platelet Count	698.09	± 136.48	795.56	± 149.25	0.012

Table 8: Complete blood counts of 8 week old animals

At 8 weeks of age, peripheral blood samples were collected by retro-orbital bleeds. Complete blood counts for 33 wildtype and 26 Runx1$^{HTY350\text{-}352AAA}$ homozygous animals are compiled in this table with means listed. Errors shown are standard deviation and p values were calculated using Student's T test.

The Runx1$^{HTY350-352AAA}$ mutation compromises growth control in bone marrow cells

Runx1 may help to preserve long-term hematopoietic repopulating capacity by maintaining HSC quiescence and appropriate apoptosis.[62] Expression of a naturally occurring, dominant negative truncated form, Runx1a, in HSC enhanced proliferation and increased short-term engraftment.[109] To examine hematopoietic progenitor properties in the Runx1$^{HTY350-352AAA}$ mice, bone marrow cells from wildtype and homozygous mutant animals were isolated and cultured ex vivo. After 7 days in culture, there were significantly more cells in cultures from the knock-in animals (Figure 22A, $p<0.001$). In contrast, when the same cells were instead plated in methocellulose for colony forming unit (CFU) assays, they formed fewer colonies (Figure 22B, $p=0.027$). These data indicate that Runx1$^{HTY350-352AAA}$ bone marrow cells, while more proliferative, have diminished progenitor capacity. The majority of cells taken from day 7 *ex vivo* cultures from both wildtype and Runx1$^{HTY350-352AAA}$ mice express the myeloid lineage antigen CD11b (Figure 22C) with very low expression of the B lymphoid B220 or T lymphoid CD3 (data not shown). Given the known roles of Runx1 in myeloid and B lymphocyte development, these results warranted further investigation of committed populations in the Runx1$^{HTY350-352AAA}$ mice.

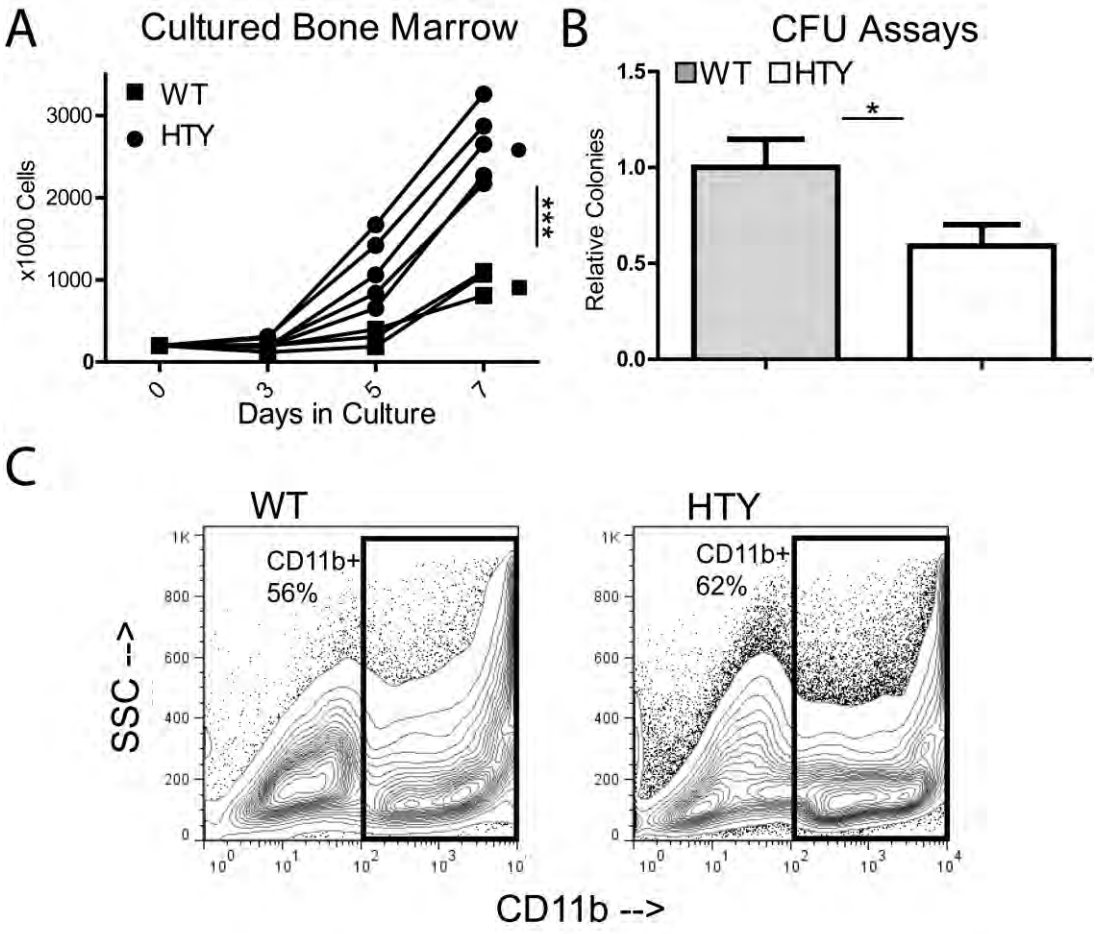

Figure 22: Increased ex vivo growth and diminished colony forming ability of Runx1$^{HTY350-352AAA}$ marrow.

(A) Ex vivo cultures of bone marrow cells from wildtype or Runx1$^{HTY350-352AAA}$ animals (each point represents the mean cell number of three technical replicates from one animal; n=3 WT, 5 HTY). (B) Myeloid colony forming unit assays performed with wildtype or Runx1$^{HTY350-352AAA}$ bone marrow cells (n=28 WT, 34 HTY). (C) Cells from the experiment reported in panel A were harvested at day 7 and the percentage of cells expressing the myeloid antigen CD11b was determined using flow cytometry (n=3 WT, 3 HTY). * $p<0.05$, *** $p<0.001$, calculated by Student's T test. All error bars are SEM.

TGF beta is involved in maintaining HSC quiescence; however, the exact mechanism is poorly understood.[146-148] SMAD proteins mediate TGF beta signaling, and Runx1 interacts with SMAD proteins during hematopoietic development. Therefore, we asked if TGF beta signaling is perturbed in the presence of Runx1$^{HTY350-352AAA}$. Both ex vivo growth and CFU assays were repeated with the addition of TGF beta in the medium. Growth was suppressed by TGF beta in both wildtype and Runx1$^{HTY350-352AAA}$ cultures, but the Runx1$^{HTY350-352AAA}$ cells proliferated more rapidly than wildtype (Figure 22A, p=0.024). Similarly, adding TGF beta to the CFU assays suppressed colony forming ability, but the difference between wildtype and Runx1$^{HTY350-352AAA}$ marrow was maintained (Figure 22B). These data reveal that the mechanism by which TGF beta causes quiescence remains intact within the bone marrow of Runx1$^{HTY350-352AAA}$ homozygous mice, indicating that TGF beta mediation of quiescence does not signal through Runx1.

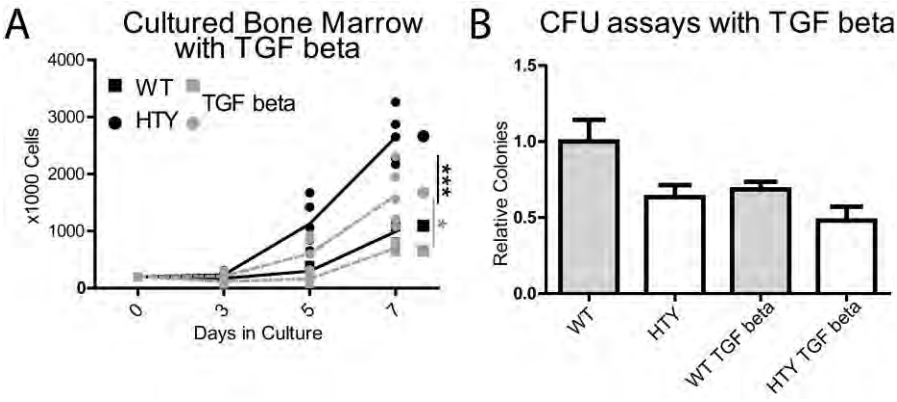

Figure 23: TGF beta mediated quiescence does not signal through Runx1.

Ex vivo culture (A) and CFU assays (B) as in Figure 22A and B, but with additional TGF beta to a final concentration of 10 ng per mL (error bars are SEM and each point represents mean cell number of three technical replicates from one animal; n=3 WT, 5 HTY). As CFU assays in (B) used only TGF beta or vehicle treated cells there were insufficient replicates to maintain statistical signifigance. * $p<0.05$, *** $p<0.001$, calculated with Student's T test.

Runx1$^{HTY350-352AAA}$ under hematopoietic stress

Treatment with 5-flourouracil (5-FU) is used to poison transit amplifying cells and thereby force repopulation of hematopoietic lineages and mobilize progenitors.[149] We treated wildtype and Runx1$^{HTY350-352AAA}$ mice with 5-FU and 6 days later analyzed peripheral blood with complete blood counts (CBC) and collected bone marrow cells for CFU assays. While the overall white blood cell counts after treatment were similar, on Day 6 after 5-FU treatment the Runx1$^{HTY350-352AAA}$ mice recovered significantly more granulocytes and monocytes than wildtype (Table 9). Also their platelet counts were higher, albeit more variable (Table 9). The CBC data implies that Runx1$^{HTY350-352AAA}$ bone marrow is able to expand myeloid cells more quickly. CFU assays were performed with bone marrow cells from animals treated with vehicle or 5-FU. As expected after 5-FU treatment, both wildtype and mutant marrow made more colonies than vehicle treated. In both vehicle and 5-FU treatment groups the Runx1$^{HTY350-352AAA}$ cells formed fewer colonies than wildtype (Figure 24), but the n was not large enough to reach statistical significance as in Figure 22B.

Complete Blood Counts Day 6 after 5-FU					
	WT	(n=11)	HTY	(n=11)	p value
White Blood Cells	2.59	± 1.27	2.96	± 1.27	0.498
Lymphocyte	2.36	± 1.15	2.49	± 1.19	0.801
Granulocyte	0.11	± 0.14	0.25	± 0.15	0.028
Monocyte	0.12	± 0.10	0.22	± 0.08	0.014
Platelet Volume	6.41	± 0.31	6.83	± 0.37	0.009
Platelet Count	388.45	± 104.04	593.82	± 311.80	0.051

Table 9: Complete blood counts of peripheral blood after 5-FU treatment

Peripheral blood was taken from wildtype and Runx1$^{HTY350\text{-}352AAA}$ mice 6 days after IP injection with 5-FU. Complete blood counts for 11 wildtype and Runx1$^{HTY350\text{-}352AAA}$ animals are compiled in this table, with means listed. Errors shown are standard deviation and p values were calculated using Student's T test.

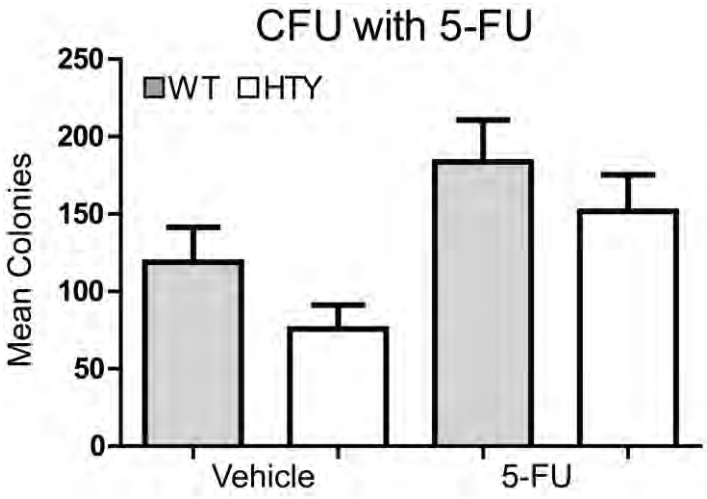

Figure 24: CFU assays of wildtype and Runx1$^{HTY350\text{-}352AAA}$ bone marrow after 5-FU treatment

Wildtype and Runx1$^{HTY350\text{-}352AAA}$ homozygous mice were treated with 5-FU or vehicle by IP injection. 6 days after injection, bone marrow cells were isolated and used in colony forming unit assays. Colonies were counted by visual inspection after 7 days of incubation (n=6 WT, 8 HTY for vehicle and 8 WT, 9 HTY for 5-FU). Error bars are SEM.

Gene expression analysis of bone marrow of Runx1$^{HTY350-352AAA}$ homozygous mice

To assess if Runx1$^{HTY350-352AAA}$ was causing dramatic changes in gene expression, bone marrow was isolated from wildtype and Runx1$^{HTY350-352AAA}$ homozygous animals for qRT-PCR analysis. The majority of genes examined showed no change in expression. Runx transcription factors, Cebp transcription factors and the GATA family of hematopoietic transcription factors were all unchanged (Figure 25A). Bmi1 is important for self-renewal in hematopoietic cells[150,151], SCL is required for long term HSC function[152,153] and Gfi1 is important for progenitor growth regulation.[154,155] These three genes also showed similar expression levels (Figure 25A). VpreB1 and Rag1 are important in B cell maturation[156,157] and their expression levels were down, but not enough to maintain statistical significance. However, LCN2 and IRF4 are inflammation regulatory genes[158-160] that were expressed at significantly lower levels (Figure 25B). Expression levels of phenotypic myeloid genes such as Neutrophil Elastase, MPO, Csf1R,Gr1 and CD11b was also generally similar, with only the reduction of GM-CSF maintaining statistical significance (Figure 25C). The platelet myosin light chain (Myl9) is important in platelet function and directly regulated by Runx1.[161,162] The gene expression of Myl9 was significantly reduced in Runx1$^{HTY350-352AAA}$ marrow (Figure 25D, $p<0.01$). In addition, Id1, a transcription factor that can contribute to myeloid leukemia[163] and is upregulated by the leukemic fusion protein Runx1-ETO[164], was markedly increased (Figure 25E, $p<0.001$). These results indicate deregulation of gene expression in several hematopoietic lineages. The analysis was performed on total bone

marrow and would therefore not be able to detect gene expression changes in a particular cell compartment or alterations of genes that are only expressed by a small population of cells. The gene expression alterations observed in total bone marrow prompted investigation of specific hematopoietic lineages.

Figure 25: qRT-PCR of bone marrow from Runx1$^{HTY350\text{-}352AAA}$ mice

RNA was isolated from bone marrow cells of 12 week old wildtype and Runx1$^{HTY350\text{-}352AAA}$ homozygous mice. qRT-PCR was performed to measure expression levels of master phenotypic transcription factors and genes important for progenitor growth control (A), genes regulating lymphoid development (B), myeloid phenotypic genes (C), a gene important in platelet function (D) and a hematopoietic gene implicated in Runx1-ETO driven malignancy (E). Expression levels were normalized to mCox. Each point represents the mean of technical replicates from one animal (n=3 to 10). * $p<0.05$, ** $p<0.01$, *** $p<0.001$, calculated by Student's T test. All error bars are SEM. All expression levels are shown relative to mCox. For specific primers please see Table 7.

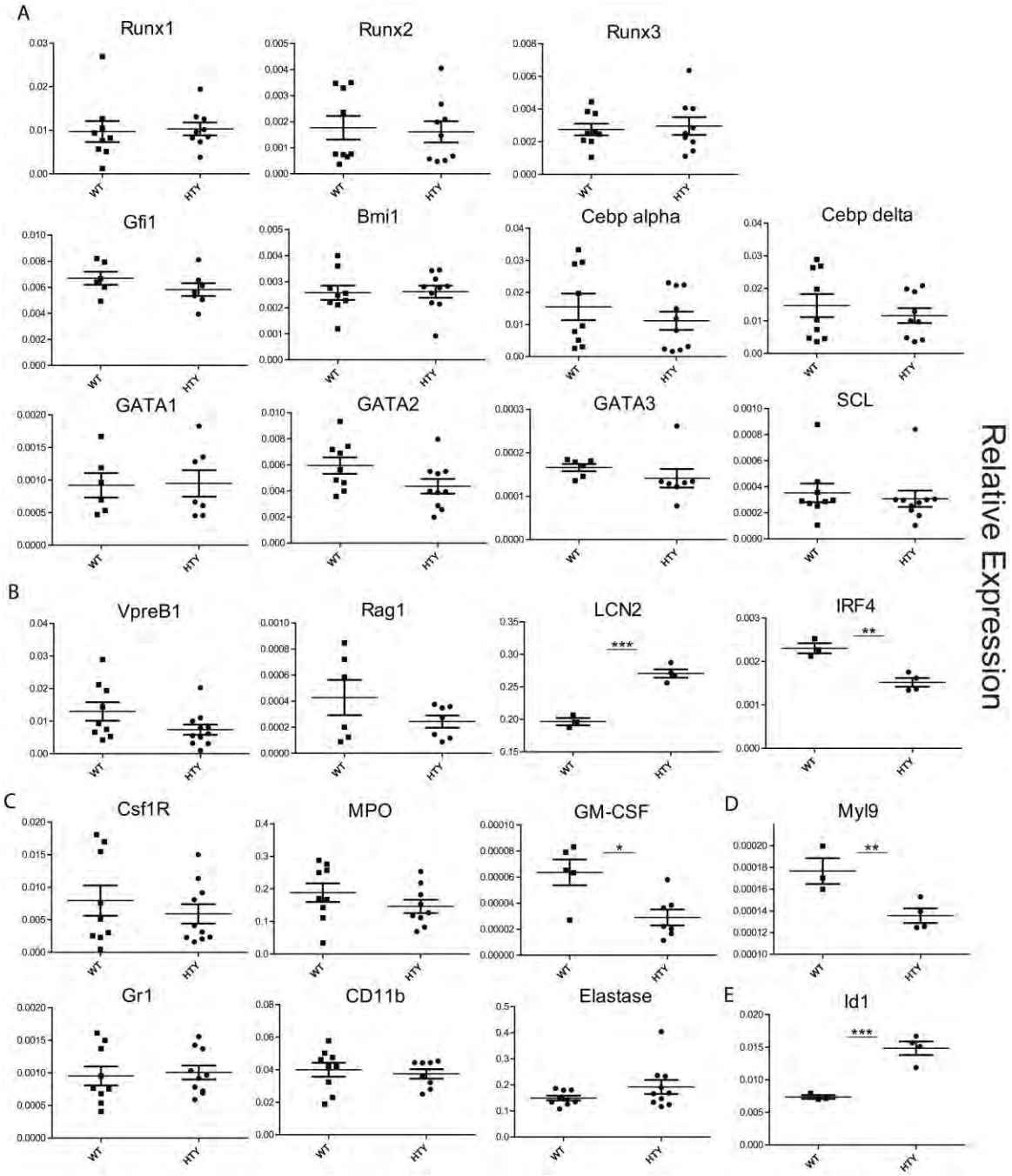
A
Runx1
Runx2
Runx3
Gfi1
Bmi1
Cebp alpha
Cebp delta
GATA1
GATA2
GATA3
SCL
B
VpreB1
Rag1
LCN2
***
IRF4
**
C
Csf1R
MPO
GM-CSF
*
D
Myl9
**
Gr1
CD11b
Elastase
E
Id1
***
WT
HTY
Relative Expression

The Runx1$^{HTY350-352AAA}$ mutation compromises maintenance of early hematopoietic progenitors

To assess alterations in the earliest progenitor populations, bone marrow from Runx1$^{HTY350-352AAA}$ mice was analyzed by flow cytometry. There was a small yet statistically significant decrease in the lineage negative, Sca1 positive, c-Kit positive population (LSK) which contains HSC, with no significant reductions in the lineage negative, Sca1 negative, c-Kit positive (LS-K+) myeloid precursors and lineage negative, Sca1 positive, c-Kit negative (LS+K-) lymphoid precursors[165] (Figure 26A and B). The frequency of common lymphoid progenitor (CLP; Lineage-, IL7Ralpha +, AA4.1+, c-Kit intermediate) cells in the Runx1$^{HTY350-352AAA}$ mice was similar to wildtype (Figure 26C and D). The LS-K+ compartment contains common myeloid progenitors (CMP), which further differentiate into either granulocyte-monocyte progenitors (GMP) or megakaryocyte erythroid progenitors (MEP). We determined that these discrete populations were not significantly different in Runx1$^{HTY350-352AAA}$ bone marrow when compared to wildtype mice (Figure 26E and F).

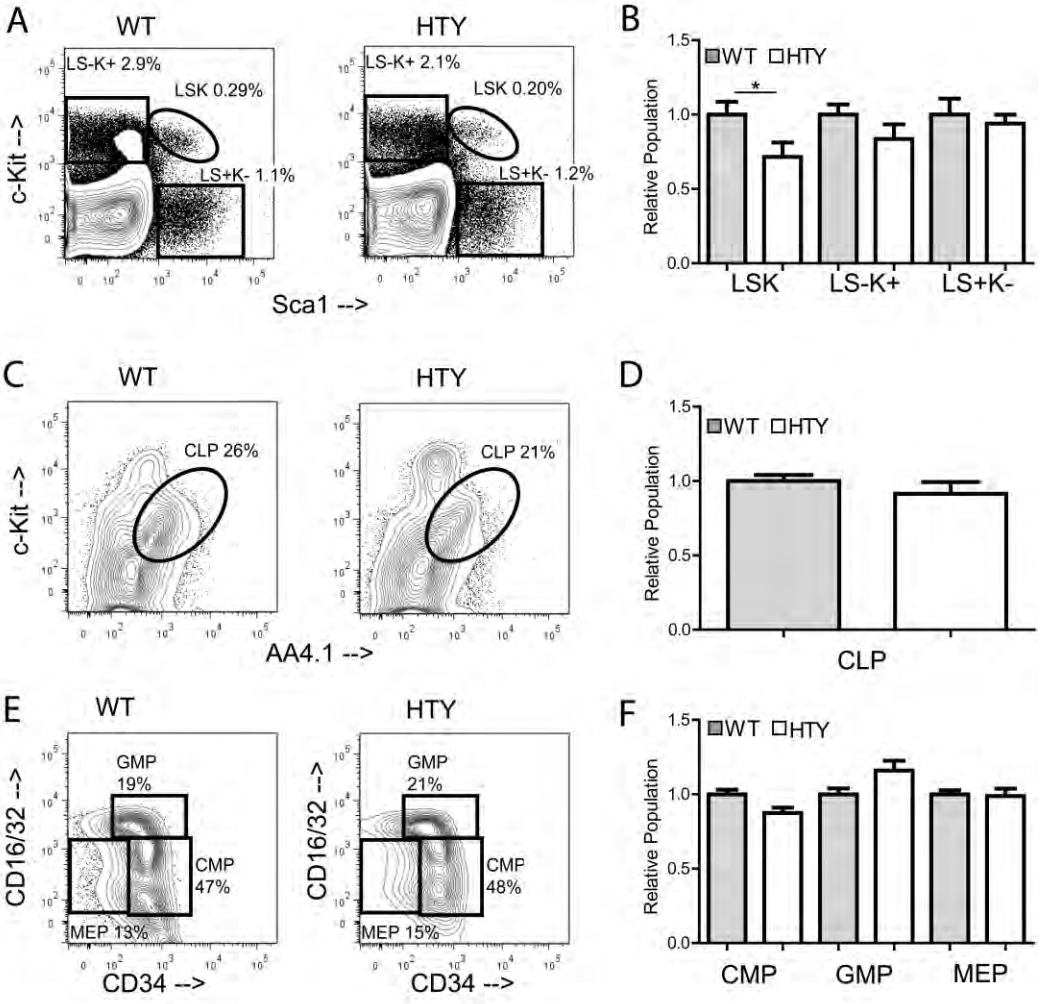

Figure 26: Progenitors in Runx1$^{HTY350-352AAA}$ bone marrow.

(A) Bone marrow cells from wildtype or Runx1$^{HTY350-352AAA}$ animals were stained using antibodies to c-Kit, Sca1, CD16/32, CD34, IL7Ralpha, AA4.1 and Lineage markers (CD3, CD11b, B220, Ter119, Gr1) and analyzed by flow cytometry. Lineage negative cells were gated and are plotted in panel A to highlight the Lin-Sca1+Kit+ (LSK), myeloid potential L-S-K+ and lymphoid potential L-S+K- fractions. (B) Quantification of multiple experiments performed as depicted in A, normalizing to the wildtype average of each experiment (n=13 WT, 13 HTY). (C) Lineage negative and IL7R alpha positive bone marrow cells were gated and c-Kit versus AA4.1 was plotted to measure AA4.1+, c-Kit intermediate CLP. (D) Quantification of multiple experiments in C (n=6 WT, 6 HTY). (E) Lineage negative, c-Kit positive, Sca1 negative (L-S-K+) cells from panel A were plotted as CD16/32 versus CD34 to measure the CMP, GMP and MEP progenitor populations. (F) Quantification of multiple experiments as in E, normalizing to the wildtype average of each experiment (n=10 WT, 10 HTY). * $p<0.05$, calculated by Student's T test. All error bars are SEM.

Deregulation of B and T lymphoid cells with Runx1$^{HTY350-352AAA}$

We further examined B and T lymphopoiesis in the Runx1$^{HTY350-352AAA}$ mice as Runx1 is known to have important biological functions in the maturation of both of these lineages. Spleens of the Runx1$^{HTY350-352AAA}$ homozygous animals were significantly enlarged (Figure 27A, p=0.019), consistent with the splenomegaly that occurs following conditional Runx1 ablation.[125] Histological examination of Runx1$^{HTY350-352AAA}$ spleens showed deregulation of the white pulp, with decreased delineation of follicles and lower cell density (Figure 27B). Bone marrow of Runx1$^{HTY350-352AAA}$ mice exhibited slightly increased mature and decreased immature B cell populations (Figure 27C and D, $p<0.0001$ and $p<0.001$), consistent with a moderate impairment of B-lymphopoiesis. Furthermore, there was a decrease in the pre-Pro-B and increase in the Pro-B populations (Figure 27E and F, p=0.005 and p=0.04). Taken together, these findings indicate that defective Runx1 function from the HTY350-352AAA mutation perturbs B-lymphopoiesis at multiple stages.

We observed fewer CD8 single positive cells in both the spleen and thymus of Runx1$^{HTY350-352AAA}$ animals (Figure 28A and B, p=0.038 and 0.038). The discrete populations of CD4/CD8 double negative T cell progenitors within the thymus were not altered (Figure 28D and E), nor was thymus size of Runx1$^{HTY350-352AAA}$ animals (Figure 28C). Our findings indicate that the knock-in mutation does not interfere with early T-lymphoid development, but alters single positive populations during T cell maturation.

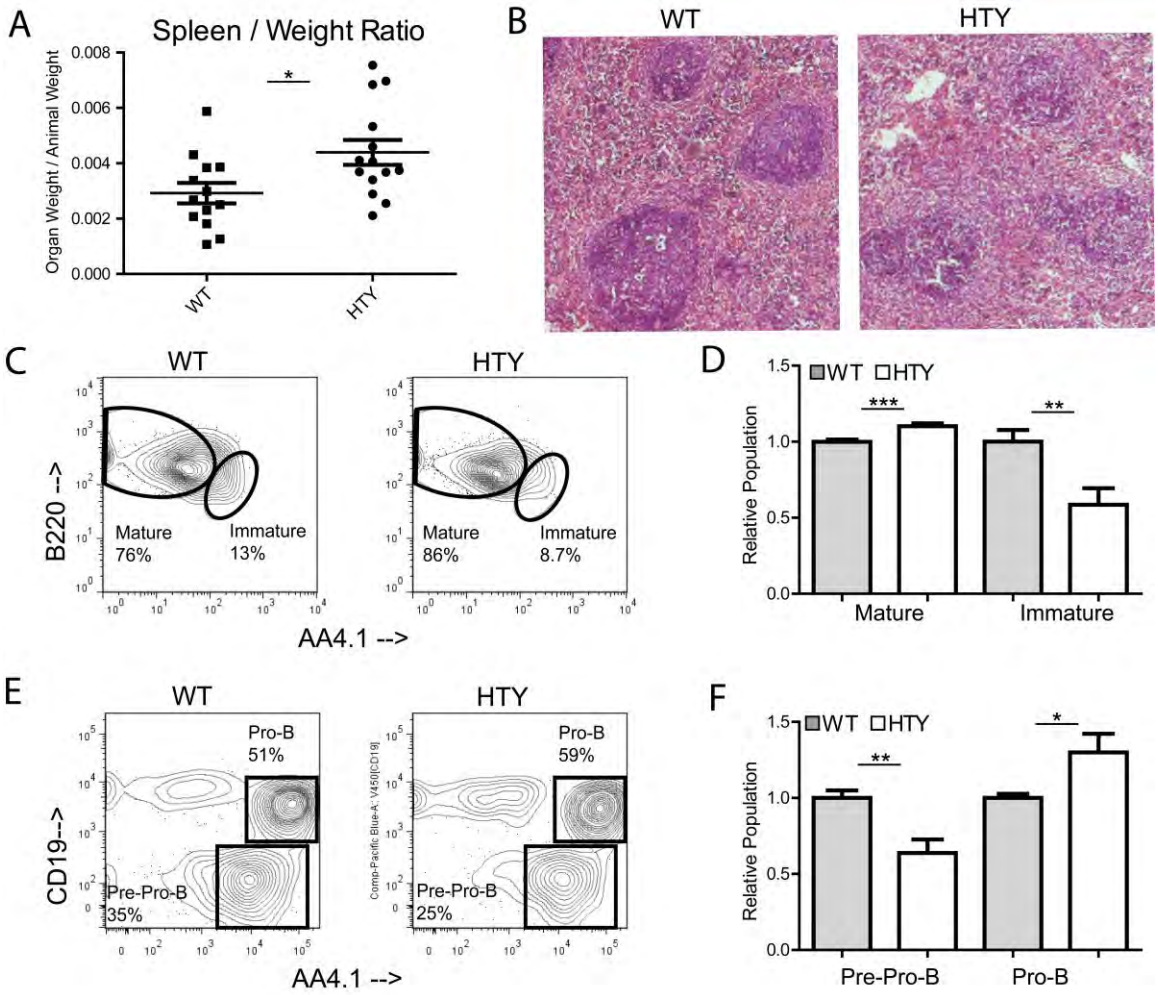

Figure 27: B lymphopoiesis in Runx1$^{HTY350\text{-}352AAA}$ animals.

(A) At sacrifice, animals were weighed then the spleen and/or thymus was removed and weighed. Displayed is the spleen weight normalized to total animal weight. Each point represents one animal (n=14 WT, 15 HTY). (B) Spleens from 12 month old wildtype or Runx1$^{HTY350\text{-}352AAA}$ mice were formalin fixed, sectioned and then stained by H & E. Representative fields are shown (n=3 WT, 3 HTY). (C) Bone marrow cells from wildtype or Runx1$^{HTY350\text{-}352AAA}$ animals were stained for B220, IgM, AA4.1 and CD43. B220 positive and IgM positive cells were gated to show expression of AA4.1 to separate Immature and Mature B cells. (D) Quantification of multiple experiments performed as in C (n=12 WT, 12 HTY). (E) Bone marrow cells from wildtype or Runx1$^{HTY350\text{-}352AAA}$ animals were stained for B220, IgM, AA4.1, Ly6C, CD49b, CD19 and CD43. Cells positive for Ly6C, CD49b and IgM were excluded by gating, and the CD43+ B220+ subset is shown to measure AA4.1+ CD19- pre-Pro-B cells and AA4.1+ CD19+ pro-B cells. (F) Quantification of multiple experiments as in E (n=6 WT, 6 HTY). * $p<0.05$, ** $p<0.01$, *** $p<0.001$, calculated by Student's T test. All error bars are SEM.

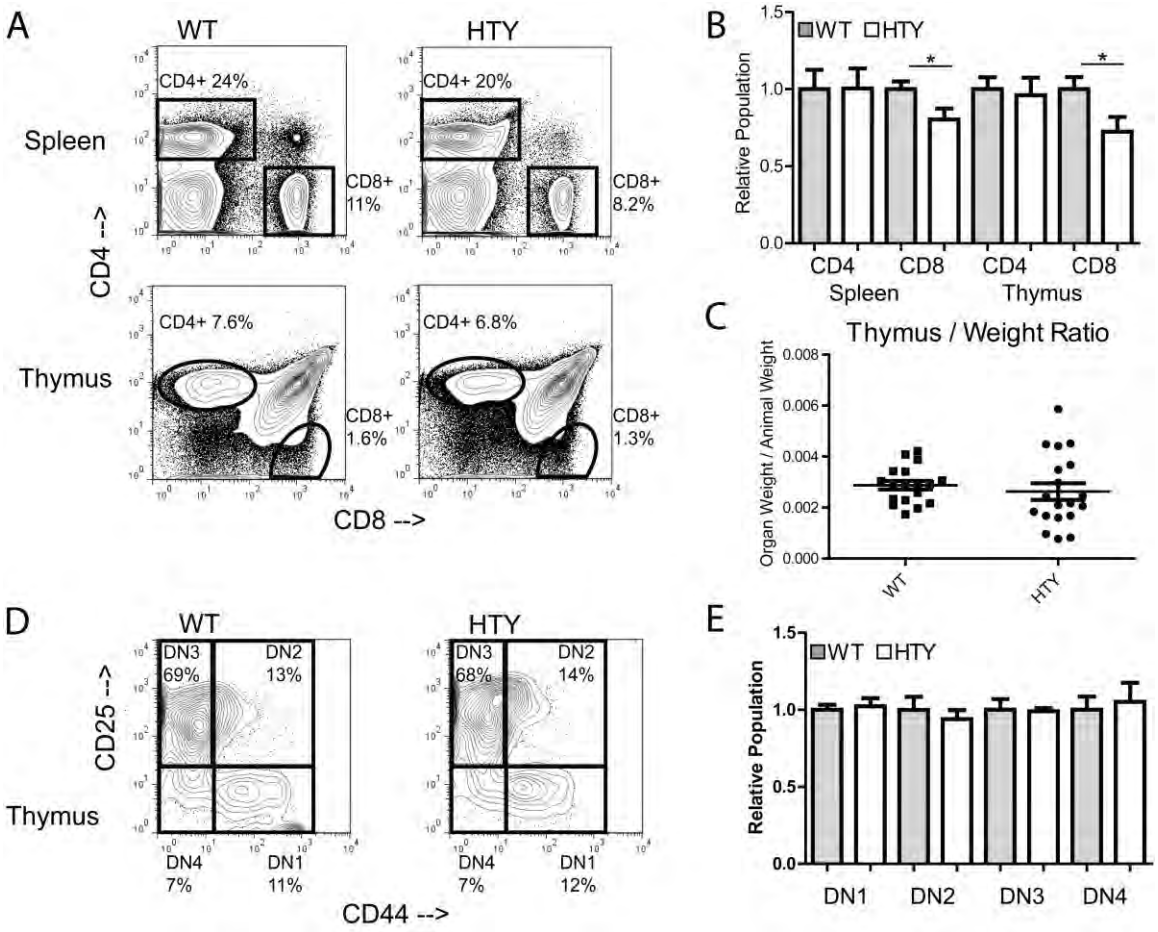

Figure 28: Altered T lymphopoiesis in Runx1$^{HTY350-352AAA}$ animals

(A) Spleen or thymus cells were isolated and stained with CD4 and CD8. Cells were gated and plotted as CD4 versus CD8 to measure CD4+ and CD8+ T cell populations. (B) Quantification of multiple experiments as shown in A (n=12 WT, 14 HTY for both spleen and thymus). (C) Displayed is the thymus weight normalized to total animal weight (n=18 WT, 19 HTY). (D) Thymus cells were stained with CD4, CD8, CD25 and CD44. CD4 and CD8 double negative cells are plotted with CD25 versus CD44 to show the DN1 through DN4 T-Cell progenitor populations. (E) Quantification of multiple experiments shown in D (n= 7 WT, 9 HTY). * $p<0.05$, calculated by Student's T test. All error bars are SEM.

Runx1$^{HTY350-352AAA}$ causes over expansion in both myeloid and megakaryocytic lineage cells

Runx1 mutations are often implicated in myeloid leukemia and Runx1 point mutations are associated with familial platelet disorders.[77,79,96] Conditional Runx1 ablation in adult mice causes defects in myeloid and megakaryocytic lineages.[79] Therefore, we anticipated the most striking differences in our knock-in mouse would be observed there. We noted a significant increase in both the mature granulocyte (CD11b positive, Gr1 high; $p<0.0001$) and immature monocyte / macrophage (CD11b positive, Gr1 intermediate; $p<0.0001$) populations in the spleens of Runx1$^{HTY350-352AAA}$ mice (Figure 29C and D). However, the granulocyte population was not significantly different in the bone marrow (Figure 29A and B). The expansion in the spleen is consistent with the growth factor independent proliferation we observed in murine myeloid cell lines harboring similar mutations.[87] The expansion also suggests that much of the observed splenomegaly (Figure 27A) may be a consequence of myeloid expansion, infiltration and/or accumulation in the spleen, similar to that observed in the Runx1 conditional mouse.[79]

Megakaryocytic maturation is known to be particularly sensitive to Runx1.[66] We observed that the CD41 positive compartment of both bone marrow and spleen was slightly expanded in Runx1$^{HTY350-352AAA}$ mice (Figure 29E and F). This finding was unexpected because conditional Runx1 ablation is known to cause thrombocytopenia.[77,125] Therefore, we next examined the maturation status of the CD41

compartment, using propidium iodide staining to assay DNA content in the CD41 positive cells. This analysis suggests maturation of megakaryocytes is delayed, as shown by the marked decrease in 8N and 16N cells compared with the wildtype reference (Figure 29G). We confirmed this finding with histological analysis of the bone marrow. While some megakaryocytes in the marrow appeared normal, we observed many smaller megakaryocytes with less nuclear hematoxylin staining compared with wildtype marrow (Figure 29H). These results indicate that Runx1$^{HTY350\text{-}352AAA}$ causes a delay in megakaryocyte maturation, but the expanded compartment apparently allows the homozygous mice to maintain normal, albeit slightly higher, platelet counts (Table 8).

Figure 29: Alterations in myeloid compartment and megakaryocytic maturation in Runx1$^{HTY350\text{-}352AAA}$ animals.

(A) Bone marrow cells stained with antibodies to Gr1 and CD11b to measure the Gr1 positive CD11b positive granulocyte population. (B) Quantification of multiple experiments shown in A (n=7 WT, 9 HTY). (C) Spleen cells were stained with antibodies to Gr1 and CD11b to measure the Gr1 high, CD11b positive granulocyte and the Gr1 intermediate CD11b positive monocyte / macrophage populations. (D) Quantification of multiple experiments performed as shown in A (n=7 WT, 9 HTY) (E) Bone marrow or spleen cells were stained for CD41 to measure the megakaryocyte population. (F) Quantification of multiple experiments shown in C (n=12 WT, 14 HTY). (G) Bone marrow cells were stained for CD41, fixed with ethanol and then stained with propidium iodide to detect DNA content. Displayed is the CD41 positive fraction, with normal hyperploidy of a representative wildtype sample plotted in black, with Runx1$^{HTY350\text{-}352AAA}$ samples plotted in red to show the reduction in 8N and 16N cells. (H) Histological sections of bone marrow from 12 month old wildtype or Runx1$^{HTY350\text{-}352AAA}$ mice were H & E stained. Megakaryocytes that appear smaller and less hyperploid in the Runx1$^{HTY350\text{-}352AAA}$ animals are shown. *** $p<0.001$, calculated by Student's T test. All error bars are SEM.

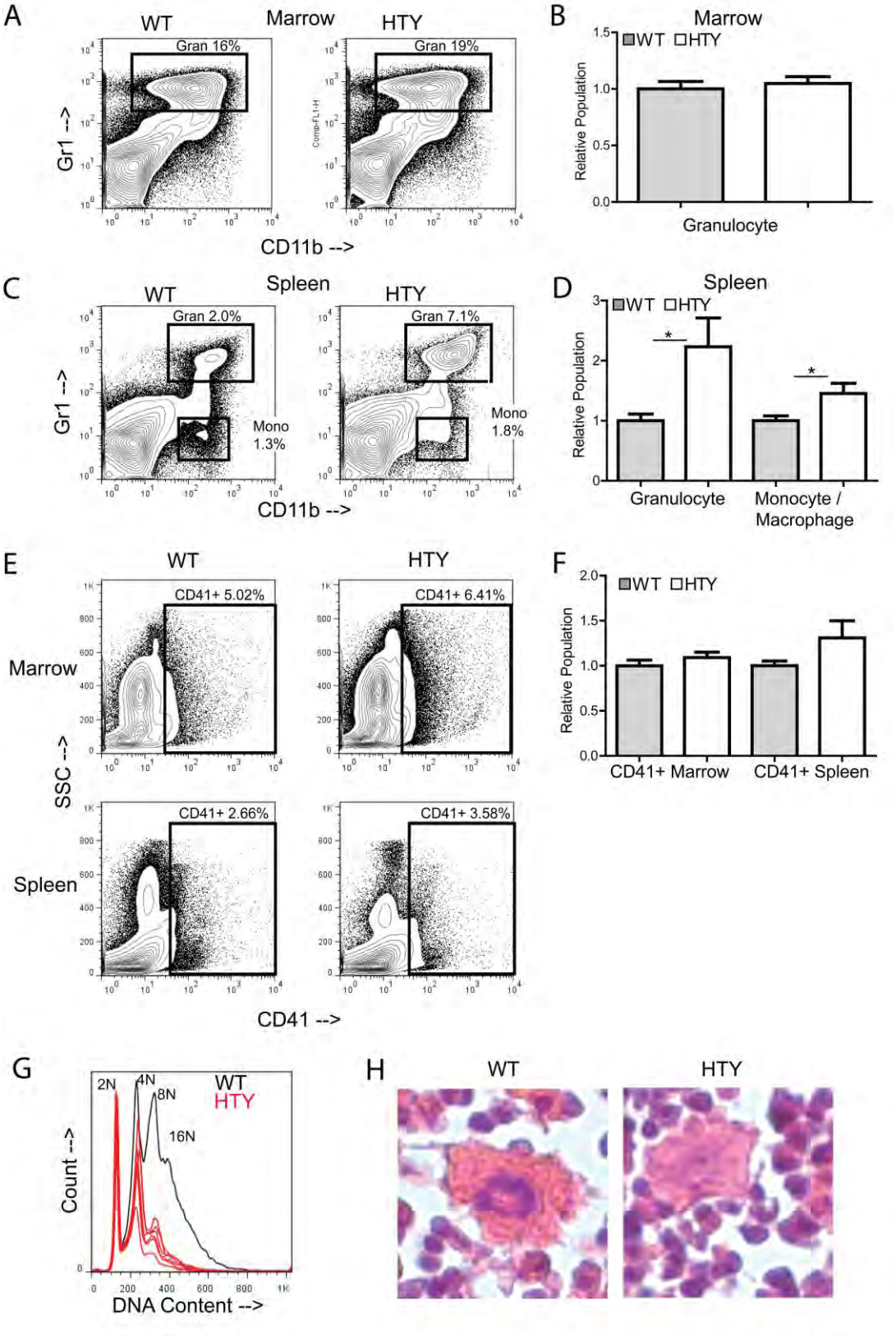
A
WT
Marrow
HTY
Gran 16%
Gran 19%
Gr1 -->
CD11b -->
B
Marrow
WT HTY
Relative Population
Granulocyte
C
WT
Spleen
HTY
Gran 2.0%
Gran 7.1%
Mono 1.3%
Mono 1.8%
Gr1 -->
CD11b -->
D
Spleen
WT HTY
Relative Population
Granulocyte
Monocyte / Macrophage
E
WT
HTY
Marrow
CD41+ 5.02%
CD41+ 6.41%
Spleen
CD41+ 2.66%
CD41+ 3.58%
SSC -->
CD41 -->
F
WT HTY
Relative Population
CD41+ Marrow
CD41+ Spleen
G
2N
4N
8N
16N
WT
HTY
Count -->
DNA Content -->
H
WT
HTY

Red blood cell maturation is perturbed in Runx1$^{HTY350-352AAA}$ homozygous mice

CBC of Runx1$^{HTY350-352AAA}$ homozygous mice revealed a significantly lower hematocrit than wildtype (Table 8, p=0.025). Because the role of Runx1 in erythropoiesis is poorly understood, these preliminary results warranted closer examination.

We characterized erythroid progenitor populations using a validated method of flow cytometry analysis with the erythroid markers Ter117 and CD71.[166,167] Examination of bone marrow cells revealed an increase in early erythroid progenitor populations (ProE, EryA and EryB) and fewer mature red cell progenitors (EryC) (Figure 30A and C). The increase in ProE and EryB progenitors and the decrease in more mature EryC cells were all statistically significant ($p<0.001$, $p=0.012$ and $p<0.01$, respectively). In the spleen of Runx1$^{HTY350-352AAA}$ mice, ProE cell populations were similar to wildtype, and the increase of EryA and EryB with a subsequent decrease in EryC was still observed (Figure 30B and D). However, none of the differences in the spleen cells reached statistical significance ($p=0.14$, $p= 0.18$ and $p=0.054$ for EryA, EryB and EryC). Additionally, qRT-PCR analysis of bone marrow cells showed a significant decrease in the transcript levels of hemoglobin beta ($p=0.025$), with no significant alterations of hemoglobin alpha (Figure 30E). Fetal hemoglobin gamma was not significantly increased, inconsistent with a delay in globin switching in the mutant mice[168] (Figure 30E). Alteration of the alpha and beta hemoglobin balance may explain the smaller size of the red blood cells (Table 8). EPO receptor expression was suppressed in the Runx1$^{HTY350-352AAA}$ marrow, consistent with a defect in erythroid progenitors (Figure 30D, $p=0.068$ due to n=3 WT

and 4 HTY). However, neither the levels of the master erythroid transcription factor GATA1, nor those of PU.1, a known Runx1 target and direct inhibitor of GATA1, were significantly altered (Figure 30D). Thus, the Runx1$^{HTY350-352AAA}$ mutation provides new information regarding the role of Runx1 in erythroid development.

Figure 30: Altered red blood cell maturation in Runx1$^{HTY350-352AAA}$ animals.

(A) Bone marrow cells were stained for CD71 and Ter119 and plotted to measure the CD71 positive, Ter119 intermediate ProE population. Ter119 high cells were plotted CD71 versus forward scatter (FSC) to measure the EryA, EryB and EryC progenitor populations. (B) Spleen cells were stained and analyzed as in A. (C) Quantification of several experiments shown in A (n=12 WT, 14 HTY). (D) Quantification of several experiments shown in B (n=12 WT, 14 HTY). (E) qRT-PCR of bone marrow cells for hemoglobin genes (F) qRT-PCR for factors important for erythroid maturation and an important antagonist of erythropoiesis. Each point represents the average of technical replicates from one animal (n=3 to 11). * $p<0.05$, ** $p<0.01$, calculated by Student's T test. All error bars are SEM.

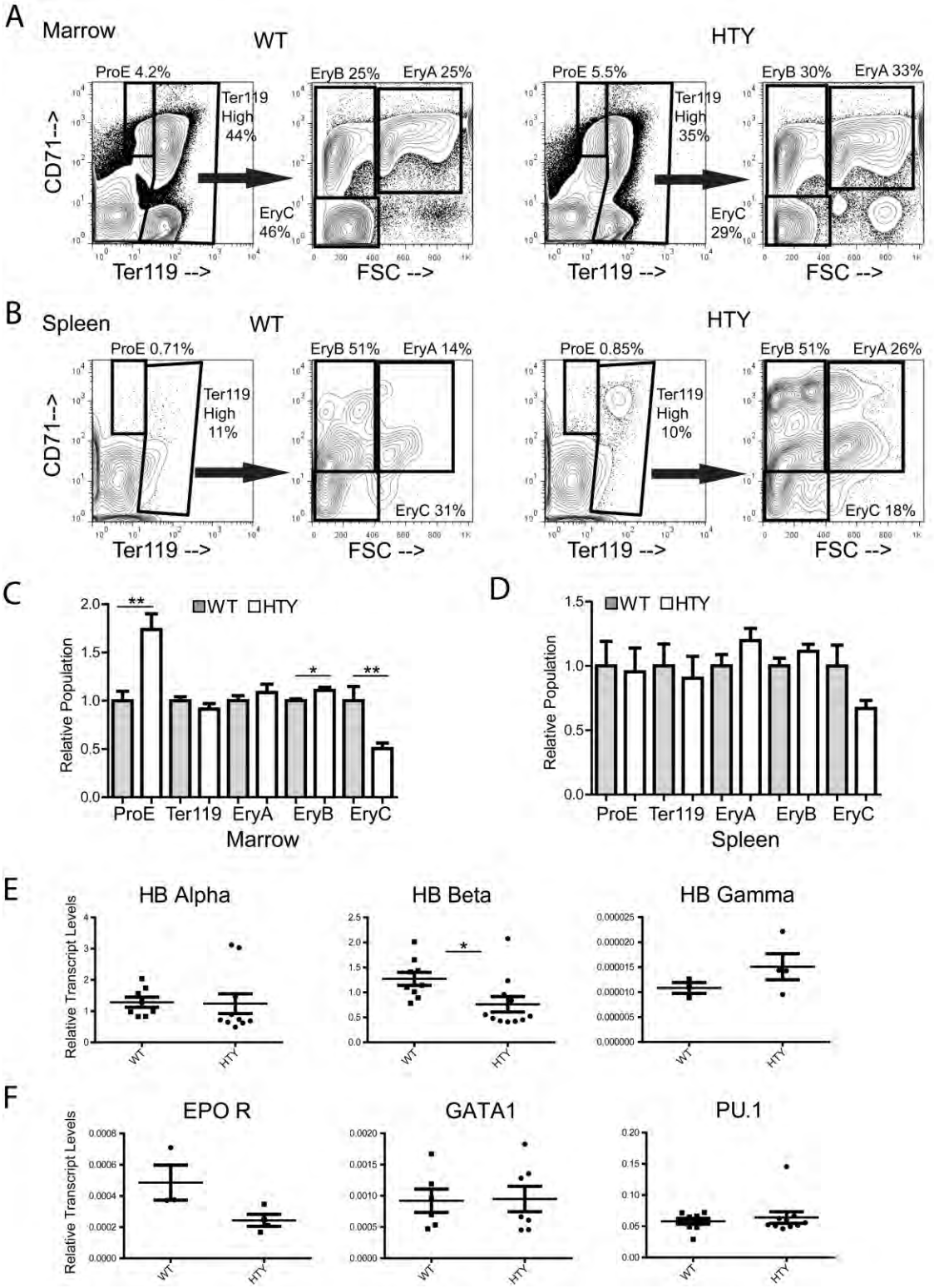
A
Marrow
WT
HTY
ProE 4.2%
EryB 25%
EryA 25%
Ter119 High 44%
EryC 46%
ProE 5.5%
EryB 30%
EryA 33%
Ter119 High 35%
EryC 29%
CD71-->
Ter119 -->
FSC -->
B
Spleen
WT
HTY
ProE 0.71%
EryB 51%
EryA 14%
Ter119 High 11%
EryC 31%
ProE 0.85%
EryB 51%
EryA 26%
Ter119 High 10%
EryC 18%
C
WT HTY
Relative Population
ProE Ter119 EryA EryB EryC
Marrow
D
WT HTY
Relative Population
ProE Ter119 EryA EryB EryC
Spleen
E
HB Alpha
HB Beta
HB Gamma
Relative Transcript Levels
WT
HTY
F
EPO R
GATA1
PU.1
Relative Transcript Levels
WT
HTY

Long term effects of Runx1$^{HTY350-352AAA}$ in aged mice

To investigate long term effects of Runx1$^{HTY350-352AAA}$ on hematopoietic progenitors and leukemogenesis, a cohort of wildtype and homozygous knock-in animals was monitored until 1 year of age. Peripheral blood was taken regularly for complete blood counts. The alterations observed in 8 week old animals (Table 8) generally remained consistent in this cohort over 12 months. There remained no difference in white blood cells or their differential (Figure 31A). Red blood cell counts and total hemoglobin were similar, but there remained lower hematocrit from smaller red blood cells in the Runx1$^{HTY350-352AAA}$ mice (Figure 31B). The increased number and size of platelets observed at 8 weeks was also maintained over 12 months (Figure 31C). Animals were sacrificed at 12 months of age and examined for any hematopoietic neoplasms. We observed one B-cell lymphoma and one liver carcinoma with severe steatosis in the 12 month old Runx1$^{HTY350-352AAA}$ mice (Figure 31D and E) with no tumors in age matched wildtype controls (n=22 wildtype and 15 mutant). These results are similar to Runx1 conditional mice which have increased myeloid infiltration of the liver and spleen and with age develop lymphomas.[125] The low tumor frequency is also reminiscent of the conditional knock-in of Runx1-ETO which, without additional mutagenesis, causes a low rate of lymphoma in aged mice.[169]

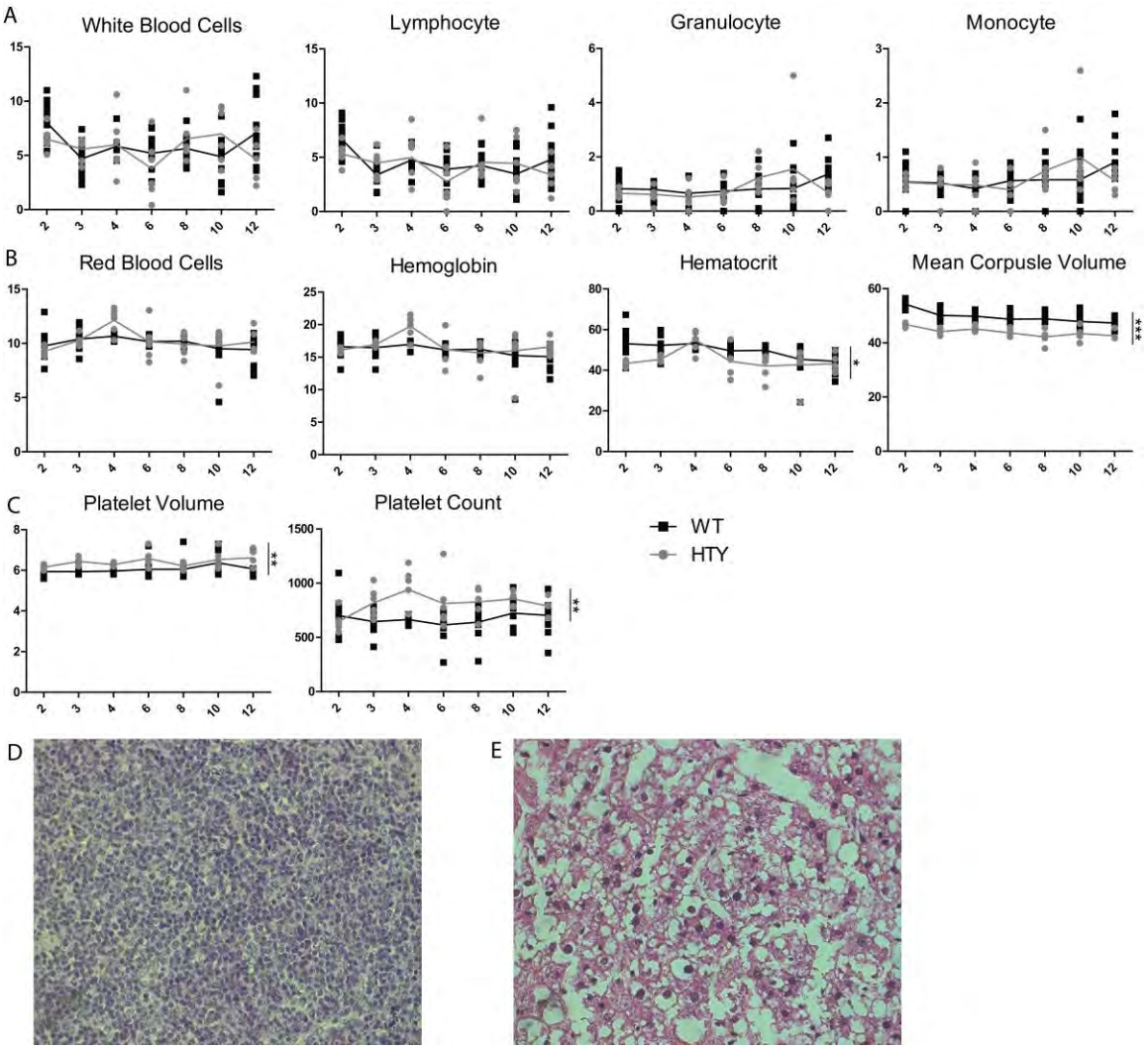

Figure 31: Long term effects of Runx1$^{HTY350\text{-}352AAA}$

A cohort of Runx1$^{HTY350\text{-}352AAA}$ mice were aged to 12 months and had blood taken at 2, 3, 4, 6, 8, 10 and 12 months of age to compare complete blood counts (n=12 WT, 6 HTY). (A) White blood cell counts and differentials remained similar. (B) Red blood cell count and hemoglobin were similar but their remained a low hematocrit from the smaller red blood cells in Runx1$^{HTY350\text{-}352AAA}$ mice. (C) Increased number and size of platelets was also maintained. * $p<0.05$, ** $p<0.01$, ***$p<0.001$ calculated by Student's T test. Mice were sacrificed at 12 months of age and examined for neoplasms. One B-cell lymphoma (D) and one liver carcinoma with severe steatosis were observed in Runx1$^{HTY350\text{-}352AAA}$ mice with no tumors in wildtype mice (n=22 WT, 15 HTY). Shown are paraffin embedded sections stained with hematoxylin and eosin at 40x magnification.

Discussion

Mutations in specific domains of Runx1 that disrupt subnuclear targeting and co-factor interactions alter target gene regulation, block differentiation and confer a pre-leukemic phenotype.[87,128] It was therefore of interest to investigate the functional activities of these domains in vivo. We developed and characterized Runx1$^{HTY350-352AAA}$ knock-in mice that bypass the embryonic lethality observed with Runx1 ablation or C-terminal truncation. When expressed in vivo, this mutant perturbs multiple hematopoietic lineages. Thus, the Runx1$^{HTY350-352AAA}$ mutation discriminates specific roles for Runx1 during embryogenesis and adult hematopoiesis.[10,143]

Primary bone marrow cells in homozygous Runx1$^{HTY350-352AAA}$ knock-in mice still retain Runx1 signal in the nuclear matrix. While the amount of Runx1 retained in the nuclear matrix is likely reduced, the heterogeneous cell population and the relatively low endogenous expression levels make quantification difficult. During the initial in vitro characterization by our lab of NMTS mutations, we found that even a C-terminal truncation could still retain some Runx1 in the matrix by biochemical fractionation. As a truncation that completely removes the NMTS does not abolish signal, and with the sensitivity of immunofluorescence, it is understandable matrix association can be perturbed while some signal is still retained.

qRT-PCR of bone marrow cells was able to provide insights about global gene deregulation occurring in the presence of Runx1$^{HTY350\text{-}352AAA}$. However, that analysis is severely limited by using whole bone marrow. Dramatic changes could be seen, but alterations with specific cell populations or in an important gene that is only expressed in a small population would be lost in the relatively high background. Sorting specific populations by flow cytometry prior to extracting RNA would be very informative, especially for genes that appeared to be changing in the whole bone marrow, but were too variable to meet statistical significance, such as VpreB1 and MPO. It is likely that their expression is being altered, but only in subsets of cells.

Bone marrow progenitor cell growth regulation is perturbed in the Runx1$^{HTY350\text{-}352AAA}$ homozygous animals, as indicated by increased growth ex vivo, and expansion or contraction of progenitor compartments in vivo. These observations are combined with the decreased progenitor ability in ex vivo colony formation assays and a reduction of LSK cells. Conditional ablation of Runx1 in adult mice causes an increase in LSK cells, which are less competitive over time.[79,125] The germline mutation likely deregulates progenitor growth control very early, and by adulthood it is possible only less competitive cells remain, explaining the smaller LSK population with reduced colony forming ability. These data suggest that Runx1$^{HTY350\text{-}352AAA}$ is compromised in the normal roles of Runx1 that maintain control of progenitor growth and proliferation.[61]

The Runx1$^{HTY350-352AAA}$ homozygous mice have splenomegaly, abnormalities in the white pulp of the spleen and deregulated B cell maturation. Several cell compartments of the B lineage are affected. Pre-Pro-B and Pro-B progenitors are altered in addition to the balance of immature and mature circulating B cells. Conditional Runx1 ablation[79,125] or expression of leukemic fusion proteins that inhibit Runx1 function[67] deplete the CLP compartment and inhibit B-cell development in its early stages. Runx1$^{HTY350-352AAA}$ contrasts by altering the balance of multiple compartments. This implies that this specific domain of Runx1 has functional roles at multiple stages of B-lymphopoiesis. Down-regulation of Runx1 is required during T-cell maturation for silencing of CD4 in CD4/CD8 double positive cells.[70] A knock-in mouse model that removed the C-terminal VWRPY motif decreased the CD8 positive T cell population in the spleen.[69] Similarly, Runx1$^{HTY350-352AAA}$ homozygous mice have fewer CD8 single positive T-cells in spleen and thymus. Thymus size and early T-cell progenitors were not significantly altered in Runx1$^{HTY350-352AAA}$ homozygous mice, in contrast to the smaller thymus and differentiation block observed after Runx1 excision in adults.[79,125] These results define contributions of precise domains with the known roles of Runx1 in control of both B and T lymphopoiesis.[64,65,67,170-173] Taken together, these data suggest that the HTY350-352 mutation compromises normal physiological functions of Runx1 and consequently deregulates B and T-lymphopoiesis.

The spleen harbors a major reserve of myeloid cells in healthy mice[174] and these cells undergo expansion with Runx1 loss.[79] We observed significant expansion of both the monocyte and granulocyte compartments in Runx1$^{HTY350-352AAA}$ homozygous spleens, suggesting that the observed splenomegaly is predominantly caused by aberrant expansion of these resident myeloid cells. These data are consistent with known contributions of Runx1 mutants to myeloid proliferative disease.[51,92]

Thrombocytopenia is one of the most common findings in patients with Runx1 mutations, and in animal models employing conditional Runx1 ablation.[77,79] The Runx1$^{HTY350-352AAA}$ homozygous mice are defective in megakaryocyte maturation and have a slight expansion of CD41 positive cells. Despite perturbed maturation, and unlike conditional Runx1 ablation[79,125], Runx1$^{HTY350-352AAA}$ homozygous mice are still able to maintain platelet counts within normal ranges. Thus Runx1 functions associated with HTY350-352 are required for megakaryocytic maturation but do not block platelet production.

Abnormalities in primitive erythrocytes from Runx1 null mice and perturbation of erythropoiesis by the leukemic fusion Runx1-ETO implicate Runx1 in erythropoiesis.[119,175] Subtle changes in the characteristics of red blood cells occur with Runx1 haploinsufficiency or conditional ablation, but these differences were not explored.[79,125] Runx1$^{HTY350-352AAA}$ homozygous mice have a lower hematocrit, resulting

from smaller red blood cells. A decrease in beta hemoglobin and the presence of alpha rich hemoglobin may explain the smaller cell size. In patients with beta thalassemia, the alpha rich hemoglobin is less stable and resultant red blood cells have difficulty retaining shape.[176] Red cell maturation was perturbed in the Runx1$^{HTY350-352AAA}$ homozygous mice, causing an increase in the earliest erythroid progenitors, with a subsequent decrease in the more mature cells. Thus, Runx1$^{HTY350-352AAA}$ causes a defect in erythroid maturation. Runx1 expression normally decreases during erythroid maturation.[63] Therefore, it is possible that the mechanism is indirect, with Runx1$^{HTY350-352AAA}$ somehow interfering with the endogenous downregulation.

Inhibition of Runx1 function does not cause leukemia without additional mutations. Even the leukemia associated t(8;21) translocation can be found in healthy individuals.[177,178] With advanced age additional mutations can occur and conditional mice with Runx1 ablation or knock-in of Runx1-ETO have a low incidence of lymphomas.[125,169] The Runx1$^{HTY350-352AAA}$ homozygous mice also have a low incidence of tumors, which supports the hypothesis that loss of function in C-terminal domain of Runx1 may promote leukemogenesis.

Runx factors organize and scaffold regulatory machinery, including factors that support chromatin structure and nucleosome organization at strategic sites of target gene promoters and in focal nuclear microenvironments.[26] Subtle alterations in the scaffolding

function of Runx1 could have profound regulatory effects. As the point mutation is within the domain important for subnuclear localization, alterations in subnuclear organization and/or perturbed protein interactions are likely responsible for the hypomorphic hematopoietic phenotypes of the Runx1$^{HTY350-352AAA}$ knock-in mouse.

Our findings reinforce the pivotal role of Runx1 as a master regulator of hematopoiesis. Runx1$^{HTY350-352AAA}$ represents a germline Runx1 mutation that bypasses embryonic lethality but alters multiple differentiated lineages in the adult. Runx1$^{HTY350-352AAA}$ homozygosity results in defective growth control of hematopoietic progenitors, deregulation of B-lymphoid and myeloid lineages, as well as maturation delays in megakaryocytic and erythroid development. Our study establishes a novel dimension in Runx1 mediated regulatory control that separates its roles in HSC emergence and differentiation across multiple hematopoietic lineages.

Chapter 5: Summary and Conclusions

Runx1 is a master regulator of hematopoiesis, important in the HSC[10,58,60,62,80,179] and throughout differentiated hematopoietic lineages.[63,79,80,102,119,142] There is some evidence for Runx1 function without CBFbeta.[180] However, Runx1 is generally thought to always act with CBFbeta as a heterodimer. CBFbeta increases DNA-binding ability of Runx1[181] and is expressed during definitive hematopoiesis at stages where Runx1 is known to be important.[100] Further supporting this concept, there are identical consequences of Runx1 and CBFbeta ablation[10,58,59,99,101,143,182] or inhibition by leukemic fusion proteins[183-185] during embryonic definitive hematopoiesis.

The essential functions of Runx1 in normal hematopoiesis are juxtaposed with frequent perturbations of Runx1 in hematopoietic disease.[92,95,97,186-188] In many cases, mutations in Runx1 correlate with poor prognosis.[92,172,188] Combined, Runx1 and CBFbeta are the most common targets for mutation and translocation in human leukemia.[88] The most frequent alteration of CBFbeta is caused by inv(16) which generates a chimeric fusion protein CBFbeta-SMMHC that sequesters Runx1 from its normal functional domains.[189] Runx1 mutations associated with leukemia cluster into two groups, either DNA-binding mutations or C-terminal frame shifts and truncations.[96,190] The majority of leukemia associated translocations involving Runx1 retain the DNA binding domain, but replace the C-terminus with a chimeric fusion.[88] With the common loss of Runx1 C-terminal domains in hematopoietic diseases, we postulated that losing the function of these

domains could be a common disease mechanism. We developed a panel of mutations to test the functions of these domains in vitro, and then developed mouse models to examine the consequences of losing Runx1 C-terminal domains on hematopoietic development and leukemogenesis in vivo.

In vitro analysis of Runx1 C-terminal mutations highlighted the context dependent nature of Runx1 function. The Runx1 C-terminal truncation bound DNA, but otherwise appeared to be a functional null. Point mutations disrupting subnuclear targeting were more sensitive to cellular context. They suppressed proliferation similar to wildtype Runx1, but caused deregulation of gene expression that blocked differentiation in a myeloid progenitor cell line. The most striking findings came from gene expression analysis of those progenitor cell lines before differentiation was initiated. Genes ontology clusters important for differentiating monocytes were suppressed, indicating that subnuclear targeting defective Runx1 was making cells less poised for differentiation in the absence of extracellular signals. Furthermore, promoters of the suppressed genes were not enriched for Runx1 binding motifs. The promoters were instead enriched for binding sites of known co-factors, whose direct protein-protein interactions with Runx1 should have been preserved. These data indicate a non-DNA-binding role of Runx1 in deregulation of those genes and provide strong evidence for Runx1 as a transcription factor scaffolding regulatory machinery within nuclear architecture as an additional layer of regulatory control.[26,27,191]

We next examined the consequences of replacing endogenous Runx1 in vivo with a C-terminal truncation, Runx1^{Q307X}. Embryos homozygous for Runx1^{Q307X} died during mid-gestation from severe central nervous system hemorrhage and a complete lack of definitive hematopoiesis. During embryonic hematopoiesis a C-terminal truncation of Runx1 that lacks domains responsible for co-factor interactions and subnuclear targeting is a phenocopy of a complete Runx1 null.[10,143] The functions of the domains lost in Runx1^{Q307X} are just as critical during hematopoietic development as the ability of Runx1 to bind DNA. These results highlight the critical importance of factors organizing with the highly complex nuclear architecture to carry out their biological functions.[26,27,29,54]

To clarify to contribution of specific domains lost in the Runx1^{Q307X} C-terminal translocation, we generated another knock-in mouse model, Runx1$^{HTY350-352AAA}$. Embryos homozygous for Runx1$^{HTY350-352AAA}$ bypass embryonic lethality, but have hypomorphic Runx1 function as adults. Runx1$^{HTY350-352AAA}$ results in defective growth control of hematopoietic progenitors, deregulation of B-lymphoid and myeloid lineages, as well as maturation delays in megakaryocytic and erythroid development. These phenotypes are likely caused by alterations in subnuclear organization and/or perturbed protein interactions. Even subtle alterations in the scaffolding function of Runx1 could have profound regulatory effects.

A hematopoietic progenitor must continue to proliferate without differentiation of the progeny in order to cause leukemia. Runx1-ETO or CBFbeta-SMMHC alone is insufficient to cause leukemia in model systems unless there is additional mutagenesis or a long latency.[169,192] In vitro expression of mSTD Runx1 impedes differentiation and Runx1$^{HTY350-352AAA}$ homozygosity in vivo deregulates growth control in early hematopoietic progenitors. Similar to Runx1-ETO or CBFbeta-SMMHC, conditional ablation of Runx1[125] and knock-in of Runx1$^{HTY350-352AAA}$ both cause a mild predisposition toward hematopoietic neoplasms with a long latency. Taken together, these data support the hypothesis that loss of function in Runx1 C-terminal domains represent a common mechanism for progenitor deregulation and potentially contribute to leukemogenesis.

Runx1 is important at many steps throughout definitive hematopoiesis in the embryo and adult. Germline and conditional knock-ins of Runx1 lacking DNA-binding ability have shown where Runx1 function is essential.[10,79,125] However, outside of later T-cell maturation,[69] little was known about the requirements for specific domains of Runx1 during hematopoiesis. Removal of the entire C-terminus is a developmental phenocopy of the complete Runx1 null,[143] and knock-in of Runx1$^{HTY350-352AAA}$ spares embryonic hematopoiesis but is hypomorphic in many lineages of adult hematopoiesis (Figure 32).

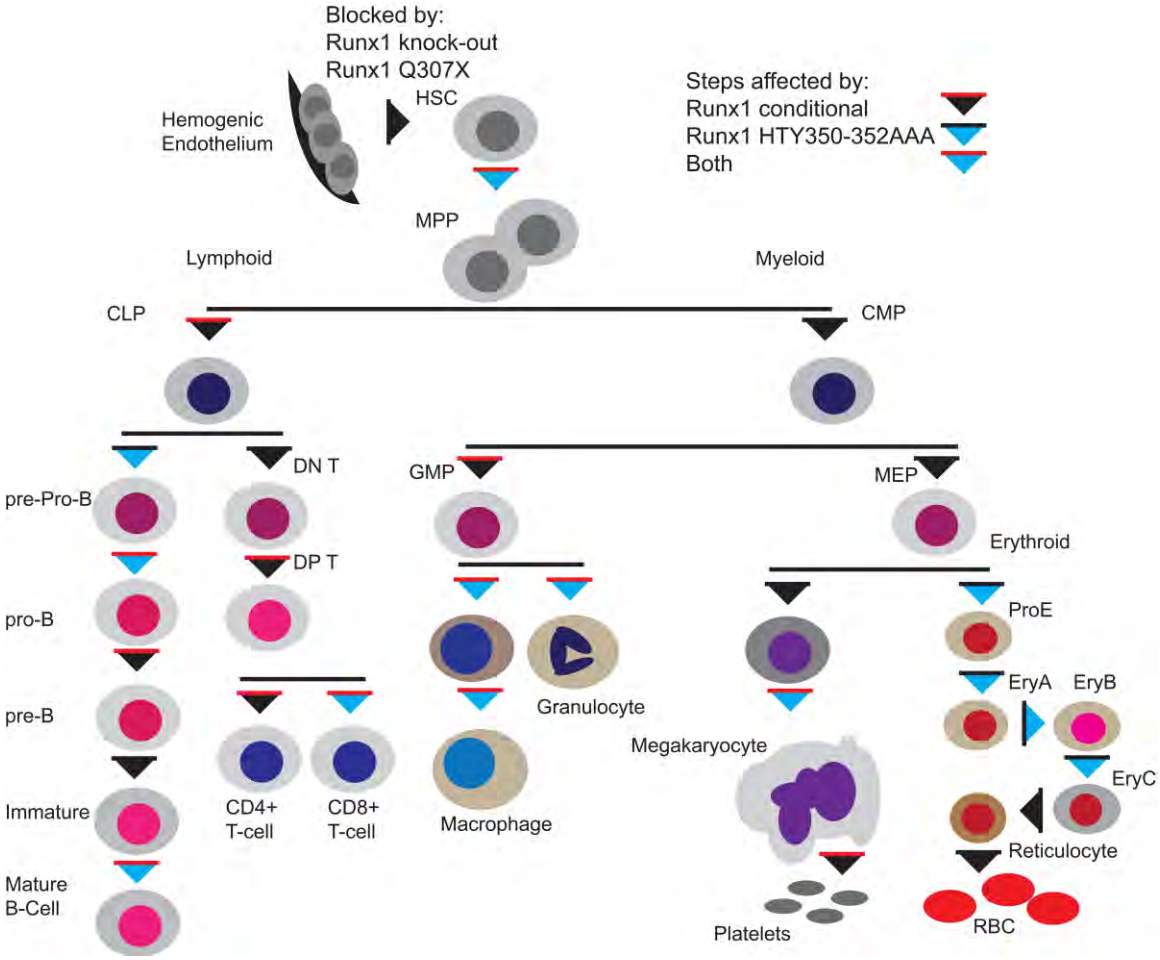

Figure 32: Definitive hematopoiesis with Runx1 mutations

Germline knockout of DNA-binding ability or knock-in Runx1^{Q307X} blocks emergence of the hematopoietic stem cells during embryonic hematopoiesis. Conditional ablation of Runx1 in adults or germline knock-in of Runx1$^{HTY350-352AAA}$ has consequences for many hematopoietic lineages.

Adapted from Larsson and Karlsson, *Oncogene* 2005; 24(37):5676-92

It is interesting to note that nuclear matrix association was not abolished in primary bone marrow cells of homozygous Runx1$^{HTY350-352AAA}$ mice. Initial in vitro characterization of the NMTS mutations showed that C-terminal truncations which completely removed the NMTS would retain some signal in the nuclear matrix. The majority of the mutant protein would not be retained, and the single or triple point mutations similarly lost most of their matrix association. The fact that when expressed at endogenous levels in vivo, Runx1$^{HTY350-352AAA}$ is still retained within the nuclear matrix indicates that these residues alone are not responsible for full subnuclear targeting. These data are also consistent with a knock-in mouse model with the equivalent mutation in Runx2 that our lab has developed. Homozygous animals for the Runx2 knock-in are also viable, with a subtle hypomorphic phenotype (Yang, et al., manuscript in preparation). Given the hypomorphic Runx1 phenotype observed in the Runx1$^{HTY350-352AAA}$ mice, we conclude that even mild perturbations of the subnuclear targeting of Runx1 can explain the altered Runx1 function throughout adult hematopoiesis.

As DNA-binding ability is retained in all of the C-terminal Runx1 mutations, gene deregulation must occur by other means. Runx factors have myriad known co-factors, and many have known interaction domains that overlap with the NMTS (Figure 33). Runx factors are known to provide a scaffold within the nucleus, organizing co-factors and chromatin regions in the highly complex three-dimensional architecture of the nucleus and this organization of regulatory machinery is important for biological

control.[26,27,29,54,110,191] The potential consequences of Runx1 not being able to perform these functions far exceed loss of a single co-factor interaction.

As a component of the nuclear architecture and functionally organizing transcriptional machinery, Runx1 can regulate genes without binding their promoters. The Runx1 consensus binding site has a hexamer as its core (TGTGGT) and statistically occurs at a high frequency. Therefore, as Runx1 is endogenously expressed at relatively modest levels, the Runx binding site is present far more frequently than there would be available Runx1 to bind it. The wide spread use of Chip-Seq and next generation sequencing technologies have provided tools to examine where Runx1 is acting throughout the genome.[193,194] Supporting the structural role of Runx proteins, ChipSeq data from our group using either Runx1 or Runx2 consistently shows the majority of Runx binding events occur outside known promoters (Dobson, et al., Wu, et al., and Trombley et al., manuscripts in preparation). Promoters of genes altered by the subnuclear targeting defective Runx1 in stable 32D cells lines were enriched with co-factor binding sites and not the Runx motif. Therefore, Runx1 mediated regulation of those genes must use its structural functions.

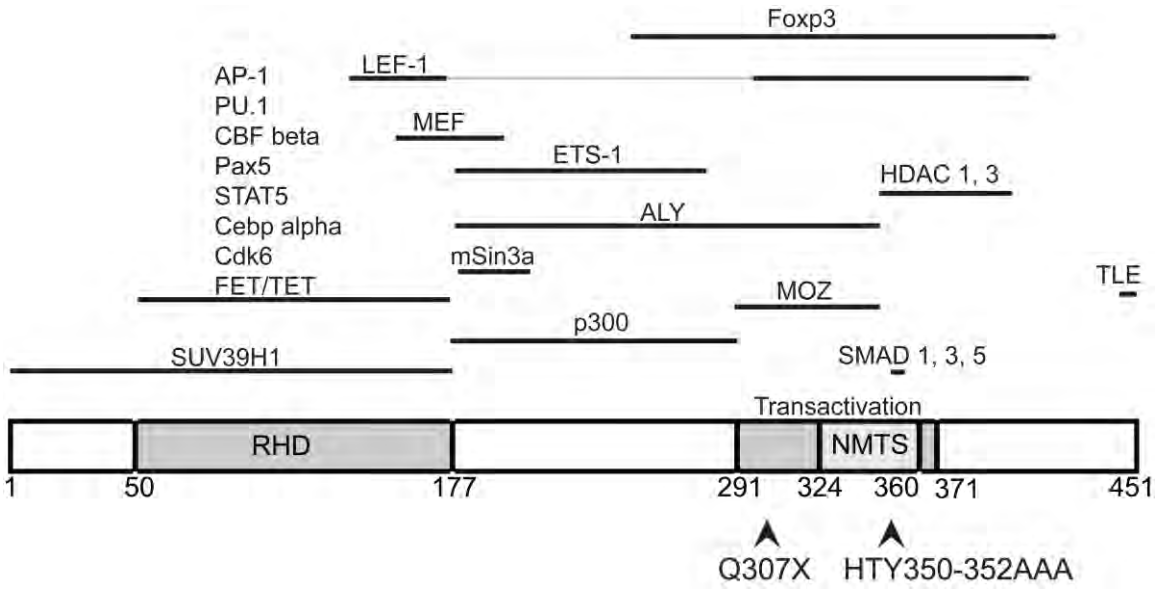

Figure 33: Schematic of Runx1 and interaction domains of known co-factors

Schematic of murine Runx1, noting the Runt-homology DNA binding domain (RHD), Transactivation Domain, nuclear matrix targeting signal (NMTS), and mutations sites for $Runx1^{Q307X}$ and $Runx1^{HTY350\text{-}352AAA}$ knock-in mice. Also shown are mapped protein interaction domains for: ALY[195], SUV39H1[196], AP-1[197], CBFbeta[198], Cdk6[199], FET/TET[200], ETS-1[117], MOZ[137], p300[19], TLE[136], LEF-1[201], PAX5[202], mSin3A[203], MEF[204], HDACs[20], SMADs[134,135,145], STAT5[205], Cebp alpha[116], Foxp3[206], and PU.1[116]. Many additional factors have been shown to bind Runx1, but are not shown because the interaction domains have not been defined.

Were this work to be continued, flow cytometry for sorting out specific cell populations should be the immediate priority. Now that flow cytometry has of multiple lineages has shown what maturation stages are affected by Runx1$^{HTY350\text{-}352AAA}$, those populations and the maturation stages immediately preceding them can be isolated. Microarray or qRT-PCR analysis of those cell populations could show the exact genes and pathways affected. Microarray analysis would also have the benefit of enabling motif analysis to understand what co-factors are mediating affects, in addition to identifying novel genes regulated directly, or indirectly, by Runx1. Sorting specific populations would also enable specialized functional assays to further dissect the defects observed in each lineage. In addition, a relatively homogenous population of primary cells would allow for replication of the in situ immunofluorescence and quantification of matrix retention in discrete cell populations. It remains a possibility that Runx1$^{HTY350\text{-}352AAA}$ may alter subnuclear targeting to different degrees among cell types. Chromatin structure and the altered expression levels of various co-factors could alter matrix retention and add an additional layer of context dependent regulatory control. Other known functions of Runx1 are highly context dependent so it stands to reason that subnuclear targeting could more affected by Runx1$^{HTY350\text{-}352AAA}$ in certain populations.

After establishing that Runx1$^{HTY350\text{-}352AAA}$ has a low rate of spontaneous tumors, similar to that of conditional knock-in of Runx1-ETO, this tumor predisposition should be further investigated. The liver and thymus of Runx1$^{HTY350\text{-}352AAA}$ homozygous and age

matched wildtype controls should be examined for subclinical hematopoietic neoplasms. The increased myeloid infiltration observed in spleen might also be present in the liver, as it is with Runx1-ETO knock-in and Runx1 conditional ablation.[79,169] Despite the lack of alterations in thymus size or double negative thymocyte populations, cellularity within the thymus should be examined as it has been in other Runx1 knock-in mutations.[69] To assess the leukemogeneicity of Runx1$^{HTY350-352AAA}$ a bone marrow transduction model could be used to ask if retroviral NRAS expression in Runx1$^{HTY350-352AAA}$ versus wildtype marrow would progress to leukemia with a shorter latency. Additional known second hits in Runx1-ETO or CBFbeta-SMMHC could be transduced into Runx1$^{HTY350-352AAA}$ marrow, or retroviral insertional mutagenesis used to look for novel co-operating genes.

This work supports the role of transcription factors interacting with nuclear architecture for greater biological control, and shows how even subtle alterations in that ability could have profound effects on gene regulation. Runx1 localizes to distinct nuclear microenvironments, and this localization is critical for normal biological function.[24,25] This localization requires a nuclear matrix targeting signal (NMTS) which is lost in many leukemic mutations and translocations, representing a potential common disease mechanism. In these studies, we show that loss of the NMTS and associated functions can in some ways mimic the presence of a leukemic fusion protein, and has in vivo consequences throughout definitive hematopoiesis.

Bibliography

1. Huang X, Crute BE, Sun C, Tang YY, Kelley JJ, 3rd, Lewis AF, Hartman KL, Laue TM, Speck NA, Bushweller JH. Overexpression, purification, and biophysical characterization of the heterodimerization domain of the core-binding factor beta subunit. *J Biol Chem*. 1998;273(4):2480-2487. Prepublished on 1998/01/27 as DOI.
2. Huang G, Shigesada K, Ito K, Wee HJ, Yokomizo T, Ito Y. Dimerization with PEBP2beta protects RUNX1/AML1 from ubiquitin-proteasome-mediated degradation. *EMBO J*. 2001;20(4):723-733. Prepublished on 2001/02/17 as DOI 10.1093/emboj/20.4.723.
3. Kamachi Y, Ogawa E, Asano M, Ishida S, Murakami Y, Satake M, Ito Y, Shigesada K. Purification of a mouse nuclear factor that binds to both the A and B cores of the polyomavirus enhancer. *J Virol*. 1990;64(10):4808-4819. Prepublished on 1990/10/01 as DOI.
4. Wang SW, Speck NA. Purification of core-binding factor, a protein that binds the conserved core site in murine leukemia virus enhancers. *Mol Cell Biol*. 1992;12(1):89-102. Prepublished on 1992/01/01 as DOI.
5. Miyoshi H, Shimizu K, Kozu T, Maseki N, Kaneko Y, Ohki M. t(8;21) breakpoints on chromosome 21 in acute myeloid leukemia are clustered within a limited region of a single gene, AML1. *Proc Natl Acad Sci U S A*. 1991;88(23):10431-10434. Prepublished on 1991/12/01 as DOI.
6. Bidwell JP, van Wijnen AJ, Fey EG, Merriman H, Penman S, Stein JL, Stein GS, Lian JB. Subnuclear distribution of the vitamin D receptor. *J Cell Biochem*. 1994;54(4):494-500. Prepublished on 1994/04/01 as DOI 10.1002/jcb.240540417.
7. Banerjee C, Hiebert SW, Stein JL, Lian JB, Stein GS. An AML-1 consensus sequence binds an osteoblast-specific complex and transcriptionally activates the osteocalcin gene. *Proc Natl Acad Sci U S A*. 1996;93(10):4968-4973. Prepublished on 1996/05/14 as DOI.
8. Hoffmann HM, Beumer TL, Rahman S, McCabe LR, Banerjee C, Aslam F, Tiro JA, van Wijnen AJ, Stein JL, Stein GS, Lian JB. Bone tissue-specific transcription of the osteocalcin gene: role of an activator osteoblast-specific complex and suppressor hox proteins that bind the OC box. *J Cell Biochem*. 1996;61(2):310-324. Prepublished on 1996/05/01 as DOI 10.1002/(SICI)1097-4644(19960501)61:2<310::AID-JCB14>3.0.CO;2-P.
9. van Wijnen AJ, Stein GS, Gergen JP, Groner Y, Hiebert SW, Ito Y, Liu P, Neil JC, Ohki M, Speck N. Nomenclature for Runt-related (RUNX) proteins. *Oncogene*. 2004;23(24):4209-4210. Prepublished on 2004/05/25 as DOI 10.1038/sj.onc.1207758.
10. Okuda T, van Deursen J, Hiebert SW, Grosveld G, Downing JR. AML1, the target of multiple chromosomal translocations in human leukemia, is essential for normal fetal liver hematopoiesis. *Cell*. 1996;84(2):321-330. Prepublished on 1996/01/26 as DOI.
11. Otto F, Thornell AP, Crompton T, Denzel A, Gilmour KC, Rosewell IR, Stamp GW, Beddington RS, Mundlos S, Olsen BR, Selby PB, Owen MJ. Cbfa1, a candidate gene for cleidocranial dysplasia syndrome, is essential for osteoblast differentiation and bone development. *Cell*. 1997;89(5):765-771. Prepublished on 1997/05/30 as DOI.
12. Komori T, Yagi H, Nomura S, Yamaguchi A, Sasaki K, Deguchi K, Shimizu Y, Bronson RT, Gao YH, Inada M, Sato M, Okamoto R, Kitamura Y, Yoshiki S, Kishimoto T. Targeted disruption of Cbfa1 results in a complete lack of bone formation owing to maturational arrest of osteoblasts. *Cell*. 1997;89(5):755-764. Prepublished on 1997/05/30 as DOI.
13. Li QL, Ito K, Sakakura C, Fukamachi H, Inoue K, Chi XZ, Lee KY, Nomura S, Lee CW, Han SB, Kim HM, Kim WJ, Yamamoto H, Yamashita N, Yano T, Ikeda T, Itohara S, Inazawa J,

Abe T, Hagiwara A, Yamagishi H, Ooe A, Kaneda A, Sugimura T, Ushijima T, Bae SC, Ito Y. Causal relationship between the loss of RUNX3 expression and gastric cancer. *Cell*. 2002;109(1):113-124. Prepublished on 2002/04/17 as DOI.

14. Levanon D, Bettoun D, Harris-Cerruti C, Woolf E, Negreanu V, Eilam R, Bernstein Y, Goldenberg D, Xiao C, Fliegauf M, Kremer E, Otto F, Brenner O, Lev-Tov A, Groner Y. The Runx3 transcription factor regulates development and survival of TrkC dorsal root ganglia neurons. *EMBO J*. 2002;21(13):3454-3463. Prepublished on 2002/07/03 as DOI 10.1093/emboj/cdf370.

15. Levanon D, Groner Y. Structure and regulated expression of mammalian RUNX genes. *Oncogene*. 2004;23(24):4211-4219.

16. Stein GS, Lian JB, Stein JL, Wijnen AJ, Montecino M, Javed A, Pratap J, Choi J, Zaidi SK, Gutierrez S, Harrington K, Shen J, Young D. Intranuclear trafficking of transcription factors: Requirements for vitamin D-mediated biological control of gene expression. *J Cell Biochem*. 2003;88(2):340-355. Prepublished on 2003/01/10 as DOI 10.1002/jcb.10364.

17. Pelletier N, Champagne N, Stifani S, Yang XJ. MOZ and MORF histone acetyltransferases interact with the Runt-domain transcription factor Runx2. *Oncogene*. 2002;21(17):2729-2740.

18. Durst KL, Lutterbach B, Kummalue T, Friedman AD, Hiebert SW. The inv(16) fusion protein associates with corepressors via a smooth muscle myosin heavy-chain domain. *Mol Cell Biol*. 2003;23(2):607-619. Prepublished on 2003/01/02 as DOI.

19. Kitabayashi I, Yokoyama A, Shimizu K, Ohki M. Interaction and functional cooperation of the leukemia-associated factors AML1 and p300 in myeloid cell differentiation. *EMBO J*. 1998;17(11):2994-3004. Prepublished on 1998/06/26 as DOI 10.1093/emboj/17.11.2994.

20. Reed-Inderbitzin E, Moreno-Miralles I, Vanden-Eynden SK, Xie J, Lutterbach B, Durst-Goodwin KL, Luce KS, Irvin BJ, Cleary ML, Brandt SJ, Hiebert SW. RUNX1 associates with histone deacetylases and SUV39H1 to repress transcription. *Oncogene*. 2006;25(42):5777-5786. Prepublished on 2006/05/03 as DOI 10.1038/sj.onc.1209591.

21. Durst KL, Hiebert SW. Role of RUNX family members in transcriptional repression and gene silencing. *Oncogene*. 2004;23(24):4220-4224. Prepublished on 2004/05/25 as DOI 10.1038/sj.onc.1207122.

22. Bristow CA, Shore P. Transcriptional regulation of the human MIP-1alpha promoter by RUNX1 and MOZ. *Nucleic Acids Res*. 2003;31(11):2735-2744.

23. Javed A, Guo B, Hiebert S, Choi JY, Green J, Zhao SC, Osborne MA, Stifani S, Stein JL, Lian JB, van Wijnen AJ, Stein GS. Groucho/TLE/R-esp proteins associate with the nuclear matrix and repress RUNX (CBF(alpha)/AML/PEBP2(alpha)) dependent activation of tissue-specific gene transcription. *J Cell Sci*. 2000;113 (Pt 12):2221-2231. Prepublished on 2000/05/29 as DOI.

24. Zeng C, McNeil S, Pockwinse S, Nickerson J, Shopland L, Lawrence JB, Penman S, Hiebert S, Lian JB, van Wijnen AJ, Stein JL, Stein GS. Intranuclear targeting of AML/CBFalpha regulatory factors to nuclear matrix-associated transcriptional domains. *Proc Natl Acad Sci U S A*. 1998;95(4):1585-1589. Prepublished on 1998/03/21 as DOI.

25. Zeng C, van Wijnen AJ, Stein JL, Meyers S, Sun W, Shopland L, Lawrence JB, Penman S, Lian JB, Stein GS, Hiebert SW. Identification of a nuclear matrix targeting signal in the leukemia and bone-related AML/CBF-alpha transcription factors. *Proc Natl Acad Sci U S A*. 1997;94(13):6746-6751. Prepublished on 1997/06/24 as DOI.

26. Stein GS, Lian JB, Stein JL, van Wijnen AJ, Javed A, Montecino M, Zaidi SK, Young DW, Choi JY, Pratap J. Combinatorial organization of the transcriptional regulatory machinery in

biological control and cancer. *Adv Enzyme Regul*. 2005;45:136-154. Prepublished on 2005/09/02 as DOI 10.1016/j.advenzreg.2005.02.009.
27. Stein GS, Lian JB, van Wijnen AJ, Stein JL, Javed A, Montecino M, Zaidi SK, Young D, Choi JY, Gutierrez S, Pockwinse S. Nuclear microenvironments support assembly and organization of the transcriptional regulatory machinery for cell proliferation and differentiation. *J Cell Biochem*. 2004;91(2):287-302. Prepublished on 2004/01/27 as DOI 10.1002/jcb.10777.
28. Stein GS, van Wijnen AJ, Stein JL, Lian JB, Montecino M, Zaidi SK, Braastad C. An architectural perspective of cell-cycle control at the G1/S phase cell-cycle transition. *J Cell Physiol*. 2006;209(3):706-710. Prepublished on 2006/09/27 as DOI 10.1002/jcp.20843.
29. Stein GS, Zaidi SK, Braastad CD, Montecino M, van Wijnen AJ, Choi JY, Stein JL, Lian JB, Javed A. Functional architecture of the nucleus: organizing the regulatory machinery for gene expression, replication and repair. *Trends Cell Biol*. 2003;13(11):584-592. Prepublished on 2003/10/24 as DOI.
30. Huang da W, Sherman BT, Lempicki RA. Systematic and integrative analysis of large gene lists using DAVID bioinformatics resources. *Nat Protoc*. 2009;4(1):44-57. Prepublished on 2009/01/10 as DOI 10.1038/nprot.2008.211.
31. Nickerson J. Experimental observations of a nuclear matrix. *J Cell Sci*. 2001;114(Pt 3):463-474. Prepublished on 2001/02/15 as DOI.
32. Herman R, Weymouth L, Penman S. Heterogeneous nuclear RNA-protein fibers in chromatin-depleted nuclei. *J Cell Biol*. 1978;78(3):663-674. Prepublished on 1978/09/01 as DOI.
33. Berezney R, Coffey DS. Identification of a nuclear protein matrix. *Biochem Biophys Res Commun*. 1974;60(4):1410-1417. Prepublished on 1974/10/23 as DOI.
34. He DC, Nickerson JA, Penman S. Core filaments of the nuclear matrix. *J Cell Biol*. 1990;110(3):569-580. Prepublished on 1990/03/01 as DOI.
35. Jackson DA, Cook PR. Visualization of a filamentous nucleoskeleton with a 23 nm axial repeat. *EMBO J*. 1988;7(12):3667-3677. Prepublished on 1988/12/01 as DOI.
36. Nickerson JA, Krockmalnic G, Wan KM, Penman S. The nuclear matrix revealed by eluting chromatin from a cross-linked nucleus. *Proc Natl Acad Sci U S A*. 1997;94(9):4446-4450. Prepublished on 1997/04/29 as DOI.
37. Berezney R, Coffey DS. Nuclear protein matrix: association with newly synthesized DNA. *Science*. 1975;189(4199):291-293. Prepublished on 1975/07/25 as DOI.
38. Pardoll DM, Vogelstein B, Coffey DS. A fixed site of DNA replication in eucaryotic cells. *Cell*. 1980;19(2):527-536. Prepublished on 1980/02/01 as DOI.
39. Hozak P, Hassan AB, Jackson DA, Cook PR. Visualization of replication factories attached to nucleoskeleton. *Cell*. 1993;73(2):361-373. Prepublished on 1993/04/23 as DOI.
40. Kimura H, Tao Y, Roeder RG, Cook PR. Quantitation of RNA polymerase II and its transcription factors in an HeLa cell: little soluble holoenzyme but significant amounts of polymerases attached to the nuclear substructure. *Mol Cell Biol*. 1999;19(8):5383-5392. Prepublished on 1999/07/20 as DOI.
41. Mika S, Rost B. NMPdb: Database of Nuclear Matrix Proteins. *Nucleic Acids Res*. 2005;33(Database issue):D160-163. Prepublished on 2004/12/21 as DOI 10.1093/nar/gki132.
42. Lian JB, Javed A, Zaidi SK, Lengner C, Montecino M, van Wijnen AJ, Stein JL, Stein GS. Regulatory controls for osteoblast growth and differentiation: role of Runx/Cbfa/AML factors. *Crit Rev Eukaryot Gene Expr*. 2004;14(1-2):1-41. Prepublished on 2004/04/24 as DOI.
43. Nakamura T, Mori T, Tada S, Krajewski W, Rozovskaia T, Wassell R, Dubois G, Mazo A, Croce CM, Canaani E. ALL-1 is a histone methyltransferase that assembles a supercomplex of proteins involved in transcriptional regulation. *Mol Cell*. 2002;10(5):1119-1128. Prepublished on 2002/11/28 as DOI.

44. Zaidi SK, Young DW, Javed A, Pratap J, Montecino M, van Wijnen A, Lian JB, Stein JL, Stein GS. Nuclear microenvironments in biological control and cancer. *Nat Rev Cancer*. 2007;7(6):454-463. Prepublished on 2007/05/25 as DOI 10.1038/nrc2149.
45. Bakshi R, Zaidi SK, Pande S, Hassan MQ, Young DW, Montecino M, Lian JB, van Wijnen AJ, Stein JL, Stein GS. The leukemogenic t(8;21) fusion protein AML1-ETO controls rRNA genes and associates with nucleolar-organizing regions at mitotic chromosomes. *J Cell Sci*. 2008;121(Pt 23):3981-3990. Prepublished on 2008/11/13 as DOI 10.1242/jcs.033431.
46. DeFranco DB, Guerrero J. Nuclear matrix targeting of steroid receptors: specific signal sequences and acceptor proteins. *Crit Rev Eukaryot Gene Expr*. 2000;10(1):39-44. Prepublished on 2000/05/17 as DOI.
47. Mancini MG, Liu B, Sharp ZD, Mancini MA. Subnuclear partitioning and functional regulation of the Pit-1 transcription factor. *J Cell Biochem*. 1999;72(3):322-338. Prepublished on 1999/02/18 as DOI.
48. McNeil S, Guo B, Stein JL, Lian JB, Bushmeyer S, Seto E, Atchison ML, Penman S, van Wijnen AJ, Stein GS. Targeting of the YY1 transcription factor to the nucleolus and the nuclear matrix in situ: the C-terminus is a principal determinant for nuclear trafficking. *J Cell Biochem*. 1998;68(4):500-510. Prepublished on 1998/03/11 as DOI.
49. McNeil S, Zeng C, Harrington KS, Hiebert S, Lian JB, Stein JL, van Wijnen AJ, Stein GS. The t(8;21) chromosomal translocation in acute myelogenous leukemia modifies intranuclear targeting of the AML1/CBFalpha2 transcription factor. *Proc Natl Acad Sci U S A*. 1999;96(26):14882-14887. Prepublished on 1999/12/28 as DOI.
50. Seo J, Lozano MM, Dudley JP. Nuclear matrix binding regulates SATB1-mediated transcriptional repression. *J Biol Chem*. 2005;280(26):24600-24609. Prepublished on 2005/04/27 as DOI 10.1074/jbc.M414076200.
51. Barseguian K, Lutterbach B, Hiebert SW, Nickerson J, Lian JB, Stein JL, van Wijnen AJ, Stein GS. Multiple subnuclear targeting signals of the leukemia-related AML1/ETO and ETO repressor proteins. *Proc Natl Acad Sci U S A*. 2002;99(24):15434-15439. Prepublished on 2002/11/13 as DOI 10.1073/pnas.242588499.
52. Hanahan D, Weinberg RA. The hallmarks of cancer. *Cell*. 2000;100(1):57-70. Prepublished on 2000/01/27 as DOI.
53. Zink D, Fischer AH, Nickerson JA. Nuclear structure in cancer cells. *Nat Rev Cancer*. 2004;4(9):677-687. Prepublished on 2004/09/03 as DOI 10.1038/nrc1430.
54. Stein GS, Zaidi SK, Stein JL, Lian JB, van Wijnen AJ, Montecino M, Young DW, Javed A, Pratap J, Choi JY, Ali SA, Pande S, Hassan MQ. Organization, integration, and assembly of genetic and epigenetic regulatory machinery in nuclear microenvironments: implications for biological control in cancer. *Ann N Y Acad Sci*. 2009;1155:4-14. Prepublished on 2009/03/03 as DOI 10.1111/j.1749-6632.2009.03697.x.
55. Fraser P, Bickmore W. Nuclear organization of the genome and the potential for gene regulation. *Nature*. 2007;447(7143):413-417. Prepublished on 2007/05/25 as DOI 10.1038/nature05916.
56. Stein GS. Gene expression in nuclear microenvironments for biological control and cancer. *Cancer Biol Ther*. 2007;6(11):1817-1821. Prepublished on 2008/04/29 as DOI.
57. Stein GS, Zaidi SK, Stein JL, Lian JB, van Wijnen AJ, Montecino M, Young DW, Javed A, Pratap J, Choi JY, Ali SA, Pande S, Hassan MQ. Genetic and epigenetic regulation in nuclear microenvironments for biological control in cancer. *J Cell Biochem*. 2008;104(6):2016-2026. Prepublished on 2008/07/11 as DOI 10.1002/jcb.21813.

58. North T, Gu TL, Stacy T, Wang Q, Howard L, Binder M, Marin-Padilla M, Speck NA. Cbfa2 is required for the formation of intra-aortic hematopoietic clusters. *Development*. 1999;126(11):2563-2575. Prepublished on 1999/05/05 as DOI.
59. Wang Q, Stacy T, Binder M, Marin-Padilla M, Sharpe AH, Speck NA. Disruption of the Cbfa2 gene causes necrosis and hemorrhaging in the central nervous system and blocks definitive hematopoiesis. *Proc Natl Acad Sci U S A*. 1996;93(8):3444-3449. Prepublished on 1996/04/16 as DOI.
60. Motoda L, Osato M, Yamashita N, Jacob B, Chen LQ, Yanagida M, Ida H, Wee HJ, Sun AX, Taniuchi I, Littman D, Ito Y. Runx1 protects hematopoietic stem/progenitor cells from oncogenic insult. *Stem Cells*. 2007;25(12):2976-2986. Prepublished on 2007/09/08 as DOI 10.1634/stemcells.2007-0061.
61. Ichikawa M, Goyama S, Asai T, Kawazu M, Nakagawa M, Takeshita M, Chiba S, Ogawa S, Kurokawa M. AML1/Runx1 negatively regulates quiescent hematopoietic stem cells in adult hematopoiesis. *J Immunol*. 2008;180(7):4402-4408. Prepublished on 2008/03/21 as DOI.
62. Cai X, Gaudet JJ, Mangan JK, Chen MJ, De Obaldia ME, Oo Z, Ernst P, Speck NA. Runx1 loss minimally impacts long-term hematopoietic stem cells. *PLoS One*. 2011;6(12):e28430. Prepublished on 2011/12/07 as DOI 10.1371/journal.pone.0028430.
63. Lorsbach RB, Moore J, Ang SO, Sun W, Lenny N, Downing JR. Role of RUNX1 in adult hematopoiesis: analysis of RUNX1-IRES-GFP knock-in mice reveals differential lineage expression. *Blood*. 2004;103(7):2522-2529. Prepublished on 2003/11/25 as DOI 10.1182/blood-2003-07-2439.
64. Lukin K, Fields S, Lopez D, Cherrier M, Ternyak K, Ramirez J, Feeney AJ, Hagman J. Compound haploinsufficiencies of Ebf1 and Runx1 genes impede B cell lineage progression. *Proc Natl Acad Sci U S A*. 2010;107(17):7869-7874. Prepublished on 2010/04/14 as DOI 10.1073/pnas.1003525107.
65. Spender LC, Whiteman HJ, Karstegl CE, Farrell PJ. Transcriptional cross-regulation of RUNX1 by RUNX3 in human B cells. *Oncogene*. 2005;24(11):1873-1881. Prepublished on 2005/02/03 as DOI 10.1038/sj.onc.1208404.
66. Ichikawa M, Asai T, Saito T, Seo S, Yamazaki I, Yamagata T, Mitani K, Chiba S, Ogawa S, Kurokawa M, Hirai H. AML-1 is required for megakaryocytic maturation and lymphocytic differentiation, but not for maintenance of hematopoietic stem cells in adult hematopoiesis. *Nat Med*. 2004;10(3):299-304. Prepublished on 2004/02/18 as DOI 10.1038/nm997.
67. Kuo YH, Gerstein RM, Castilla LH. Cbfbeta-SMMHC impairs differentiation of common lymphoid progenitors and reveals an essential role for RUNX in early B-cell development. *Blood*. 2008;111(3):1543-1551. Prepublished on 2007/10/18 as DOI 10.1182/blood-2007-07-104422.
68. Satake M, Nomura S, Yamaguchi-Iwai Y, Takahama Y, Hashimoto Y, Niki M, Kitamura Y, Ito Y. Expression of the Runt domain-encoding PEBP2 alpha genes in T cells during thymic development. *Mol Cell Biol*. 1995;15(3):1662-1670. Prepublished on 1995/03/01 as DOI.
69. Nishimura M, Fukushima-Nakase Y, Fujita Y, Nakao M, Toda S, Kitamura N, Abe T, Okuda T. VWRPY motif-dependent and -independent roles of AML1/Runx1 transcription factor in murine hematopoietic development. *Blood*. 2004;103(2):562-570. Prepublished on 2003/09/25 as DOI 10.1182/blood-2003-06-2109.
70. Wong WF, Nakazato M, Watanabe T, Kohu K, Ogata T, Yoshida N, Sotomaru Y, Ito M, Araki K, Telfer J, Fukumoto M, Suzuki D, Sato T, Hozumi K, Habu S, Satake M. Over-expression of Runx1 transcription factor impairs the development of thymocytes from the double-negative to double-positive stages. *Immunology*. 2010;130(2):243-253. Prepublished on 2010/01/28 as DOI 10.1111/j.1365-2567.2009.03230.x.

71. Telfer JC, Rothenberg EV. Expression and function of a stem cell promoter for the murine CBFalpha2 gene: distinct roles and regulation in natural killer and T cell development. *Dev Biol*. 2001;229(2):363-382. Prepublished on 2001/02/24 as DOI 10.1006/dbio.2000.9991.
72. Telfer JC, Hedblom EE, Anderson MK, Laurent MN, Rothenberg EV. Localization of the domains in Runx transcription factors required for the repression of CD4 in thymocytes. *J Immunol*. 2004;172(7):4359-4370. Prepublished on 2004/03/23 as DOI.
73. Satoh Y, Matsumura I, Tanaka H, Ezoe S, Fukushima K, Tokunaga M, Yasumi M, Shibayama H, Mizuki M, Era T, Okuda T, Kanakura Y. AML1/RUNX1 works as a negative regulator of c-Mpl in hematopoietic stem cells. *J Biol Chem*. 2008;283(44):30045-30056. Prepublished on 2008/08/09 as DOI 10.1074/jbc.M804768200.
74. Gilles L, Guieze R, Bluteau D, Cordette-Lagarde V, Lacout C, Favier R, Larbret F, Debili N, Vainchenker W, Raslova H. P19INK4D links endomitotic arrest and megakaryocyte maturation and is regulated by AML-1. *Blood*. 2008;111(8):4081-4091. Prepublished on 2008/02/16 as DOI 10.1182/blood-2007-09-113266.
75. Ben-Ami O, Pencovich N, Lotem J, Levanon D, Groner Y. A regulatory interplay between miR-27a and Runx1 during megakaryopoiesis. *Proc Natl Acad Sci U S A*. 2009;106(1):238-243. Prepublished on 2008/12/31 as DOI 10.1073/pnas.0811466106.
76. Kostyak JC, Naik UP. Megakaryopoiesis: transcriptional insights into megakaryocyte maturation. *Front Biosci*. 2007;12:2050-2062. Prepublished on 2006/11/28 as DOI.
77. Song WJ, Sullivan MG, Legare RD, Hutchings S, Tan X, Kufrin D, Ratajczak J, Resende IC, Haworth C, Hock R, Loh M, Felix C, Roy DC, Busque L, Kurnit D, Willman C, Gewirtz AM, Speck NA, Bushweller JH, Li FP, Gardiner K, Poncz M, Maris JM, Gilliland DG. Haploinsufficiency of CBFA2 causes familial thrombocytopenia with propensity to develop acute myelogenous leukaemia. *Nat Genet*. 1999;23(2):166-175. Prepublished on 1999/10/03 as DOI 10.1038/13793.
78. Michaud J, Wu F, Osato M, Cottles GM, Yanagida M, Asou N, Shigesada K, Ito Y, Benson KF, Raskind WH, Rossier C, Antonarakis SE, Israels S, McNicol A, Weiss H, Horwitz M, Scott HS. In vitro analyses of known and novel RUNX1/AML1 mutations in dominant familial platelet disorder with predisposition to acute myelogenous leukemia: implications for mechanisms of pathogenesis. *Blood*. 2002;99(4):1364-1372. Prepublished on 2002/02/07 as DOI.
79. Growney JD, Shigematsu H, Li Z, Lee BH, Adelsperger J, Rowan R, Curley DP, Kutok JL, Akashi K, Williams IR, Speck NA, Gilliland DG. Loss of Runx1 perturbs adult hematopoiesis and is associated with a myeloproliferative phenotype. *Blood*. 2005;106(2):494-504. Prepublished on 2005/03/24 as DOI 10.1182/blood-2004-08-3280.
80. North TE, Stacy T, Matheny CJ, Speck NA, de Bruijn MF. Runx1 is expressed in adult mouse hematopoietic stem cells and differentiating myeloid and lymphoid cells, but not in maturing erythroid cells. *Stem Cells*. 2004;22(2):158-168. Prepublished on 2004/03/03 as DOI 10.1634/stemcells.22-2-158.
81. Tanaka T, Tanaka K, Ogawa S, Kurokawa M, Mitani K, Nishida J, Shibata Y, Yazaki Y, Hirai H. An acute myeloid leukemia gene, AML1, regulates hemopoietic myeloid cell differentiation and transcriptional activation antagonistically by two alternative spliced forms. *EMBO J*. 1995;14(2):341-350. Prepublished on 1995/01/16 as DOI.
82. Zhang DE, Hohaus S, Voso MT, Chen HM, Smith LT, Hetherington CJ, Tenen DG. Function of PU.1 (Spi-1), C/EBP, and AML1 in early myelopoiesis: regulation of multiple myeloid CSF receptor promoters. *Curr Top Microbiol Immunol*. 1996;211:137-147. Prepublished on 1996/01/01 as DOI.
83. Zhang DE, Hetherington CJ, Meyers S, Rhoades KL, Larson CJ, Chen HM, Hiebert SW, Tenen DG. CCAAT enhancer-binding protein (C/EBP) and AML1 (CBF alpha2) synergistically

activate the macrophage colony-stimulating factor receptor promoter. *Mol Cell Biol*. 1996;16(3):1231-1240. Prepublished on 1996/03/01 as DOI.
84. Rhoades KL, Hetherington CJ, Rowley JD, Hiebert SW, Nucifora G, Tenen DG, Zhang DE. Synergistic up-regulation of the myeloid-specific promoter for the macrophage colony-stimulating factor receptor by AML1 and the t(8;21) fusion protein may contribute to leukemogenesis. *Proc Natl Acad Sci U S A*. 1996;93(21):11895-11900. Prepublished on 1996/10/15 as DOI.
85. Huang G, Zhang P, Hirai H, Elf S, Yan X, Chen Z, Koschmieder S, Okuno Y, Dayaram T, Growney JD, Shivdasani RA, Gilliland DG, Speck NA, Nimer SD, Tenen DG. PU.1 is a major downstream target of AML1 (RUNX1) in adult mouse hematopoiesis. *Nat Genet*. 2008;40(1):51-60. Prepublished on 2007/11/13 as DOI 10.1038/ng.2007.7.
86. Hu Z, Gu X, Baraoidan K, Ibanez V, Sharma A, Kadkol S, Munker R, Ackerman S, Nucifora G, Saunthararajah Y. RUNX1 regulates corepressor interactions of PU.1. *Blood*. 2011;117(24):6498-6508. Prepublished on 2011/04/27 as DOI 10.1182/blood-2010-10-312512.
87. Vradii D, Zaidi SK, Lian JB, van Wijnen AJ, Stein JL, Stein GS. Point mutation in AML1 disrupts subnuclear targeting, prevents myeloid differentiation, and effects a transformation-like phenotype. *Proc Natl Acad Sci U S A*. 2005;102(20):7174-7179. Prepublished on 2005/05/05 as DOI 10.1073/pnas.0502130102.
88. Look AT. Oncogenic transcription factors in the human acute leukemias. *Science*. 1997;278(5340):1059-1064. Prepublished on 1997/11/14 as DOI.
89. Osato M. Point mutations in the RUNX1/AML1 gene: another actor in RUNX leukemia. *Oncogene*. 2004;23(24):4284-4296.
90. Ratain MJ, Rowley JD. Therapy-related acute myeloid leukemia secondary to inhibitors of topoisomerase II: from the bedside to the target genes. *Ann Oncol*. 1992;3(2):107-111. Prepublished on 1992/02/01 as DOI.
91. Felix CA. Secondary leukemias induced by topoisomerase-targeted drugs. *Biochim Biophys Acta*. 1998;1400(1-3):233-255. Prepublished on 1998/09/28 as DOI.
92. Kuo MC, Liang DC, Huang CF, Shih YS, Wu JH, Lin TL, Shih LY. RUNX1 mutations are frequent in chronic myelomonocytic leukemia and mutations at the C-terminal region might predict acute myeloid leukemia transformation. *Leukemia*. 2009;23(8):1426-1431. Prepublished on 2009/03/14 as DOI 10.1038/leu.2009.48.
93. Downing JR, Higuchi M, Lenny N, Yeoh AE. Alterations of the AML1 transcription factor in human leukemia. *Semin Cell Dev Biol*. 2000;11(5):347-360. Prepublished on 2000/12/06 as DOI 10.1006/scdb.2000.0183.
94. Buijs A, Poddighe P, van Wijk R, van Solinge W, Borst E, Verdonck L, Hagenbeek A, Pearson P, Lokhorst H. A novel CBFA2 single-nucleotide mutation in familial platelet disorder with propensity to develop myeloid malignancies. *Blood*. 2001;98(9):2856-2858. Prepublished on 2001/10/25 as DOI.
95. Osato M, Yanagida M, Shigesada K, Ito Y. Point mutations of the RUNx1/AML1 gene in sporadic and familial myeloid leukemias. *Int J Hematol*. 2001;74(3):245-251. Prepublished on 2001/11/28 as DOI.
96. Harada H, Harada Y, Niimi H, Kyo T, Kimura A, Inaba T. High incidence of somatic mutations in the AML1/RUNX1 gene in myelodysplastic syndrome and low blast percentage myeloid leukemia with myelodysplasia. *Blood*. 2004;103(6):2316-2324. Prepublished on 2003/11/15 as DOI 10.1182/blood-2003-09-3074.
97. Matheny CJ, Speck ME, Cushing PR, Zhou Y, Corpora T, Regan M, Newman M, Roudaia L, Speck CL, Gu TL, Griffey SM, Bushweller JH, Speck NA. Disease mutations in

RUNX1 and RUNX2 create nonfunctional, dominant-negative, or hypomorphic alleles. *EMBO J*. 2007;26(4):1163-1175. Prepublished on 2007/02/10 as DOI 10.1038/sj.emboj.7601568.
98. Talebian L, Li Z, Guo Y, Gaudet J, Speck ME, Sugiyama D, Kaur P, Pear WS, Maillard I, Speck NA. T-lymphoid, megakaryocyte, and granulocyte development are sensitive to decreases in CBFbeta dosage. *Blood*. 2007;109(1):11-21. Prepublished on 2006/08/31 as DOI 10.1182/blood-2006-05-021188.
99. Sasaki K, Yagi H, Bronson RT, Tominaga K, Matsunashi T, Deguchi K, Tani Y, Kishimoto T, Komori T. Absence of fetal liver hematopoiesis in mice deficient in transcriptional coactivator core binding factor beta. *Proc Natl Acad Sci U S A*. 1996;93(22):12359-12363. Prepublished on 1996/10/29 as DOI.
100. Kundu M, Liu PP. Cbf beta is involved in maturation of all lineages of hematopoietic cells during embryogenesis except erythroid. *Blood Cells Mol Dis*. 2003;30(2):164-169. Prepublished on 2003/05/07 as DOI.
101. Wang Q, Stacy T, Miller JD, Lewis AF, Gu TL, Huang X, Bushweller JH, Bories JC, Alt FW, Ryan G, Liu PP, Wynshaw-Boris A, Binder M, Marin-Padilla M, Sharpe AH, Speck NA. The CBFbeta subunit is essential for CBFalpha2 (AML1) function in vivo. *Cell*. 1996;87(4):697-708. Prepublished on 1996/11/15 as DOI.
102. Yamagata T, Maki K, Mitani K. Runx1/AML1 in normal and abnormal hematopoiesis. *Int J Hematol*. 2005;82(1):1-8.
103. Li X, Vradii D, Gutierrez S, Lian JB, van Wijnen AJ, Stein JL, Stein GS, Javed A. Subnuclear targeting of Runx1 is required for synergistic activation of the myeloid specific M-CSF receptor promoter by PU.1. *J Cell Biochem*. 2005;96(4):795-809. Prepublished on 2005/09/09 as DOI 10.1002/jcb.20548.
104. Zaidi SK, Javed A, Choi JY, van Wijnen AJ, Stein JL, Lian JB, Stein GS. A specific targeting signal directs Runx2/Cbfa1 to subnuclear domains and contributes to transactivation of the osteocalcin gene. *J Cell Sci*. 2001;114(Pt 17):3093-3102. Prepublished on 2001/10/09 as DOI.
105. Hawley RG, Lieu FH, Fong AZ, Hawley TS. Versatile retroviral vectors for potential use in gene therapy. *Gene Ther*. 1994;1(2):136-138. Prepublished on 1994/03/01 as DOI.
106. Behre G, Smith LT, Tenen DG. Use of a promoterless Renilla luciferase vector as an internal control plasmid for transient co-transfection assays of Ras-mediated transcription activation. *Biotechniques*. 1999;26(1):24-26, 28. Prepublished on 1999/01/23 as DOI.
107. Javed A, Barnes GL, Pratap J, Antkowiak T, Gerstenfeld LC, van Wijnen AJ, Stein JL, Lian JB, Stein GS. Impaired intranuclear trafficking of Runx2 (AML3/CBFA1) transcription factors in breast cancer cells inhibits osteolysis in vivo. *Proc Natl Acad Sci U S A*. 2005;102(5):1454-1459. Prepublished on 2005/01/25 as DOI 10.1073/pnas.0409121102.
108. Javed A, Barnes GL, Jasanya BO, Stein JL, Gerstenfeld L, Lian JB, Stein GS. runt homology domain transcription factors (Runx, Cbfa, and AML) mediate repression of the bone sialoprotein promoter: evidence for promoter context-dependent activity of Cbfa proteins. *Mol Cell Biol*. 2001;21(8):2891-2905. Prepublished on 2001/04/03 as DOI 10.1128/MCB.21.8.2891-2905.2001.
109. Tsuzuki S, Hong D, Gupta R, Matsuo K, Seto M, Enver T. Isoform-specific potentiation of stem and progenitor cell engraftment by AML1/RUNX1. *PLoS Med*. 2007;4(5):e172. Prepublished on 2007/05/17 as DOI 10.1371/journal.pmed.0040172.
110. Stein GS, Stein JL, Van Wijnen AJ, Lian JB, Montecino M, Croce CM, Choi JY, Ali SA, Pande S, Hassan MQ, Zaidi SK, Young DW. Transcription factor-mediated epigenetic regulation of cell growth and phenotype for biological control and cancer. *Adv Enzyme Regul*. 2010;50(1):160-167. Prepublished on 2009/11/10 as DOI 10.1016/j.advenzreg.2009.10.026.

111. Pratap J, Galindo M, Zaidi SK, Vradii D, Bhat BM, Robinson JA, Choi JY, Komori T, Stein JL, Lian JB, Stein GS, van Wijnen AJ. Cell growth regulatory role of Runx2 during proliferative expansion of preosteoblasts. *Cancer Res*. 2003;63(17):5357-5362. Prepublished on 2003/09/23 as DOI.
112. Wolyniec K, Wotton S, Kilbey A, Jenkins A, Terry A, Peters G, Stocking C, Cameron E, Neil JC. RUNX1 and its fusion oncoprotein derivative, RUNX1-ETO, induce senescence-like growth arrest independently of replicative stress. *Oncogene*. 2009;28(27):2502-2512. Prepublished on 2009/05/19 as DOI 10.1038/onc.2009.101.
113. Coffman JA. Runx transcription factors and the developmental balance between cell proliferation and differentiation. *Cell Biol Int*. 2003;27(4):315-324.
114. Lichtinger M, Hoogenkamp M, Krysinska H, Ingram R, Bonifer C. Chromatin regulation by RUNX1. *Blood Cells Mol Dis*. 2010;44(4):287-290. Prepublished on 2010/03/03 as DOI 10.1016/j.bcmd.2010.02.009.
115. Friedman AD. Cell cycle and developmental control of hematopoiesis by Runx1. *J Cell Physiol*. 2009;219(3):520-524. Prepublished on 2009/02/25 as DOI 10.1002/jcp.21738.
116. Petrovick MS, Hiebert SW, Friedman AD, Hetherington CJ, Tenen DG, Zhang DE. Multiple functional domains of AML1: PU.1 and C/EBPalpha synergize with different regions of AML1. *Mol Cell Biol*. 1998;18(7):3915-3925. Prepublished on 1998/06/25 as DOI.
117. Kim WY, Sieweke M, Ogawa E, Wee HJ, Englmeier U, Graf T, Ito Y. Mutual activation of Ets-1 and AML1 DNA binding by direct interaction of their autoinhibitory domains. *EMBO J*. 1999;18(6):1609-1620. Prepublished on 1999/03/17 as DOI 10.1093/emboj/18.6.1609.
118. Ito Y. Oncogenic potential of the RUNX gene family: 'overview'. *Oncogene*. 2004;23(24):4198-4208.
119. Yokomizo T, Hasegawa K, Ishitobi H, Osato M, Ema M, Ito Y, Yamamoto M, Takahashi S. Runx1 is involved in primitive erythropoiesis in the mouse. *Blood*. 2008;111(8):4075-4080. Prepublished on 2008/02/06 as DOI 10.1182/blood-2007-05-091637.
120. Hoi CS, Lee SE, Lu SY, McDermitt DJ, Osorio KM, Piskun CM, Peters RM, Paus R, Tumbar T. Runx1 directly promotes proliferation of hair follicle stem cells and epithelial tumor formation in mouse skin. *Mol Cell Biol*. 2010;30(10):2518-2536. Prepublished on 2010/03/24 as DOI 10.1128/MCB.01308-09.
121. Osorio KM, Lee SE, McDermitt DJ, Waghmare SK, Zhang YV, Woo HN, Tumbar T. Runx1 modulates developmental, but not injury-driven, hair follicle stem cell activation. *Development*. 2008;135(6):1059-1068. Prepublished on 2008/02/08 as DOI 10.1242/dev.012799.
122. Osorio KM, Lilja KC, Tumbar T. Runx1 modulates adult hair follicle stem cell emergence and maintenance from distinct embryonic skin compartments. *J Cell Biol*. 2011;193(1):235-250. Prepublished on 2011/04/06 as DOI 10.1083/jcb.201006068.
123. Liakhovitskaia A, Lana-Elola E, Stamateris E, Rice DP, van 't Hof RJ, Medvinsky A. The essential requirement for Runx1 in the development of the sternum. *Dev Biol*. 2010;340(2):539-546. Prepublished on 2010/02/16 as DOI 10.1016/j.ydbio.2010.02.005.
124. Lian JB, Balint E, Javed A, Drissi H, Vitti R, Quinlan EJ, Zhang L, Van Wijnen AJ, Stein JL, Speck N, Stein GS. Runx1/AML1 hematopoietic transcription factor contributes to skeletal development in vivo. *J Cell Physiol*. 2003;196(2):301-311. Prepublished on 2003/06/18 as DOI 10.1002/jcp.10316.
125. Putz G, Rosner A, Nuesslein I, Schmitz N, Buchholz F. AML1 deletion in adult mice causes splenomegaly and lymphomas. *Oncogene*. 2006;25(6):929-939. Prepublished on 2005/10/26 as DOI 10.1038/sj.onc.1209136.
126. Watanabe-Okochi N, Kitaura J, Ono R, Harada H, Harada Y, Komeno Y, Nakajima H, Nosaka T, Inaba T, Kitamura T. AML1 mutations induced MDS and MDS/AML in a mouse

BMT model. *Blood*. 2008;111(8):4297-4308. Prepublished on 2008/01/15 as DOI 10.1182/blood-2007-01-068346.
127. Watanabe-Okochi N, Oki T, Komeno Y, Kato N, Yuji K, Ono R, Harada Y, Harada H, Hayashi Y, Nakajima H, Nosaka T, Kitaura J, Kitamura T. Possible involvement of RasGRP4 in leukemogenesis. *Int J Hematol*. 2009;89(4):470-481. Prepublished on 2009/04/08 as DOI 10.1007/s12185-009-0299-0.
128. Zaidi SK, Dowdy CR, van Wijnen AJ, Lian JB, Raza A, Stein JL, Croce CM, Stein GS. Altered Runx1 subnuclear targeting enhances myeloid cell proliferation and blocks differentiation by activating a miR-24/MKP-7/MAPK network. *Cancer Res*. 2009;69(21):8249-8255. Prepublished on 2009/10/15 as DOI 10.1158/0008-5472.CAN-09-1567.
129. Levanon D, Glusman G, Bangsow T, Ben-Asher E, Male DA, Avidan N, Bangsow C, Hattori M, Taylor TD, Taudien S, Blechschmidt K, Shimizu N, Rosenthal A, Sakaki Y, Lancet D, Groner Y. Architecture and anatomy of the genomic locus encoding the human leukemia-associated transcription factor RUNX1/AML1. *Gene*. 2001;262(1-2):23-33. Prepublished on 2001/02/17 as DOI.
130. Liu X, Zhang Q, Zhang DE, Zhou C, Xing H, Tian Z, Rao Q, Wang M, Wang J. Overexpression of an isoform of AML1 in acute leukemia and its potential role in leukemogenesis. *Leukemia*. 2009;23(4):739-745. Prepublished on 2009/01/20 as DOI 10.1038/leu.2008.350.
131. Okuda T, Takeda K, Fujita Y, Nishimura M, Yagyu S, Yoshida M, Akira S, Downing JR, Abe T. Biological characteristics of the leukemia-associated transcriptional factor AML1 disclosed by hematopoietic rescue of AML1-deficient embryonic stem cells by using a knock-in strategy. *Mol Cell Biol*. 2000;20(1):319-328. Prepublished on 1999/12/14 as DOI.
132. Goyama S, Yamaguchi Y, Imai Y, Kawazu M, Nakagawa M, Asai T, Kumano K, Mitani K, Ogawa S, Chiba S, Kurokawa M, Hirai H. The transcriptionally active form of AML1 is required for hematopoietic rescue of the AML1-deficient embryonic para-aortic splanchnopleural (P-Sp) region. *Blood*. 2004;104(12):3558-3564. Prepublished on 2004/07/24 as DOI 10.1182/blood-2004-04-1535.
133. Pande S, Ali SA, Dowdy C, Zaidi SK, Ito K, Ito Y, Montecino MA, Lian JB, Stein JL, van Wijnen AJ, Stein GS. Subnuclear targeting of the Runx3 tumor suppressor and its epigenetic association with mitotic chromosomes. *J Cell Physiol*. 2009;218(3):473-479. Prepublished on 2008/11/14 as DOI 10.1002/jcp.21630.
134. Javed A, Bae JS, Afzal F, Gutierrez S, Pratap J, Zaidi SK, Lou Y, van Wijnen AJ, Stein JL, Stein GS, Lian JB. Structural coupling of Smad and Runx2 for execution of the BMP2 osteogenic signal. *J Biol Chem*. 2008;283(13):8412-8422. Prepublished on 2008/01/22 as DOI 10.1074/jbc.M705578200.
135. Leboy P, Grasso-Knight G, D'Angelo M, Volk SW, Lian JV, Drissi H, Stein GS, Adams SL. Smad-Runx interactions during chondrocyte maturation. *J Bone Joint Surg Am*. 2001;83-A Suppl 1(Pt 1):S15-22. Prepublished on 2001/03/27 as DOI.
136. Imai Y, Kurokawa M, Tanaka K, Friedman AD, Ogawa S, Mitani K, Yazaki Y, Hirai H. TLE, the human homolog of groucho, interacts with AML1 and acts as a repressor of AML1-induced transactivation. *Biochem Biophys Res Commun*. 1998;252(3):582-589. Prepublished on 1998/12/05 as DOI 10.1006/bbrc.1998.9705.
137. Kitabayashi I, Aikawa Y, Nguyen LA, Yokoyama A, Ohki M. Activation of AML1-mediated transcription by MOZ and inhibition by the MOZ-CBP fusion protein. *EMBO J*. 2001;20(24):7184-7196. Prepublished on 2001/12/18 as DOI 10.1093/emboj/20.24.7184.
138. Levanon D, Goldstein RE, Bernstein Y, Tang H, Goldenberg D, Stifani S, Paroush Z, Groner Y. Transcriptional repression by AML1 and LEF-1 is mediated by the TLE/Groucho

corepressors. *Proc Natl Acad Sci U S A*. 1998;95(20):11590-11595. Prepublished on 1998/09/30 as DOI.
139. Yagi R, Chen LF, Shigesada K, Murakami Y, Ito Y. A WW domain-containing yes-associated protein (YAP) is a novel transcriptional co-activator. *EMBO J*. 1999;18(9):2551-2562. Prepublished on 1999/05/06 as DOI 10.1093/emboj/18.9.2551.
140. Zaidi SK, Sullivan AJ, Medina R, Ito Y, van Wijnen AJ, Stein JL, Lian JB, Stein GS. Tyrosine phosphorylation controls Runx2-mediated subnuclear targeting of YAP to repress transcription. *EMBO J*. 2004;23(4):790-799. Prepublished on 2004/02/07 as DOI 10.1038/sj.emboj.7600073.
141. Choi JY, Pratap J, Javed A, Zaidi SK, Xing L, Balint E, Dalamangas S, Boyce B, van Wijnen AJ, Lian JB, Stein JL, Jones SN, Stein GS. Subnuclear targeting of Runx/Cbfa/AML factors is essential for tissue-specific differentiation during embryonic development. *Proc Natl Acad Sci U S A*. 2001;98(15):8650-8655. Prepublished on 2001/07/05 as DOI 10.1073/pnas.151236498.
142. Woolf E, Xiao C, Fainaru O, Lotem J, Rosen D, Negreanu V, Bernstein Y, Goldenberg D, Brenner O, Berke G, Levanon D, Groner Y. Runx3 and Runx1 are required for CD8 T cell development during thymopoiesis. *Proc Natl Acad Sci U S A*. 2003;100(13):7731-7736. Prepublished on 2003/06/11 as DOI 10.1073/pnas.1232420100.
143. Dowdy CR, Xie R, Frederick D, Hussain S, Zaidi SK, Vradii D, Javed A, Li X, Jones SN, Lian JB, van Wijnen AJ, Stein JL, Stein GS. Definitive hematopoiesis requires Runx1 C-terminal-mediated subnuclear targeting and transactivation. *Hum Mol Genet*. 2010;19(6):1048-1057. Prepublished on 2009/12/26 as DOI 10.1093/hmg/ddp568.
144. Fukushima-Nakase Y, Naoe Y, Taniuchi I, Hosoi H, Sugimoto T, Okuda T. Shared and distinct roles mediated through C-terminal subdomains of acute myeloid leukemia/Runt-related transcription factor molecules in murine development. *Blood*. 2005;105(11):4298-4307. Prepublished on 2005/02/17 as DOI 10.1182/blood-2004-08-3372.
145. Javed A, Afzal F, Bae JS, Gutierrez S, Zaidi K, Pratap J, van Wijnen AJ, Stein JL, Stein GS, Lian JB. Specific residues of RUNX2 are obligatory for formation of BMP2-induced RUNX2-SMAD complex to promote osteoblast differentiation. *Cells Tissues Organs*. 2009;189(1-4):133-137. Prepublished on 2008/08/30 as DOI 10.1159/000151719.
146. Fortunel NO, Hatzfeld A, Hatzfeld JA. Transforming growth factor-beta: pleiotropic role in the regulation of hematopoiesis. *Blood*. 2000;96(6):2022-2036. Prepublished on 2000/09/09 as DOI.
147. Ruscetti FW, Akel S, Bartelmez SH. Autocrine transforming growth factor-beta regulation of hematopoiesis: many outcomes that depend on the context. *Oncogene*. 2005;24(37):5751-5763. Prepublished on 2005/08/27 as DOI 10.1038/sj.onc.1208921.
148. Larsson J, Karlsson S. The role of Smad signaling in hematopoiesis. *Oncogene*. 2005;24(37):5676-5692. Prepublished on 2005/08/27 as DOI 10.1038/sj.onc.1208920.
149. Yeager AM, Levin J, Levin FC. The effects of 5-fluorouracil on hematopoiesis: studies of murine megakaryocyte-CFC, granulocyte-macrophage-CFC, and peripheral blood cell levels. *Exp Hematol*. 1983;11(10):944-952. Prepublished on 1983/11/01 as DOI.
150. Schuringa JJ, Vellenga E. Role of the polycomb group gene BMI1 in normal and leukemic hematopoietic stem and progenitor cells. *Curr Opin Hematol*. 2010;17(4):294-299. Prepublished on 2010/03/24 as DOI 10.1097/MOH.0b013e328338c439.
151. Rizo A, Olthof S, Han L, Vellenga E, de Haan G, Schuringa JJ. Repression of BMI1 in normal and leukemic human CD34(+) cells impairs self-renewal and induces apoptosis. *Blood*. 2009;114(8):1498-1505. Prepublished on 2009/06/27 as DOI 10.1182/blood-2009-03-209734.

152. Lacombe J, Herblot S, Rojas-Sutterlin S, Haman A, Barakat S, Iscove NN, Sauvageau G, Hoang T. Scl regulates the quiescence and the long-term competence of hematopoietic stem cells. *Blood*. 2010;115(4):792-803. Prepublished on 2009/10/24 as DOI 10.1182/blood-2009-01-201384.
153. Brunet de la Grange P, Armstrong F, Duval V, Rouyez MC, Goardon N, Romeo PH, Pflumio F. Low SCL/TAL1 expression reveals its major role in adult hematopoietic myeloid progenitors and stem cells. *Blood*. 2006;108(9):2998-3004. Prepublished on 2006/07/20 as DOI 10.1182/blood-2006-05-022988.
154. Khandanpour C, Kosan C, Gaudreau MC, Duhrsen U, Hebert J, Zeng H, Moroy T. Growth factor independence 1 protects hematopoietic stem cells against apoptosis but also prevents the development of a myeloproliferative-like disease. *Stem Cells*. 2011;29(2):376-385. Prepublished on 2011/07/07 as DOI 10.1002/stem.575.
155. Horman SR, Velu CS, Chaubey A, Bourdeau T, Zhu J, Paul WE, Gebelein B, Grimes HL. Gfi1 integrates progenitor versus granulocytic transcriptional programming. *Blood*. 2009;113(22):5466-5475. Prepublished on 2009/04/07 as DOI 10.1182/blood-2008-09-179747.
156. Sabbattini P, Dillon N. The lambda5-VpreB1 locus--a model system for studying gene regulation during early B cell development. *Semin Immunol*. 2005;17(2):121-127. Prepublished on 2005/03/02 as DOI 10.1016/j.smim.2005.01.004.
157. Igarashi H, Gregory SC, Yokota T, Sakaguchi N, Kincade PW. Transcription from the RAG1 locus marks the earliest lymphocyte progenitors in bone marrow. *Immunity*. 2002;17(2):117-130. Prepublished on 2002/08/28 as DOI.
158. Biswas PS, Bhagat G, Pernis AB. IRF4 and its regulators: evolving insights into the pathogenesis of inflammatory arthritis? *Immunol Rev*. 2010;233(1):79-96. Prepublished on 2010/03/03 as DOI 10.1111/j.0105-2896.2009.00864.x.
159. Biswas PS, Gupta S, Stirzaker RA, Kumar V, Jessberger R, Lu TT, Bhagat G, Pernis AB. Dual regulation of IRF4 function in T and B cells is required for the coordination of T-B cell interactions and the prevention of autoimmunity. *J Exp Med*. 2012;209(3):581-596. Prepublished on 2012/03/01 as DOI 10.1084/jem.20111195.
160. Aigner F, Maier HT, Schwelberger HG, Wallnofer EA, Amberger A, Obrist P, Berger T, Mak TW, Maglione M, Margreiter R, Schneeberger S, Troppmair J. Lipocalin-2 regulates the inflammatory response during ischemia and reperfusion of the transplanted heart. *Am J Transplant*. 2007;7(4):779-788. Prepublished on 2007/03/30 as DOI 10.1111/j.1600-6143.2006.01723.x.
161. Jalagadugula G, Mao G, Kaur G, Goldfinger LE, Dhanasekaran DN, Rao AK. Regulation of platelet myosin light chain (MYL9) by RUNX1: implications for thrombocytopenia and platelet dysfunction in RUNX1 haplodeficiency. *Blood*. 2010;116(26):6037-6045. Prepublished on 2010/09/30 as DOI 10.1182/blood-2010-06-289850.
162. Sun L, Gorospe JR, Hoffman EP, Rao AK. Decreased platelet expression of myosin regulatory light chain polypeptide (MYL9) and other genes with platelet dysfunction and CBFA2/RUNX1 mutation: insights from platelet expression profiling. *J Thromb Haemost*. 2007;5(1):146-154. Prepublished on 2006/10/25 as DOI 10.1111/j.1538-7836.2006.02271.x.
163. Suh HC, Leeanansaksiri W, Ji M, Klarmann KD, Renn K, Gooya J, Smith D, McNiece I, Lugthart S, Valk PJ, Delwel R, Keller JR. Id1 immortalizes hematopoietic progenitors in vitro and promotes a myeloproliferative disease in vivo. *Oncogene*. 2008;27(42):5612-5623. Prepublished on 2008/06/11 as DOI 10.1038/onc.2008.175.
164. Wang L, Gural A, Sun XJ, Zhao X, Perna F, Huang G, Hatlen MA, Vu L, Liu F, Xu H, Asai T, Deblasio T, Menendez S, Voza F, Jiang Y, Cole PA, Zhang J, Melnick A, Roeder RG,

Nimer SD. The leukemogenicity of AML1-ETO is dependent on site-specific lysine acetylation. *Science*. 2011;333(6043):765-769. Prepublished on 2011/07/19 as DOI 10.1126/science.1201662.
165. Kumar R, Fossati V, Israel M, Snoeck HW. Lin-Sca1+kit- bone marrow cells contain early lymphoid-committed precursors that are distinct from common lymphoid progenitors. *J Immunol*. 2008;181(11):7507-7513. Prepublished on 2008/11/20 as DOI.
166. Liu Y, Pop R, Sadegh C, Brugnara C, Haase VH, Socolovsky M. Suppression of Fas-FasL coexpression by erythropoietin mediates erythroblast expansion during the erythropoietic stress response in vivo. *Blood*. 2006;108(1):123-133. Prepublished on 2006/03/11 as DOI 10.1182/blood-2005-11-4458.
167. Koulnis M, Porpiglia E, Porpiglia PA, Liu Y, Hallstrom K, Hidalgo D, Socolovsky M. Contrasting dynamic responses in vivo of the Bcl-xL and Bim erythropoietic survival pathways. *Blood*. 2012;119(5):1228-1239. Prepublished on 2011/11/17 as DOI 10.1182/blood-2011-07-365346.
168. Lal A, Vichinsky E. The role of fetal hemoglobin-enhancing agents in thalassemia. *Semin Hematol*. 2004;41(4 Suppl 6):17-22. Prepublished on 2004/11/10 as DOI.
169. Higuchi M, O'Brien D, Kumaravelu P, Lenny N, Yeoh EJ, Downing JR. Expression of a conditional AML1-ETO oncogene bypasses embryonic lethality and establishes a murine model of human t(8;21) acute myeloid leukemia. *Cancer Cell*. 2002;1(1):63-74. Prepublished on 2002/06/28 as DOI.
170. Blyth K, Slater N, Hanlon L, Bell M, Mackay N, Stewart M, Neil JC, Cameron ER. Runx1 promotes B-cell survival and lymphoma development. *Blood Cells Mol Dis*. 2009;43(1):12-19. Prepublished on 2009/03/10 as DOI 10.1016/j.bcmd.2009.01.013.
171. Egawa T. Runx and ThPOK: a balancing act to regulate thymocyte lineage commitment. *J Cell Biochem*. 2009;107(6):1037-1045. Prepublished on 2009/05/30 as DOI 10.1002/jcb.22212.
172. Grossmann V, Kern W, Harbich S, Alpermann T, Jeromin S, Schnittger S, Haferlach C, Haferlach T, Kohlmann A. Prognostic relevance of RUNX1 mutations in T-cell acute lymphoblastic leukemia. *Haematologica*. 2011;96(12):1874-1877. Prepublished on 2011/08/11 as DOI 10.3324/haematol.2011.043919.
173. Hashidate T, Murakami N, Nakagawa M, Ichikawa M, Kurokawa M, Shimizu T, Nakamura M. AML1 enhances the expression of leukotriene B4 type-1 receptor in leukocytes. *FASEB J*. 2010;24(9):3500-3510. Prepublished on 2010/04/17 as DOI 10.1096/fj.10-156844.
174. Swirski FK, Nahrendorf M, Etzrodt M, Wildgruber M, Cortez-Retamozo V, Panizzi P, Figueiredo JL, Kohler RH, Chudnovskiy A, Waterman P, Aikawa E, Mempel TR, Libby P, Weissleder R, Pittet MJ. Identification of splenic reservoir monocytes and their deployment to inflammatory sites. *Science*. 2009;325(5940):612-616. Prepublished on 2009/08/01 as DOI 10.1126/science.1175202.
175. Choi Y, Elagib KE, Delehanty LL, Goldfarb AN. Erythroid inhibition by the leukemic fusion AML1-ETO is associated with impaired acetylation of the major erythroid transcription factor GATA-1. *Cancer Res*. 2006;66(6):2990-2996. Prepublished on 2006/03/17 as DOI 10.1158/0008-5472.CAN-05-2944.
176. Old JM. Screening and genetic diagnosis of haemoglobin disorders. *Blood Rev*. 2003;17(1):43-53. Prepublished on 2002/12/20 as DOI.
177. Basecke J, Cepek L, Mannhalter C, Krauter J, Hildenhagen S, Brittinger G, Trumper L, Griesinger F. Transcription of AML1/ETO in bone marrow and cord blood of individuals without acute myelogenous leukemia. *Blood*. 2002;100(6):2267-2268. Prepublished on 2002/09/17 as DOI.

178. Song J, Mercer D, Hu X, Liu H, Li MM. Common leukemia- and lymphoma-associated genetic aberrations in healthy individuals. *J Mol Diagn*. 2011;13(2):213-219. Prepublished on 2011/03/01 as DOI 10.1016/j.jmoldx.2010.10.009.
179. Cai Z, de Bruijn M, Ma X, Dortland B, Luteijn T, Downing RJ, Dzierzak E. Haploinsufficiency of AML1 affects the temporal and spatial generation of hematopoietic stem cells in the mouse embryo. *Immunity*. 2000;13(4):423-431. Prepublished on 2000/11/09 as DOI.
180. Yokomizo T, Yanagida M, Huang G, Osato M, Honda C, Ema M, Takahashi S, Yamamoto M, Ito Y. Genetic evidence of PEBP2beta-independent activation of Runx1 in the murine embryo. *Int J Hematol*. 2008;88(2):134-138. Prepublished on 2008/07/03 as DOI 10.1007/s12185-008-0121-4.
181. Ogawa E, Inuzuka M, Maruyama M, Satake M, Naito-Fujimoto M, Ito Y, Shigesada K. Molecular cloning and characterization of PEBP2 beta, the heterodimeric partner of a novel Drosophila runt-related DNA binding protein PEBP2 alpha. *Virology*. 1993;194(1):314-331. Prepublished on 1993/05/01 as DOI 10.1006/viro.1993.1262.
182. Niki M, Okada H, Takano H, Kuno J, Tani K, Hibino H, Asano S, Ito Y, Satake M, Noda T. Hematopoiesis in the fetal liver is impaired by targeted mutagenesis of a gene encoding a non-DNA binding subunit of the transcription factor, polyomavirus enhancer binding protein 2/core binding factor. *Proc Natl Acad Sci U S A*. 1997;94(11):5697-5702. Prepublished on 1997/05/27 as DOI.
183. Castilla LH, Wijmenga C, Wang Q, Stacy T, Speck NA, Eckhaus M, Marin-Padilla M, Collins FS, Wynshaw-Boris A, Liu PP. Failure of embryonic hematopoiesis and lethal hemorrhages in mouse embryos heterozygous for a knocked-in leukemia gene CBFB-MYH11. *Cell*. 1996;87(4):687-696. Prepublished on 1996/11/15 as DOI.
184. Yergeau DA, Hetherington CJ, Wang Q, Zhang P, Sharpe AH, Binder M, Marin-Padilla M, Tenen DG, Speck NA, Zhang DE. Embryonic lethality and impairment of haematopoiesis in mice heterozygous for an AML1-ETO fusion gene. *Nat Genet*. 1997;15(3):303-306. Prepublished on 1997/03/01 as DOI 10.1038/ng0397-303.
185. Okuda T, Cai Z, Yang S, Lenny N, Lyu CJ, van Deursen JM, Harada H, Downing JR. Expression of a knocked-in AML1-ETO leukemia gene inhibits the establishment of normal definitive hematopoiesis and directly generates dysplastic hematopoietic progenitors. *Blood*. 1998;91(9):3134-3143. Prepublished on 1998/05/23 as DOI.
186. Beri-Dexheimer M, Latger-Cannard V, Philippe C, Bonnet C, Chambon P, Roth V, Gregoire MJ, Bordigoni P, Lecompte T, Leheup B, Jonveaux P. Clinical phenotype of germline RUNX1 haploinsufficiency: from point mutations to large genomic deletions. *Eur J Hum Genet*. 2008;16(8):1014-1018. Prepublished on 2008/05/15 as DOI 10.1038/ejhg.2008.89.
187. Mangan JK, Speck NA. RUNX1 Mutations in Clonal Myeloid Disorders: From Conventional Cytogenetics to Next Generation Sequencing, A Story 40 Years in the Making. *Crit Rev Oncog*. 2011;16(1-2):77-91. Prepublished on 2011/12/14 as DOI.
188. Schnittger S, Dicker F, Kern W, Wendland N, Sundermann J, Alpermann T, Haferlach C, Haferlach T. RUNX1 mutations are frequent in de novo AML with noncomplex karyotype and confer an unfavorable prognosis. *Blood*. 2011;117(8):2348-2357. Prepublished on 2010/12/15 as DOI 10.1182/blood-2009-11-255976.
189. Adya N, Stacy T, Speck NA, Liu PP. The leukemic protein core binding factor beta (CBFbeta)-smooth-muscle myosin heavy chain sequesters CBFalpha2 into cytoskeletal filaments and aggregates. *Mol Cell Biol*. 1998;18(12):7432-7443. Prepublished on 1998/11/20 as DOI.
190. Osato M, Asou N, Abdalla E, Hoshino K, Yamasaki H, Okubo T, Suzushima H, Takatsuki K, Kanno T, Shigesada K, Ito Y. Biallelic and heterozygous point mutations in the runt

domain of the AML1/PEBP2alphaB gene associated with myeloblastic leukemias. *Blood*. 1999;93(6):1817-1824. Prepublished on 1999/03/09 as DOI.
191. Stein GS, van Wijnen AJ, Imbalzano AN, Montecino M, Zaidi SK, Lian JB, Nickerson JA, Stein JL. Architectural genetic and epigenetic control of regulatory networks: compartmentalizing machinery for transcription and chromatin remodeling in nuclear microenvironments. *Crit Rev Eukaryot Gene Expr*. 2010;20(2):149-155. Prepublished on 2010/12/08 as DOI.
192. Kuo YH, Landrette SF, Heilman SA, Perrat PN, Garrett L, Liu PP, Le Beau MM, Kogan SC, Castilla LH. Cbf beta-SMMHC induces distinct abnormal myeloid progenitors able to develop acute myeloid leukemia. *Cancer Cell*. 2006;9(1):57-68. Prepublished on 2006/01/18 as DOI 10.1016/j.ccr.2005.12.014.
193. Stender JD, Kim K, Charn TH, Komm B, Chang KC, Kraus WL, Benner C, Glass CK, Katzenellenbogen BS. Genome-wide analysis of estrogen receptor alpha DNA binding and tethering mechanisms identifies Runx1 as a novel tethering factor in receptor-mediated transcriptional activation. *Mol Cell Biol*. 2010;30(16):3943-3955. Prepublished on 2010/06/16 as DOI 10.1128/MCB.00118-10.
194. Zhao L, Glazov EA, Pattabiraman DR, Al-Owaidi F, Zhang P, Brown MA, Leo PJ, Gonda TJ. Integrated genome-wide chromatin occupancy and expression analyses identify key myeloid pro-differentiation transcription factors repressed by Myb. *Nucleic Acids Res*. 2011;39(11):4664-4679. Prepublished on 2011/02/15 as DOI 10.1093/nar/gkr024.
195. Bruhn L, Munnerlyn A, Grosschedl R. ALY, a context-dependent coactivator of LEF-1 and AML-1, is required for TCRalpha enhancer function. *Genes Dev*. 1997;11(5):640-653. Prepublished on 1997/03/01 as DOI.
196. Chakraborty S, Sinha KK, Senyuk V, Nucifora G. SUV39H1 interacts with AML1 and abrogates AML1 transactivity. AML1 is methylated in vivo. *Oncogene*. 2003;22(34):5229-5237. Prepublished on 2003/08/15 as DOI 10.1038/sj.onc.1206600.
197. Hess J, Porte D, Munz C, Angel P. AP-1 and Cbfa/runt physically interact and regulate parathyroid hormone-dependent MMP13 expression in osteoblasts through a new osteoblast-specific element 2/AP-1 composite element. *J Biol Chem*. 2001;276(23):20029-20038. Prepublished on 2001/03/29 as DOI 10.1074/jbc.M010601200.
198. Kagoshima H, Akamatsu Y, Ito Y, Shigesada K. Functional dissection of the alpha and beta subunits of transcription factor PEBP2 and the redox susceptibility of its DNA binding activity. *J Biol Chem*. 1996;271(51):33074-33082. Prepublished on 1996/12/20 as DOI.
199. Fujimoto T, Anderson K, Jacobsen SE, Nishikawa SI, Nerlov C. Cdk6 blocks myeloid differentiation by interfering with Runx1 DNA binding and Runx1-C/EBPalpha interaction. *EMBO J*. 2007;26(9):2361-2370. Prepublished on 2007/04/14 as DOI 10.1038/sj.emboj.7601675.
200. Li X, Decker M, Westendorf JJ. TEThered to Runx: novel binding partners for runx factors. *Blood Cells Mol Dis*. 2010;45(1):82-85. Prepublished on 2010/04/07 as DOI 10.1016/j.bcmd.2010.03.002.
201. Li FQ, Person RE, Takemaru K, Williams K, Meade-White K, Ozsahin AH, Gungor T, Moon RT, Horwitz M. Lymphoid enhancer factor-1 links two hereditary leukemia syndromes through core-binding factor alpha regulation of ELA2. *J Biol Chem*. 2004;279(4):2873-2884. Prepublished on 2003/11/05 as DOI 10.1074/jbc.M310759200.
202. Libermann TA, Pan Z, Akbarali Y, Hetherington CJ, Boltax J, Yergeau DA, Zhang DE. AML1 (CBFalpha2) cooperates with B cell-specific activating protein (BSAP/PAX5) in activation of the B cell-specific BLK gene promoter. *J Biol Chem*. 1999;274(35):24671-24676. Prepublished on 1999/08/24 as DOI.

203. Lutterbach B, Westendorf JJ, Linggi B, Isaac S, Seto E, Hiebert SW. A mechanism of repression by acute myeloid leukemia-1, the target of multiple chromosomal translocations in acute leukemia. *J Biol Chem*. 2000;275(1):651-656. Prepublished on 2000/01/05 as DOI.
204. Mao S, Frank RC, Zhang J, Miyazaki Y, Nimer SD. Functional and physical interactions between AML1 proteins and an ETS protein, MEF: implications for the pathogenesis of t(8;21)-positive leukemias. *Mol Cell Biol*. 1999;19(5):3635-3644. Prepublished on 1999/04/17 as DOI.
205. Ogawa S, Satake M, Ikuta K. Physical and functional interactions between STAT5 and Runx transcription factors. *J Biochem*. 2008;143(5):695-709. Prepublished on 2008/02/26 as DOI 10.1093/jb/mvn022.
206. Ono M, Yaguchi H, Ohkura N, Kitabayashi I, Nagamura Y, Nomura T, Miyachi Y, Tsukada T, Sakaguchi S. Foxp3 controls regulatory T-cell function by interacting with AML1/Runx1. *Nature*. 2007;446(7136):685-689. Prepublished on 2007/03/23 as DOI 10.1038/nature05673.